

# Sheffield Hallam University

*HBC fuse models based on fundamental arc mechanisms.*

GOMEZ, J. C.

Available from the Sheffield Hallam University Research Archive (SHURA) at:

<http://shura.shu.ac.uk/19696/>

## A Sheffield Hallam University thesis

This thesis is protected by copyright which belongs to the author.

The content must not be changed in any way or sold commercially in any format or medium without the formal permission of the author.

When referring to this work, full bibliographic details including the author, title, awarding institution and date of the thesis must be given.

Please visit <http://shura.shu.ac.uk/19696/> and <http://shura.shu.ac.uk/information.html> for further details about copyright and re-use permissions.

101 435 909 0



BLN 306 954

Sheffield Hallam University

**REFERENCE ONLY**

ProQuest Number: 10696996

All rights reserved

INFORMATION TO ALL USERS

The quality of this reproduction is dependent upon the quality of the copy submitted.

In the unlikely event that the author did not send a complete manuscript and there are missing pages, these will be noted. Also, if material had to be removed, a note will indicate the deletion.



ProQuest 10696996

Published by ProQuest LLC (2017). Copyright of the Dissertation is held by the Author.

All rights reserved.

This work is protected against unauthorized copying under Title 17, United States Code  
Microform Edition © ProQuest LLC.

ProQuest LLC.  
789 East Eisenhower Parkway  
P.O. Box 1346  
Ann Arbor, MI 48106 – 1346

**H.B.C. Fuse Models Based on  
Fundamental Arc Mechanisms**

**J. C. Gomez**

**Degree of Doctor of Philosophy**

**1994**

# **H.B.C. Fuse Models Based on Fundamental Arc Mechanisms**

Juan Carlos Gomez

A thesis submitted in partial fulfilment of the  
requirements of  
Sheffield Hallam University  
for the degree of Doctor of Philosophy

September 1994

## Abstract

The Thesis presents an in-depth study of arcing behaviour of H.B.C. Fuses for a range of fuse elements and fillers, under critical current conditions. The methodologies used were the standard breaking capacity short-circuit test plus the application of crow-bar, X-ray studies, metallographic microscopic and optical fiber arc detection techniques.

Due to the observation of some unknown and puzzling arc phenomena, it was decided to pursue the arc investigation by an extensive test programme of single uniform wire fuse elements.

From the investigation a basic arc mechanism for the pre-peak and post-peak arcs period was discovered.

The new mechanism was applied to single wire, strip, long notched, medium notched and short notched fuse elements and to paralleled wires and strips immersed in three quartz filler types: standard sand, high quality granular quartz and bound quartz in two different sizes.

The proposed arc mechanism was modelled by a computer program which was used to simulate the described fuse constructions. The results of over 800 tests and subsequent simulation undoubtedly confirm that the proposed arc mechanism is applicable for the described fuse types.

The experimental and analytical results are close enough to justify the model application for fuse designers and fuse users.

A critical comparison of the experimental and analytical results with previous findings published by other researchers is presented.

A detailed arc mechanism and the key behaviour rules are proposed, they are:

- Maximum column voltage can not exceed the arc-root voltage.
- The arc-root voltage and the initial  $dv/dt$  values are influenced by filler characteristics and are able to precisely characterize the filler behaviour.
- The  $dv/dt$ , and consequently, the burn-back are instantaneous current density functions

The application of the above rules allows the fuse designer to tailor the fuse element in order to obtain specific current and arc voltage waveforms.

It is believed that the proposed arc mechanism and computer model is able to explain some puzzling arc phenomena and eventually could be applied to predicting other low overload H.B.C. fuse behaviour.

# Contents

	Page
Abstract	i
Contents	ii
<b>1 Chapter 1 : Review of Research into H.B.C. Fuse Arcing Behaviour</b>	
1.1. Introduction	1
1.2. Scope of the thesis	2
1.3. Historical background	3
1.3.1. Fuse development stages	3
1.4. Arc model research of filled fuses	4
1.5. Assessment of principal arc research work	12
1.5.1. Arc physics models	12
1.5.1.1. The Wright model	12
1.5.1.2. Merits and limitations of the Wright model	17
1.5.2. Arc voltage-current electrical equivalent circuit models	18
1.5.2.1. The Dowlegowski model	18
1.5.2.2. Merits and limitations	21
1.5.3. Hybrid models	22
1.5.3.1. The Daaldder model	22
1.5.3.2. Merits and limitations	27
1.6. Unknown arc phenomena	27
1.6.1. Fundamental issues	27
1.6.2. Development of author's research of arc mechanisms	28
1.7. References	28
<b>2. Chapter 2 : Basic arc mechanisms</b>	
2.1. Basic arc mechanisms in wires immersed in fillers	31
2.2. Wall stabilised arc model applied to axi-symmetric arc problem	36
2.3. Wall stabilised arc mechanism model	38
2.3.1. Experimental investigation	38
I. Crow-bar fuse tests	39
I-1. Samples	39
I-2. Test circuit	40
I-3. Methodology	45
II. Optical fibre fuse tests	47
II-1. Samples	47
II-2. Test circuit	51
II-3. Fibre optic methodology	51
2.3.2. Arc model for rising arc voltage	62
2.3.3. Basic arc model for falling arc voltage	69
2.3.4. Limitations of basic arc mechanism model	74
2.3.5. Evaluation of model for wires in fillers	74
2.4. References	80

	Page
3. Chapter 3 : Arc models for practical fuse links	
3.1. Evaluation of arc model for practical H.B.C. fuses	83
3.1.1. Fuse element types and arc quenching media	83
3.2. Evaluation of arc model for compacted filler	84
3.2.1. Single strip fuse element	84
3.2.2. Single notched strip fuse element	93
3.2.2.1. Long notch arcs	94
3.2.2.2. Medium notch arcs	96
3.2.2.3. Short notch arcs	103
3.3. Evaluation of model for varying filler media	103
3.4. Evaluation of simple parallel elements	109
3.5. Complex notched shaped elements (round and rhomboid holes)	110
4. Chapter 4 : Determination of fuse short-circuit arc characteristics and critical design parameters	
4.1. Determination of arc model critical parametric values	113
4.1.1. Determination of arc-root voltage	113
4.1.2. Determination of the pre-peak dv/dt parametric value	114
4.1.3. Determination of the post-peak dv/dt parametric value	120
4.2. Prediction of arc performance characteristics	122
4.2.1. Fuse characteristic determination	122
4.2.2. Experimental simulation and model accuracy	125
4.2.3. Practical limitations of proposed arc model	126
4.3. Fuse design considerations	126
4.3.1. Ideal fuse arc characteristics	126
4.4. References	130
5. Chapter 5 : Review of research and concluding observations	
5.1. Review of H.B.C. fuse arc mechanistic model	132
5.1.1. Pre-peak arc voltage mechanism	132
5.1.2. Post-peak arc voltage mechanism	133
5.2. Review of arc physical formation and extinction processes	136
5.2.1. Arc physical formation processes	136
5.2.2. Arc physical extinction processes	141
5.3. Fuse arcing and circuit interaction	142
5.4. Unresolved problems and future work	145
5.5. References	145
6. The Author	146
7. Acknowledgments	147
8. Appendix 1 : Fuse data Tables 1 ~ 8	148

### List of symbols:

$A_e$  = cross-sectional area of electrode,  $\text{mm}^2$   
 $C_f$  = specific heat of filler,  $\text{J/g}^\circ\text{C}$   
 $b$  = channel width, mm  
 $d$  = wire diameter, mm  
 $D$  = channel thickness, mm  
 $E$  = axial arc gradient,  $\text{V/mm}$   
 $E_c$  = energy input to column, J  
 $E_j$  = ionisation energy  
 $G$  = electrical conductivity,  $\omega\text{m}$   
 $h$  = striation module, mm  
 $H$  = enthalpy,  
 $i$  = current, A  
 $i_o$  = peak current, A  
 $J$  = current density,  $\text{A/mm}^2$   
 $l$  = length, mm  
 $l_z$  = fuse length, mm  
 $L_f$  = latent heat of fusion,  $\text{J/g}$   
 $L_s$  = source inductance,  $\omega$   
 $m_t$  = total electrode mass which is melted, g  
 $m_v$  = mass of electrode which is vaporised, g  
 $N_a$  = number of atoms evaporated  
 $K_B$  = Boltzmann's constant  
 $N_e$  = number of electrons  
 $N_d$  = number of atoms scattered  
 $n$  = number of arcs  
 $n_s$  = number of restrictions in series  
 $n_p$  = number of paralleled restrictions  
 $R_s$  = source resistance,  $\omega$   
 $S_o$  = initial cross-section,  $\text{mm}^2$   
 $S_z$  = striction cross-section,  $\text{mm}^2$   
 $t$  = time, s  
 $t_a$  = arcing time, s  
 $T$  = temperature, C  
 $U_{con}$  = power loss per A., V  
 $V_s$  = source voltage, V  
 $V_{ak}$  = arc-root voltage, V  
 $V_{arc}$  = arc voltage, V  
 $V_{af}$  = voltage associated with anode fall, V  
 $V_{wf}$  = voltage associated with the work function, V  
 $v_j$  = vapour jet velocity,  $\text{mm/s}$

X = ionization fraction

Z = ion charge

$\ln \Lambda$  = Coulomb cut-off

$\delta_t$  = time interval, s

$\sigma$  = column electrical conductivity  $(\omega \text{ m})^{-1}$

$\rho$  = density,  $\text{g}/\text{mm}^3$

$\rho_f$  = filler density,  $\text{g}/\text{mm}^3$

$\varphi$  = volumetric radiation intensity, W

# **Chapter 1: Review of Research into H.B.C. Fuse Arcing Behaviour**

## **1.1 Introduction:**

The fuse as a electrical protection device is a rather ancient device [1, 2]. Its application today covers more that 90% of overcurrent electric protection needs at the three levels: transmission (high voltage), distribution (medium voltage) and sub-distribution (low voltage).

The first fuse was really a very simple device; in fact just a piece of wire across two terminal contacts. Today the fuse has reached a high degree of complexity. The fuse designs available now are able to cover a very wide field of application. These designs are very different for example, for a high voltage system protecting a transformer of some dozens of MVA or in a modern video recorder. These examples show not only the power capability and size difference of both applications but the huge manufacture variance. In the first case the production techniques require the skill and care of a craftsman whilst in the second case the level of automation is incredibly high.

For the whole fuse spectrum the design is a vast problem characterized by its cost and time consuming complexity. For this reason it is very important to utilize simulation and modelling tools whenever possible. The problem of the modelling of the prearcing phenomena has been solved for several methodologies, but the arcing behaviour is without a clear and reliable simulation.

## 1.2 Scope of the thesis

The aim of the work presented in this thesis was to create mathematical or computer arcing models which represent in a simple and precise way the arcing phenomena in H.B.C. fuses. The required degree of simplicity and accuracy would be of the order necessary for the design and manufacture of fuses for any application.

A good model must be able to represent the whole of the arc process for each of the three parts in which the arc phenomena is traditionally divided, i.e. the periods pertaining to:

- the pre-peak arc voltage
- post-peak arc voltage
- post-arc period

Most of the researcher effort has been devoted to the first and second part, while the third is under recent investigation .

Until today several models have been presented, but all of them suffer from at least one of the following basic drawbacks:

- the complexity is so high that the application is limited to only highly qualified specialists;
- low accuracy, where the errors may be anywhere between 50 or 100% and
- the impossibility of relating the model parameters with the dimensions and physical characteristics of the different fuse components.

Today it is possible to represent practically in a perfect way the prearcing phenomena, using any of the three most important and precise methodologies: Finite elements [3,4,5], Finite differences [6,7] and Transmission Line Matrix TLM [8].

These methods are now available for the application engineer and designer, using personal computers and commercial software. Given that the prearcing studies are basically completed, it is appropriate to attempt to similarly conclude the study of the arcing behaviour in fuses to enable designers, ideally, to use either computer models or apply empirical methodologies to the prediction of the complete fuse performance.

The current situation is that any necessary change to a fuse design must be done starting practically from fundamental principles when the arc behaviour is critical.

Furthermore there are several arc quenching phenomena which could not be explained based on the available theories or models. These drawbacks have produced a true halt in the development, implementation and exploitation of new ideas, and furthermore they discourage the application of more imaginative designs and alternative materials for the fuse element and for the filler.

The understanding of arcing as a process can therefore unleash a radical approach to fuse design. This is the hope of the author for the presented work.

### 1.3 Historical Background

#### 1.3.1 Fuse Development Stages

The development of fuses could be generally described in six stages. The first stage started in 1774, with the first reference to melting wires published by Nairne [9]. This was followed by a series of papers describing many fuse experiments and explaining some simple applications [2].

The second stage could be considered as starting with Meyer's book in 1906 [10] in which a more scientific approach to analysing melting is presented. During this second stage, the researchers were mainly involved in the prediction of the relation between the fuse element dimensions and the melting time of elements. The idea was that if the fuse melts it will cut the overcurrent. In a short time it was realized that satisfying the first requirement not always resulted in the achievement of the second.

The third stage started with the birth of the filled fuse, which was introduced by German researchers in 1940. During this time extensive studies were devoted to arc extinction phenomena. The fourth stage, could be considered as the dark fuse age, because it was the time of the Second World War. During this period there was a rapid increase in the available energy of national electric power systems which quickly surpassed fuse

developments and furthermore a new device had been introduced, this being the molded case circuit breaker, (MCCB) which threatened to replace the out-moded fuse. This situation was maintained until the end of World War II, after which new H.B.C. fuse types were developed. The fifth stage, introduced several fuse improvements such as the use of M-effect, filler material, notched fuse elements, etc. These features made the fuse more competitive and reliable than the emerging MCCB.

This period coincided with the expansion of national developments after World War II and led to the creation of large fuse companies.

The sixth stage was the introduction of power semiconductors in the early fifties, which were highly different to all other electrical equipment in use, due to its very high power to mass ratio and their consequent sensitivity to overcurrents. This requirement necessitated a new type of protective device. The fuse was able to protect these devices but this solution was not straight-forward. Initially the traditional fuse manufacturer was not able of develop satisfactory fuses, and the semiconductor factories were obliged in some countries to create their own semiconductor fuses.

Fuse development since the fifties has slowed down, despite the strong position of the fuse in electric systems, to the extent that nothing exceptional in fuse research has occurred during the last ten years.

The fuse historic development can be easily tracked by reading Läßle's [11] and Baxter's [12] books together with UK Electrical Research Association Digests [13].

#### 1.4 Arc Model Research of Filled Fuses

The best known fuse arc models or methodologies are summarised in chronological order as follows:

1.4.1. Kroemer H. 1942 [14] investigated arcs in sand filled single notched fuses under d.c. short-circuit conditions. The arc behaviour was studied experimentally using probes. The axial electric field was measured for several arc quenching mediums and currents. A

charge-controlled model was proposed, in which the mass of electrode metal eroded was assumed to be directly proportional to electric charge passing through the arc column. Based on this concept he proposed a linear dependence between the burn-back velocity and the current density. It was concluded that the best arc quenching material is quartz sand and that the electric field is independent of current and decreasing as the arc extends.

1.4.2. Voshall R.E. 1969 [15] investigated the positive column of a high-current metal-vapor arc in vacuum. The author concluded that the dominant mechanisms for controlling the arc column are magnetic pinch forces and radiation energy losses. A set of equations based on arc physics allows the calculation of the thermal conductivity, electrical conductivity, temperatures and finally the electric field and current as time functions. Values for anode and cathode fall voltages of  $\cong 25$  V are inferred from the experiments.

1.4.3. Schonholzer E.T. 1972 [16] developed mathematical models for simulating the fuse prearcing and arcing characteristics for use with analog computers. The models are very simple being applicable to fuse-thyristor first step coordination. These models were the first analog models to be presented. The proposed value for anode-cathode voltage drop is 60V, and it is concluded that the burn-back speed is proportional to the instantaneous value of current.

1.4.4. Hirose A. 1976 [17] developed the idea of a simple arc model based on analog computer. The arc voltage is considered to be of constant value with an added voltage which is a function of the current. No specific test values are given for the two voltages, although several classical arc voltage wave forms are shown. The principle of "bad and good fuse" is also introduced.

1.4.5. Dolegowski M. 1976 [18] advocated a semi-empirical model characterised by a set of equations. The equation coefficients were based on experimental parameters or values

for the anode/cathode voltage drops, axial voltage gradient, arc length and burn-back speed. The model considered that just one arc is established in each notch. He proposed that the equation for the voltage drop in the electrodes, comprises a constant value plus a voltage based on both current and current density functions. The equations for arc length and axial voltage gradient are complex and somewhat artificial, and; as a result, very difficult to apply. The claimed accuracy is +/- 10 %. Analytical experimental comparison are presented.

1.4.6. Wright A., Beaumont K.J. 1976 [19] developed a mathematical fuse model for high current levels based on fundamental arc physic principles and phenomena. Though the model has many simplifying assumptions, for example constant electric field was assumed, it results in solving 10 simultaneous equations in 10 unknowns. The correspondence claimed by the authors between the presented analytical and experimental results is very good. The model allows the calculations of temperature and pressure inside the arc channel, giving an idea of the ionization fraction, electron density and atomic density. This was the first report on tracking the arcing processes analytically. Applications of the model to other fuse types and operating conditions has not been reproduced to the same accuracy.

1.4.7. Oliver R. 1976 [20] developed a set of equations based on Kroemer's charge-controlled model . The experimental results under d.c overcurrent conditions are explained and the merits and drawbacks are analyzed. It is concluded that the main error is caused by the constant electric field assumption. A stepped arc behaviour is observed where sudden changes in arc voltage occur followed by a steady rise. The amplitude of the steps were of the order of 60 V.

1.4.8. Oliver R, 1977 [21] reported on an in-depth study of d.c. arcs in which the factors influencing the arc structure were analysed. Evidence is presented for the classification of the fuse arc as generally wall-stabilized and cooled by conduction. The behaviour with wire and strip elements is compared together with the influence of the cartridge internal

diameter. It is concluded that the element geometry and the filler packing plays an important role in the lumen size, which in turn controls column losses and voltage gradient.

1.4.9. Wilkins R. 1977 [22] proposed a simple simulation of arcing under short-circuit conditions which gives results which compare reasonably well with tests. A review of methods of simulation were also given. The experimental work proposed for the improvement of the model is indicated.

1.4.10. Ranjan R., Barrault M.R. 1980 [23] advanced a model for notched fuse elements, based on equations derived from low overcurrent d.c. tests. An equation for the axial electric field of the fuse element is given. Their results show that the electric field is inversely proportional to the thickness of the lumen. The results supported the classification of the fuse arc in filler as a "wall-stabilized arc".

1.4.11. Gnanalingam S., Wilkins R. 1980 [24] proposed a semi-empirical model for fuses under critical current conditions. They report on the results using a computer program to simulate the transient heating, disruption of constrictions, extension and coalescence of the arcs and fulgurite growth. A set of generalised equations are given, using several constants and coefficients, determined experimentally. The model is claimed to be easy to apply, provided that the constants for particular fuses are known. The solution is applicable for each notch assuming one arc per notch, and that the notch arc phenomena can be replicated for the whole fuse element.

1.4.12. Daalder J.E., Schreus E.F. 1983 [25] proposed a 'quasi' analytical-experimental model based on extensive test using a L-C circuit under constant current conditions over a range of several kA. An experimental relation was obtained for the burn-back rate from this work. They concluded that the lumen thickness increased proportionally with the root of the arcing time. The results of arc voltages were obtained using the proposed fully ionized quasi static arc model. This model showed good agreement with the

measured values. The initial arc voltage and arc merging, together with a comparison of previous results, were discussed.

1.4.13. Leistad P.O., Kongsjorden H., Kulsetas J. 1984 [26] developed a simulation model for prediction of the arcing behaviour of high voltage (12 kV and 36 kV) fuses. This simulation is based on the Daalder-Schreus model, with minor modifications, mainly in the values and dependence of the constants. The comparison between the experimental results and calculations is reasonable. The simulation program is interactive allowing the specification of the circuit and fuse construction characteristic data to be specified by the user. The results of the simulation are given in graphic form.

1.4.14. Hibner J. 1986 [27] proposed equations to enable calculations of the peak value of the arc voltage in filled fuses. The formula is applicable to low voltage DIN-type wire fuse elements in a.c. or d.c. circuits, provided that the current density and circuit trapped energy exceed specified values. The fulgurite striation and unduloid structures are discussed.

1.4.15. Masayuki Okazaki, Tsuginori Inaba 1987 [28] proposed the high voltage fuse arc as a electric circuit composed of resistances and voltage sources. The resistances are considered as having two parts, a central and a peripheral one, where the voltage sources are functions of arc energy and time. The model constant parameters were determined by trial and error method. The reported experimental results for 20 kV and 36 kV notched fuses agree very well with the calculated values using the model.

1.4.16. Sloot J., et all 1990 [29] proposed a two dimensional numerical model which describes the dynamic burn back processes in fuse elements over a wide range of current densities. The analysis indicates that the heat loss by conduction in the silver and to the filler has a delaying influence on the burn back velocity. For current densities above 4 kA/mm<sup>2</sup> the model predicts an exponential increase in the burn back velocity, where multiple arc is dominant.

1.4.17. Barrow D. 1988 [30] advanced a summary of previous arcing research together with his explanations of the processes occurring during arcing. One hypothesis examined is that a chemical reaction takes place within the fuse during arcing. This was investigated using fulgurite wet analysis, electron spectroscopy, calorimetric test, mass spectrometry and gas collecting. The conclusion was that no net chemical change happens.

The physics of the arc phenomena was studied by scanning electron microscopy and arc spectroscopy. Burn-back was investigated using optical fibers and thermal expansion measurements. The fulgurite surface and arc electron temperatures were determined as 2523 K° and 7000 K°. Arc wandering and air emission were observed.

A model for the burn-back process based on the energy balance between the input and that required for melting and vaporization is presented. Reasonable correlation with experiments is obtained.

1.4.18. Eger D., Rother W. 1989 [31] presented a model for high voltage fuse arc simulation based on a set of equations for the axial electric field, burn-back rates and electrode fall voltage. Some of the equation constants were experimentally determined. The model was applied to circular cross-section constricted fuse elements. The energy and time constant have to be used in the equation describing the arc cross section enlargement.

1.4.19. Petit A., St-Jean, G., Fecteau G. 1989 [32] proposed an empirical arc model for current-limiting fuses. The various stages of fuse operation are modelled using equivalent circuit R, C components. The circuit is solved by the application of the Electromagnetic Transient Program (EMTP). The model is limited in application but its simplicity enables a non expert to use it. As a tool it is valuable to designers/users since the influence of the voltage-time profile (rise time, peak value and tail wave form) on the fault energy can be easily demonstrated. The comparison between the calculated and experimental values are reasonable.

1.4.20. Shang Zhenqiu, Yang Yuaniong 1989 [33] reported on a study of d.c. arcs in a quartz sand fuse based on the mathematical model developed by Mayr. It was reported that the arc time constant changes during the arcing period; it being a function of fuse element diameter and current. From the comparison between experimental and analytical results it is concluded that the arc could be considered to be in steady state, and that the arc inertia could be neglected.

1.4.21. Wilkins R. 1991 [34] proposed a dynamic model to explain the commutation of arcing current between parallel elements at low and high currents. The results show good agreement despite being a very simple model. It is concluded that much of experimental data and in-depth research on logic and programming is still necessary.

1.4.22. Xie Yunxiang 1991 [35] described a mathematical model for the arc phenomena. The results using this model to calculate the arcing process provide good agreement with their presented experiments results. The basic characteristics of the anode, cathode and arc column behaviour during the arc process are analyzed. The structure of the model is the same as Wright's model, the main difference is that the mathematical approach involves solution of twelve simultaneous equations.

1.4.23 Wilkins 1991 [36] described a number of extensions and improvements to the modelling of short-circuit tests on current-limiting fuses. Some of these improvements are concerned with the physical models (burn-back, fillers flow properties and the representation of the fuse body inner diameter) whilst others are concerned with the numerical methods required to obtain fast and accurate solutions. Some typical results are given and the need for improvements to the test plant model is discussed.

1.4.24. Bizjak M., Zunko P., Poberaj S. 1991 [37] analysed an electro-chemical model of current-carrying silver elements in silica filler by applying thermodynamic laws. The model is applicable for the simulation of arcs burning in a narrow quartz channel, as in

HBC fuses under short circuit conditions. The arc plasma is considered as an ideal gas of neutral and partially ionized elementary particles, coming from the channel wall ablation (quartz sand) . The result of the modelling is a set of graphs of voltage gradients as functions of current density for several channel thicknesses and pressures. The main conclusion of the study is that for normal arc channels, considered up to 1 mm in thickness and pressures not greater than  $10E6$  Pa, heat conductive losses prevail over radiative, hence radiative losses could be neglected in the study. Graphs of thermal conductivity, electrical conductivity and radiation intensity as well as temperature and pressure functions are given.

1.4.25. Onuphrienko Yu I. Rzhewsky A. N. 1991 [38] proposed a fuse model based on thermodynamic laws, using classical equations and assumptions. It is concluded that the plasma could be considered as a silicon-oxygen one and that the time constant is so low that a static model may be used. The model is applied to the simulation of a semiconductor aluminum fuse - thyristor combination. No comparison between experiments and the modelling is given. The model was used for the design of a fuse available in the market place.

1.4.26. Xie Yunxiang, Wan Jimei 1992 [39] proposed a mathematical model for the arcing process under short circuit conditions. A set of equations are given, which follow the same structure as Wright's. The comparison claimed between experimental and analytical results is very good but as with Wright's model they are difficult to replicate and extremely complex to use.

1.4.27 Lipski T. 1993 [40] proposed an improvement to Daalder-Shreurs arc model. The presented results are difficult to assess.

## 1.5 Assessment of Principal Arc Research Work

Fuse arc models fall into one of three main groups i.e. those based on:

arc physic, electric equivalent circuit (voltage and current) and hybrids of the arc physics and electric equivalent circuit

### 1.5.1 Arc Physic models

#### 1.5.1.1 The Wright model

This model is based on relations and equations derived from in-depth physical representation of the arc plasma phenomena. The model has been slightly modified by other researchers.

The most important feature claimed for the model is that they are applicable to the short-circuit behaviour of notched fuse elements, where under the short circuit conditions, the available time is very short. The element material is considered to be at boiling temperature and that vaporization will occur throughout the whole of each notch. It is considered that the arcs would be of the same length and equal to the notch length. When the first gap across the notch appears, the vapour would not be fully ionized and a small capacitance would be present. The voltage across the capacitance would rise quickly and breakdown will take place. It is estimated that the voltage breakdown value is approximately 17 V. At this voltage level the arc is initiated, due to the voltage gradient value which is enough to enable electrons to escape from the cathodes. After that the gaps will increase their length by vaporization due to Joule heating.

For the study the arc is divided in three regions: the cathode fall region, anode fall region and the positive column.

The cathode fall region is very small, 0.001 mm in length, being the transition between liquid or solid and metal vapour. The voltage drop was assumed as 10 V.

The anode fall region is of the same length as cathode region, and its voltage drop is 7.56 V, based on the silver ionization potential.

The positive column exists between the anode and cathode regions and its electrical charge is considered neutral. Non uniformity is neglected, assuming that the conductivity and the cross-section are constants throughout its length.

The length of the positive column is obtained from the power balance, between inputs and losses. Based on the anode and cathode burn-back rate being equal the available power for vaporizing the electrodes is given by:

$$Power = (V_{af} + V_{wf} + V_T) \times i$$

As is well known only a fraction of the fuse element material is vaporized during the arcing process, however the fraction is complex to determine. In order to assess the vaporized proportion several high current tests were conducted and the fulgurite analyzed using X-ray technique.

The relation used for the energy provided for melting and vaporizing are:

$$E_{MV} = 2 \times (V_{af} + V_{wf} + V_T) \int_0^{t_a} i dt$$

$$E_{MV} = m_i + m_v + m_i \times (melt .temp. - 200) \times spec.heat$$

It was experimentally determined that the vaporized proportion was only 40% of the mass which was melted, and that the latent heat of fusion of the total mass melted represented 20 % of the total energy entering the electrode. This latter mass is determined from the solution of the following equations.

$$\begin{aligned}
l_2 - l_1 / \delta_t &= \\
&= 2 \times (V_{af} + V_{wf} + V_T) \times \left( \frac{i_1 - i_2}{2} \right) \times \left( \frac{0.2}{L_f} \right) \times \\
&\times \left( \frac{1}{A_e \times \text{elect. density}} \right)
\end{aligned}$$

In any small interval of time the energy given to the column is:

$$E_c = \frac{1}{2} \times (V_{c1} \times i_1 + V_{c2} \times i_2) \times \delta_t$$

It is assumed that the power given to the column is dissipated to the surrounding filler, which will melt back. Considering that 2100 J are required to produce a gram of molten quartz, the volume of the liquid quartz is 64% of the original, due to the random packing of 60% and 7% of volume increase when melted.

The total volume increase in a time interval is:

$$vol_{c2} - vol_{c1} = \left\{ k \times (V_{c1} i_1 + V_{c2} i_2) \times \delta_t + 2(l_2 - l_1) \times A_e \right\}$$

where:

$$k = \frac{(1 - 0.64)}{(2 \times 2100 \times 1.6 \times 10^6)}$$

After the breaking of a large current, there is a big cavity in the fuse filler, where notched existed. It was considered that the positive column is of constant cross-section.

The column area is therefore:

$$A_{c2} = \frac{vol_{c2}}{l_{c2}}$$

The authors conducted a number of tests and it was established that vapour jets were present. The jets, between the electrodes, collide and create turbulence which in turn cause the temperature and electron densities within the column to be relatively uniform.

Over a time interval, a number of atoms of the vaporized electrode material are accelerated into a column in the jets and a fraction ( X ) of them become ionized.

During this time the same number of atoms and ions are assumed to be scattered out of the column, in order to keep the pressure and conductivity near the experimentally values obtained from voltage and current traces.

The following equations were assumed to apply:

$$N_d = N_a$$

$$\text{and } N_e = X N_a$$

It was further assumed that the positive column loses energy in the following main ways:

- Kinetic energy of atoms and ions, scattered out of the column, is dissipated in the surrounding filler, given by;

$$K E_{ai} = 1.5 \times N_d \times K_B \times \left( T_1 + T_2 / 2 \right)$$

where  $K_B$  is Boltzmann's constant.

- Kinetic energy of electrons scattered out of the column

$$K E_{ei} = 1.5 \times N_e \times K_B \times \left( T_1 + T_2 / 2 \right)$$

- Energy required to ionize Ne atoms taken out of the column and given to the filler.

$$I E = N_e \times E_J$$

- Energy lost by radiation to the surroundings of the column, based upon black-body radiation.

$$R E = \text{surf. area of column} \times K_s \times \left( \frac{T_1 + T_2}{2} \right)^4$$

Assuming the column is to be cylindrical, the following energy balance equation may be formed.

$$\left( V_{c1} \times i_1 + V_{c2} \times i_2 / 2 \right) \times \delta_i = K E_{ai} + K E_e + IE + RE$$

Saha's equation is applicable because of the many collisions that the atoms/electrons will experience. It is assumed that the temperature of atoms and electrons will be the same at any time, hence;

$$n_{e2} = \left( 1 - X_2 / X_2 \right) \times \text{antilog} \left\{ -3.878 \times 10^4 / T_2 + 1.5 \text{Log } T_2 + 15.385 \right\}$$

The atomic and electron densities are:

$$V_a = A_e v_J \delta_i$$

$$n_{a2} = N_a / (A_e \times v_J \times \delta_i)$$

$$n_{e2} = (N_a \times X) / (A_e \times v_J \times \delta_i)$$

At ionization levels of more than 0.01% Spitzer's [41] conductivity equation is valid:

$$\sigma_2 = \left\{ \frac{\left( 1.55 \times 10^{-2} \times T_2^{3/2} \right)}{\log \left( 1.242 \times 10^4 \times T_2^{3/2} / n_{e2}^{0.5} \right)} \right\}$$

The jet velocity is one of the unknown values, therefore it was approximated using experimental results. However, due to the small influence in the column conductivity, an average value was adopted despite the scattering of the results.

The electric circuit equation is given as:

$$V_s = i \times (R_c \times n + R_s) + \frac{d(L_s \times i)}{dt} + (V_{af} + V_{cf}) \times n$$

The overall model therefore results in a set of 10 simultaneous equations in 10 unknowns, which are capable of being solved by computer.

The initial values were obtained from the end of the prearcing study, considering that the arc initiation occurs when the vaporization starts.

The main problem was the value of the voltage along the column. From experiments it was observed that always the voltage changes abruptly from a small prearcing value to about 50 V. The column value associated with this one is 33 V obtained by the subtraction of the 17 V associated with the anode/cathode fall minimum value previously referred to.

#### 1.5.1.2 Merits and limitations of the Wright Model

##### Merits:

The claimed agreement achieved between computed and experimentally obtained results is very good. The model permits average values of pressure, arc temperature, electrical conductivity and lumen cross-section/length to be computed from the fuse materials and dimensions, together with the voltage and current traces.

##### Limitations:

The model is difficult to apply, requiring a deep knowledge of arc physics and the user must be able to determine many coefficients and solve a system of ten equation in ten unknowns. The mechanism used for the arc initiation is based on the assumption that only one arc burns in each notch. The model also neglects the effects due to any change in filler properties. The assumption that the anode and cathode voltage drops are constant values is highly simplistic based on classical experimental observations.

## 1.5.2 Arc voltage - current electrical equivalent circuit models

### 1.5.2.1 The Dolegowski Model

The basic idea of this group of models is based on the empirical determination of equivalent electric circuit arc parameters to produce arc voltage versus current wave forms. The proposed relations and equations, results in many constants to be determined which need to be validated by extensive experimental work. The ideas based on this approach were initiated and developed by Dolegowski. Other researchers have extended the model.

The principal characteristics of this model are:

The study is applicable to the simulation of the arcing phenomena behaviour of high breaking capacity fuses under short circuit current conditions.

For a single arc of length  $x$ , the arc voltage is:

$$u_a = u_b + \int_0^x E dx = u_b + \int_0^x \left( E \cdot \frac{dx}{dt} \right) dt$$

Heat from the arc at its roots causes the element to burn back  $\left( \frac{dx}{dt} \right)$ , increasing the length  $x$ . From experimental studies, the burn back rate for silver elements is given by:

$$\frac{dx}{dt} = (a + b \times i^{0.6}) \times \frac{i}{S}$$

where  $a$  and  $b$  are experimental constants. The burn back rate depends only on the instantaneous value of the current.

Several authors, Fraser [42], Maecker [43] and Wheeler [44], determined that the voltage gradient is proportional to  $i^{0.4}$ .

The governing equation could be termed "quasi-static", because it is considered that the arc 'time constant' is negligible. In other words the stored energy in the arc column is neglected, but the  $E / i$  characteristics shift dynamically as the lumen area changes according to:

$$E = k \times i^{0.4} / A^\gamma$$

where  $k$  and  $\gamma$  are empirical values.

If the volume of silica melted per unit axial length is  $v_1$  then:

$$dv_1/dt = E \times i / (\rho_f \times (C_f \times \Delta T + L_f))$$

As the melting of a volume of silica causes an increase in lumen area, then:

$$dA/dt = \alpha \times \left( E \times i / (\rho_f \times (C_f \times \Delta T + L_f)) \right)$$

Experiments with constant arc length indicate that:

$$\alpha = \alpha_0 + (\alpha_m - \alpha_0) \times (1 - e^{-t/\tau})$$

$\alpha_0, \alpha_m, \tau$  are empirical constants.

Several authors have developed empirical formulae for  $u_b$ , which indicated that the anode-cathode voltage drop increases with the current. Based on the fact that there is a sudden voltage drop when two arcs coalesce the following relation was determined:

$$u_b = 15 + 1.0 \times i^{0.39}$$

The initial values following Hibner's equations were applied to give:

$$E_0 = 0.4 \times \sqrt{i_0 / S_0}$$

The rise in voltage to  $u_0$  does not occur instantaneously. Arai's formula was used to determine the time delay from molten to disruption states as:

$$t_d = 0.27 \times S_0 / i_0$$

This value of time is very small ( $\cong 40 \mu s$ ) compared with the arcing time, so its effect, being only marginal, is neglected [24].

The initial value for the lumen area was assumed, given that the element has a large cross-section in comparison with the quartz grain size. If the condition does not apply, an empirical value  $S'$  is used.

In a practical fuselink there are usually several series notches per element. If arcing persists for a sufficient length of time the series arcs will coalesce into a single arc. The effect can be taken into account by the model.

The state variables representing the arcing process are described as:

$$di/dt = (u(t) - R \times i - u_f) / L$$

$$dx/dt = \left\{ a + b \times \left( \frac{i}{n_p} \right)^{0.6} \right\} \times i / (n_p \times s)$$

$$\frac{d A_j}{dt} = \left\{ \alpha_0 + (\alpha_m - \alpha_0) \times (1 - e^{-t/\tau}) \right\} \times$$

$$\times \frac{E_j \times \left( \frac{i}{n_p} \right)}{\left( \rho_f \times (C_f \times \Delta T + L_f) \right)}$$

$$j = 1, \dots, k$$

A simulation program is used to solve the differential equations using a 4th-order Runge-Kutta method. The initial values for the current and voltage result from a prearcing simulation using finite difference or finite element methodologies.

#### 1.5.2.2 Merits and limitations

Merits:

The arc voltage and current experimental and computed wave forms bear a striking resemblance. The model allows the investigation of the effect of varying test parameters such as frequency, power factor, making angle, test voltage, etc. The model provides the possibility of simulating short circuit faults in circuits with nonstandard wave forms as in power converters and conditions difficult to reproduce in test stations.

It is claimed that the application of this model can be easily performed by fuse designers with a reasonable knowledge of arc physics. The mathematics is not too complex either for the normal user.

Limitations:

The great number of empirical coefficients presents difficulties for application of this model to conditions different from those used for the determination of the parameters. The constants used in the model change with the filler (material, size and porosity) and type of notch (deep or shallow, square, triangle or circular, etc.). The initial conditions

are also determined in an artificial way. As with the previous case, the model assumes only one arc occurs in constrictions.

### 1.5.3 Hybrid arc models

#### 1.5.3.1 The Daalder Model

Daalder's model enables the coupling of the basic variables of arc plasma and filler material and equivalent circuit using empirical relations for the arc voltage and current. The idea was first pursued by Leistad et al [26] and slightly modified by Jakubiuk and Lipski [40].

The main idea is that the arc voltage can be calculated by the equation:

$$U_{arc} = u_b + \int_0^l E \times dx = u_b + \int_0^l (\rho \times i / A) \times dx$$

where E is the column gradient and  $\rho$  is the specific resistance of arc plasma, i the current and A the arc channel cross-section.

The solution of the equation is complex because the arc plasma length, resistivity and cross-section vary with the current, position and time. The chosen approach was to keep the current constant and to study the behaviour of the other parameters as functions of time. In this way the coupling between the different variables could be established.

It is assumed that the arc burns within an enclosed wall of molten and granular sand, referred to as a wall-stabilized arc. The arc channel increases by erosion of the fuse element and by melting of silica. As this process takes milliseconds while the arc thermal time constant is in the order of microseconds, the arc process is considered to be a quasi-static one. From experimental results of several authors it has been determined that the voltage-current characteristic has a positive gradient and that the arc is burning in a fully ionized silica plasma [43].

The analysis follows:

a- Voltage gradient:

The stationary power balance of a flat arc having a rectangular cross section is given by:

$$-div(\lambda \times grad.T) = G \times E^2$$

Applying Lorentz gas law and Spitzer's formulas gives:

$$\lambda = \lambda_0 \times T^{2.5}$$

$$G = G_0 \times T^{\frac{1}{2}}$$

Which in a semi-numerically form results in:

$$E = p \times \frac{(\lambda_0^{0.3} \times i^{0.4})}{(G_0^{0.7} \times b^{0.4} \times D)}$$

where p is a numerical constant, and the values of  $\lambda_0, G_0$  are given by Spitzer's relations.

$$\lambda_0 = \frac{\alpha}{(Z \times \ln. \Lambda)}$$

$$G_0 = \frac{\beta}{(Z \times \ln. \Lambda)}$$

Here Z is the ion charge and  $\Lambda$  is the Coulomb cut-off. Using Spitzer's values for the constants results:

$$E = q \times (Z \times \ln. \Lambda)^{0.4} \times \left( \frac{i^{0.4}}{(b^{0.4} \times D)} \right)$$

Which for flat arc becomes:

$$E = 5.65 \times 10^{-2} \times \left( \frac{i^{0.4}}{(b^{0.4} \times D)} \right)$$

An extensive series of experiments are necessary to determine the constants, based on the constant current methodology.

b- Burn-back rate:

The next step is to determine the burn-back rate, using probe methodology.

The experimental results showed that the burn-back rate is proportional to the current density. Daalder and Hartings [45] demonstrated that the erosion is mainly due to local electrode effects, from which the following formula was derived:

$$V_{th} = U_{con} \times J / H$$

$$H = C_s \times \rho_s \times (T_m - T_b) + L \times \rho_s + C_1 \times \rho_s \times (T_d - T_m)$$

The value of  $T_d$  was experimentally assessed as 1700 K for silver.

The proposed equation for burn-back rate results:

$$V_{th} = C \times J$$

$$C = U_{con} / H$$

Were the C is 1.06 E-09 for copper and 1.03 E-09 for silver.

c- Arc channel expansion:

For the calculation of the arc-voltage the change in arc channel dimensions as a function of time must be determined.

From experiments it is concluded that the variation of the thickness  $D$  was the most significant effect in determining lumen growth, and that the channel growth could be analyzed using a one-dimensional model.

The energy balance between the input and the value necessary to increase the sand filler from room temperature to a value greater than the melting one is:

$$E(x,t) \times i \times \Delta x \times dt = H \times d v_s$$

Given that the sand is molten, its volume will be:

$$d v_1 = \left( \frac{\rho_s}{\rho_l} \right) \times d v_s$$

The increase of the lumen volume  $d v$  is:

$$d v = d v_s - d v_1 = d v_s \times \left( 1 - \frac{\rho_s}{\rho_l} \right)$$

The maximum volume will be attained if the molten silica is entirely removed from its volume,  $d v = d v_s$ , as this extension is not known a factor is introduced.

$$d v = \gamma \times \left( 1 - \frac{\rho_s}{\rho_l} \right) \times d v_s$$

where:

$$1 \leq \gamma \leq \left( \frac{\rho_l}{\rho_l - \rho_s} \right)$$

Combining all the equations results in:

$$E(x,t) \times i \times dt = \frac{(H \times 2b \times dD)}{\left( \gamma \times \left( 1 - \frac{\rho_s}{\rho_1} \right) \right)}$$

$$dD/dt = \frac{\left( E(x,t) i \gamma \left( 1 - \frac{\rho_s}{\rho_1} \right) \right)}{(H2b)}$$

The solution of which is :

$$D = \sqrt{\left( (D_0)^2 + B \times t \right)}$$

where:

$$B = \frac{q [z \ln \Lambda]^{0.4} i^{1.4} \gamma \left( 1 - \frac{\rho_s}{\rho_1} \right)}{(b^{1.4} H)}$$

The solution of the equations were evaluated experimentally, which resulted in reasonable agreement.

An in-depth study of the arc voltage wave form during notch disintegration was undertaken. During the prearcing phenomena the voltage is small and essentially constant. Just before disruption the voltage increases a few volts due to the increased resistance caused by Joule heating.

It is assumed that disruption takes place in a very short time after the melting temperature is reached. In 0.5  $\mu$ s a voltage rise occurs. The value obtained ranges from 9 to 33 V after which a further increase of voltage occurs due to the burn-back. This occur at high speed because the arc is still in the notch, but is followed by a lower speed burn-back. No voltage drop was measured when two series arcs merged.

### 1.5.3.2 Merits and limitations

Merits: The agreement between the experiments and the computed values are very good. The arc physics is related to the circuit parameters, which is meaningful for the designer and fuse user. Fuse element material, quartz sand and general dimensions could be changed and their influence assessed.

Limitations: The mathematical solution is very complex and the equations must be solved using a second order Runge-Kutta method. There are two main constant parameters (D' and B) to be determined by experiments, which may produce considerable discrepancy. It has been proposed that the channel expansion rate and initial thickness may be time dependent. The model assumes only a single arc burns in each constriction, and also neglects the effects of any change in filler properties.

## 1.6 Unknown Arc Phenomena in Fuses

### 1.6.1 Fundamental Issues

The unknown behaviour of arc phenomena in high breaking capacity fuses are still fundamental ones as given hereon:

- Arc disruption phenomena
- Arc mechanism during the early arcing, a few microseconds after disruption.
- Arc mechanism producing current limiting.
- Arc mechanism producing current interruption
- The sudden jump phenomena in the arc voltage during disruption is not clear.

- Influence of the filler material, grain size, compaction, hardness, etc. on arc mechanisms.

### 1.6.2 Development of Author's Research of Arc Mechanisms

The original aim of the study was to use finite element (FE) CAD techniques to analyse the hybrid arc model and evaluate the equation constants from experiments. The FE modelling involved adjusting the mesh size of the model to represent the growth of the positive column and the element burn-back rate. This rate required a long series of tests and the complexity of the geometry necessitated wires (axi-symmetric geometries) were the best to evaluate first.

The initial experimental results of wire break-up were confusing and some observations of short and long arcs were new to the author. The study thereon shifted to understanding the basic arc mechanism by further experiment which led to a change in the direction of the fuse research towards studying the modelling of fundamental arc mechanisms of HBC fuses.

## 1.7 References

1. Edison, T.A.; United State Patent n° 227226, May 4th, 1880.
2. Sir W. H. Preece; On the Heating Effects of Electric Currents; Proceedings of Royal Society, Vol. 36, pp. 464-471, 1884.
3. Hofmann, M. Lindmayer, M.; Pre-calculation of time/current characteristics of "M"-effect fuse elements; Third Int. Conf. on Elec. Fuses and their App.; pp. 30-38, Eindhoven, 1987.
4. Gomez, J.C. McEwan, P. M.; Determination of the time/current characteristic of fuses using Finite Element methodology; Sixth Int. Conf. on Swit. arc Phen.; pp. 194-197, Lodz, 1989.
5. Gomez, J.C. et al; Investigation of the pre-arcing behaviour of dissimilar uniform double-elemented filled fuses, using FE CAD techniques; Fourth Int. Conf. on Elec. Fuses and their App.; pp. 65-67, Nottingham, 1991.
6. Leach, J.G. et al; Analysis of high-rupturing-capacity fuselink prearcing phenomena by a finite-difference method; Proc. IEE, vol. 120, n° 9, pp. 987-993, 1973.

7. Wilkins, R. McEwan, P. M.; A.C. short-circuit performance of notched fuse elements; Proc. IEE, vol. 122, n° 3, pp.289-292, March 1975.
8. de Cogan, D. Henini, M.; TLM modelling of thin film fuses on silica and alumina; Third Int. Conf. on Elec. Fuses and their App.; pp. 12-17, Eindhoven, 1987.
9. Nairne, E.; Electrical Experiments by Mr. Edward Nairne; Phil. Trans. Royal Soc., vol. LXIV, pp. 79-89, London, 1774.
10. Mayr, G.J.; Zur Theorie der Abschmelzsicherung, (On the theory of Fuses); Munchen, 1906.
11. Läpple, H.; Electric Fuses, A critical review of published information; Butterworths, London, 1952.
12. Baxter H.W.; Electric Fuses; Edward Arnold, London, 1950.
13. Electric Research Association; Digests of information on protective devices; Turner, H. and Turner, C.; Surrey, 1976-1993.
14. Kroemer, H.; Der Lichtbogen an Schmelzleitern in sand, (The arc in Elements Fusing in Sand); Archiv fur Elektrotechnik; Heft 8, Band 36, pp.455-470, 1942.
15. Voshall, R.E. ; Investigation of the positive column of high-current metal-vapor arcs; IEEE Trans. on PAS, vol. pas-88, n° 2, pp. 120-126, February 1969.
16. Schonholzer, E.T.; Fuse protection for power thyristors, IEEE Trans. on IA, vol. ia-8, n° 3, pp. 301-309, May/June 1972.
17. Hirose, A.; Mathematical analysis of breaking performance of current-limiting fuses; First Int. Conf. on Elec. Fuses and their App.; pp.182-191, Liverpool, 1976.
18. Dolegowski, M.; Calculation of the course of the current and voltage of a current-limiting fuse; First Int. Conf. on Elec. Fuses and their App.; pp.218-232, Liverpool, 1976.
19. Wright, A. Beaumont, K.J.; Analysis of high-breaking-capacity fuselink arcing phenomena; Proc. IEE, vol. 123, n° 3, pp. 252-258, March 1976.
20. Oliver, R.; The behaviour of d.c. overcurrent arcs in cartridge fuselinks; First Int. Conf. on Elec. Fuses and their App.; pp. 101-109, Liverpool, 1976.
21. Oliver, R.; The elementary structure of the cartridge fuse arc; Third Int. Conf. on Swit. Arc Phen., pp. 310-314, Lodz, 1977.
22. Wilkins, R.; Semiempirical models of arcing in current-limiting fuses; Third. Int. Conf. on Swit. Arc Phen., pp. 338-342, Lodz, 1977.
23. Ranjan, R. Barrault, M.R.; Axial electric-field measurements of d.c. arcs in current-limiting fuses; IEE Proc., vol. 127, Pt. C, n° 3, pp. 199-202, May 1980.
24. Gnanalingam, S. Wilkins, R.; Digital simulation of fuse breaking tests; IEE Proc., vol. 127, Pt. C, n° 6, pp. 434-440, November 1980.
25. Daalder, J.E. Schreurs, E.F.; Arcing Phenomena in High Voltage Fuses; EUT Report 83-E-137, Eindhoven University of Technology the Netherlands, March 1983.
26. Leistad, P.O. et al; Simulation of short circuit testing of high voltage fuses; Second Int. Conf. on Elec. Fuses and their App.; pp. 220-226, Trondheim, 1984.
27. Hibner, J.; Berechnung des Scheitelwertes von Überspannungen beim Ansprechen von Niederspannungs-Schmelzsicherungen mit Draht-Schmelzleitern; Intern. Wiss. Koll.; pp.133-136, TH Ilmenau 1986.
28. Masayuki Okazaki Tsuginori Inaba; Development of a simulation method for operation of current limiting fuse and confirmation of its effectiveness; Elect. Eng. in Japan; vol. 107, n° 3, pp. 21-29, 1987.
29. Sloom, J. et al; A two dimensional mathematical model for the dynamical burn-back velocity of silver strips; 1990.
30. Barrow, D.; Evaluation of arcing parameters in High Breaking Capacity Fuses; PhD Thesis, Nottingham University, October 1988.

31. Eger, D. Rother, W.; A mathematical model for the arcing period of high-voltage fuses; ICECAAA, pp. 51-55, Xi'an, May 1989.
32. Petit A. et al; Empirical model of a current-limiting fuse using EMTP; IEEE Trans. on PD, vol. 4, n° 1, pp.335-341, January 1989.
33. Shang Zhenqiu Yang Yuaniong; Study on the characteristic of the arc in quartz sand by means of Mayr's mathematical model of arc; ICECAAA, pp.129-132, Xi'an, May 1989.
34. Wilkins, R.; Commutation of arcs between parallel fuse elements; Sixth Int. Conf. on Swit. Arc Phen.; pp. 237-241, Lodz, 1989.
35. Xie Yunxiang; The computer analysis of breaking current process in sand filler fuses; Fourth Int. Conf. on Elec. Fuses and their App.; pp. 173-177, Nottingham, 1991.
36. Wilkins, R. et al; Developments in the modelling of fuse breaking tests; Fourth Int. Conf. on Elec. Fuses and their App.; pp. 211-215, Nottingham, 1991.
37. Bizjak, M. et al; Characteristics of Arc in Melting Fuse Element filled with Quartz Sand; 6th. Medit. Elec.Conf. IEEE, pp.1493-1496, Ljubljana, 1991.
38. Onuphrienko, Yu.I. Rzhewsky; Investigation of electric arc properties in sand-filled fuses; Sixth Int. Conf. on Swit. Arc Phen.; pp. 255-258, Lodz, 1989.
39. Xie Yunxiang Wang Jimei; Mathematical Model for Arcing Process of fuses; Proc. CSEE, vol. 12, n° 1, pp.27-33, January 1992.
40. Jakubiuk, K. Lipski, T.; Improvement of Daalder's arc model for H.B.C. fuses; Seventh Int. Conf. on Swit. Arc Phen.; pp.215-219, Lodz, 1993.
41. Spitzer, L.; Physics of fully ionized gases, Interscience Publishers, New York, 1956.
42. Fraser, S. G.; Extinguishing an arc; in HAYDAN, S.C. (Ed.); An Introduction to Discharge and Plasma Physics; (The University of New England, Armidale, Australia, 1964), chap. 23.
43. Maecker, H.; Theory of thermal plasma and application to observed phenomena; *ibid.*, chap. 18.
44. Wheeler, C. B.; The high-power constricted plasma discharge column, I. Theoretical Analysis; Journal Physics, Part D, Vol. 3, pp.1374-1380, 1970.
45. Daalder, J.E. Hartings, R.M.; The burn-back rate of high voltage fuses; Fourth Int. Conf. on Swit. Arc Phen.; part 2, pp.158-164, Lodz, 1981.
46. Lipski, T.; On the theory of the striated fuse-wire disintegration; IEEE Transactions on Plasma Science, Vol. PS-10, n°4, pp.339-344, December 1982.
47. Hibner, J.; Calculation of the arc-ignition voltage on single disruption of uniform fuse-elements by its independent disintegration in h.b.c. fuses; Fifth Int. Conf. on Swit. Arc Phen.; pp. 368-371, Lodz, 1985.

## Chapter 2 : Basic Arc Mechanisms

### 2.1 Basic arc mechanisms in wires immersed in fillers

The first reported observation of wire disintegration as a mechanism was made a long time ago by Nairne[1]. The author was studying, among other things, the safest way of discharging accumulators using different wires to short batteries. He observed that the melted wires formed into structures very similar to a string of pearls.

Later research by Kleen, appeared in 1931 [2], which described the processes and phenomena that occur when thin wires are suddenly vaporized by electric current surges, generally produced by capacitor discharges. Four different processes are shown, according to the energy levels. The formation of the pearls called "unduloids" is explained and discussed for copper, silver, platinum and gold wires. An analytical explanation of the phenomena is shown. The computed module (the ratio of the distance between two successive balls in reference to the wire diameter) for silver was 2.67 compared with the experimental value of 2.31. Baxter explained this phenomena [3] based on the surface tension and magnetic pinch pressure, which produce melted fuse element deformation into a number of globules. Carne [4] studied the same process using Rayleigh conditions, obtaining a very similar figure, 2.26 for the disintegration module.

Two structures referred to as unduloids and striation were identified. The difference between them was due to the formation of the necks and swelling during the fuse element liquid state. The fulgurite under both conditions is very similar, the only discrepancy being the increased regularity of the black and white rings in the case of striated disintegration.

Several equations for the disintegration module were proposed [5], the most consistent being:

$$h = 16/3 d \text{ for unduloids}$$

$$h = 0.555 + 2.08 d \text{ for striation}$$

where h and d are module and diameter in mm.

For fuse elements immersed in quartz sand, the grain size and shape have some influence on the module. The effect is greatest when the grain size is of the same order as that of the fuse element diameter or thickness.

Vermij [6] determined a threshold current density value of 8 kA/mm<sup>2</sup>, where lower values generate unduloids and higher values produce striations.

Ossowicki [7] identified five types of disintegration depending on the current and wire hardness, namely: single arc, chaotic, drop or unduloid, mixed and striated disintegration.

Much effort was devoted to the study of the fuse element disintegration and why unduloid and striations occur. Some of the explanations simply related unduloid formation to the wire hardness (obtaining the same behaviour when heating wire using a gas torch[8]). Some explanations were very complex, being based on the magneto-thermal-viscous-elastic mechanism [9]. Others considered that the outer oxide layer has a decisive influence on module formation.[10, 11]. No clear explanation of the melting mechanism in wires has been established, however, to date.

Analyses suggests that metal between globules is superheated liquid which changes state to vapour at very high temperature (around 7000 °K) at which the vapour is more or less thermally ionized and conductive. Short discharges then take place, comprising the anode and cathode voltage drop, which together with the positive column voltage comprise the arc fuse voltage.

Many values were proposed for the anode/cathode voltage drop per arc, termed the arc ignition voltage. The values ranged between 20 V and 200V. The more realistic and justified values were between 25 and 40V. [12, 13, 14]

During the same period, other researchers were investigating the relationship between the overvoltage peak and the current density, length and diameter of the fuse element, separate to consideration of the disintegration phenomena [3, 15]. These workers determined that the peak voltage value increases with the current and the fuse element length and inversely with the element diameter.

Several assumptions were made in order to explain the observed phenomena, for example:

- the number of arcs were assumed as a constant during the arcing time
- arc ignition will appear at all the constrictions simultaneously
- one arc ignites in each constriction, which extend by electrode burning.

Several equations were developed for the maximum voltage value, using constants which were determined by tests. These formulae were applicable to wire, strip, multi-wire, multi-strip and notched strip fuse elements. The most well known equation is Hibner's [16, 17], viz :

$$U_p = k_1 \times l_z \times \sqrt{i_0 / S_z}$$

where:  $k_1$  is an experimental constant equal to 16 for wire and 12.5 for notched ribbon element,  $l_z$  is the fuse element length,  $i_0$  the peak current value and  $S_z$  is the constriction cross-section.

The relation assumes that:

- the restricted cross-section is less than 60% of the shoulder cross-section.
- the disintegration current density greater than  $2.4/d$ , with  $d$  = equivalent diameter.

The relation reduces to  $j \geq 4660 \times S^{-0.29}$  where  $j$  is current density and  $S$  the fuse element cross-section.

- the magnetic field energy of the circuit per fuse element volume complies with the equation :

$$\frac{1}{2} L i_0^2 / v \geq 25$$

where: L is the circuit inductance,  $i_0$  the peak current and  $v$  the fuse element volume.

Lipski [18] later proposed an arc-pinch-force-interaction (APFI) theory to explain the striation modules, applicable for wire and strip fuse elements. Another approach was presented by Jakubiuk in 1991 [19] based on an electro-thermal fuse element disintegration mechanism.

Dolegowski [20] proposed that the arc burn-back rate is a function of the power density in the electrode zone, the temperature and fuse element physical properties. He also proposed the value for the ignition voltage (30-150 $\mu$ s after the arc start) from 11+/- 0.8 to 30+/-5V. Until this moment the authors considered that the arc ignited instantaneously.

Arai [21] proposed the relation given below for the time for element deformation following melting and prior to arc ignition.

$$t_d = k_2 \times \frac{S_z}{i_0}$$

Where  $k_2$  is a experimental constant equal to 0.27 A.s/mm<sup>2</sup> for silver,  $S_z$  notch cross section and  $i_0$  maximum instantaneous value of current.

This study of the unduloid/striation phenomena concluded that the unduloids appeared under moderate currents and for small diameter wires, whilst the striation (sharp squarish necks and swells) were observed under conditions of very high current density and very big diameter arises. It was suggested that for larger currents flowing through wires of larger diameter, the deformations are caused by pinch effect, whilst for moderate

currents and smaller diameter wires, the deformations are due both to pinch effect and surface tension.

It was suggested later that the voltage variation in time, based on extension of Hibner's equation [22] below, is related directly to the instantaneous current value instead of the maximum one. This equation did not give consistent results. Lipski [23] explained the difference for example between Arai's and Nasilowski's number of arcs (20:1) as being that not all the wire volume resulted in arcs. Hibner [24] suggested the possibility that more than one arc may ignite in each notch during its disintegration, especially if the notch is a long one.

$$U_a = k_1 \times I_z \times \sqrt{\frac{i}{S_z}} \quad \text{Hibner's equation.}$$

From the foregoing findings on fuse wire disintegration the following generalizations appear not to be in dispute:

- the disintegration time is inversely proportional to the current density at the end of the prearcing period.
- the fuse element disintegrates into a number of portions, the number of portions being functions of the energy trapped in the circuit inductance and of the fuse element volume.
- between the disintegrated portions a short arc is initially drawn, with a voltage value greater than 25 V and less than 40 V (including anode and cathode voltage drops plus positive column voltage), and finally,
- the arc or length of positive column increases as a function of the available energy.

## 2.2 Wall stabilised arc model applied to axi-symmetric arc problem

The proposed study of the arc behaviour has been based on the principle of conservation of energy and the energy loss mechanisms. It has however not been possible to study the simultaneous effects of convection, conduction and radiation loss. The complexity of the problem is such that theoretical analysis is only practicable on the basis of over-simplifying assumptions.

The most common approach is to consider the electric arc as a cylindrical high pressure arc column. Experiments on wires in filler supports that the arc burns in a tube. For these conditions, referred to as wall stabilised arcing, the arc column properties are determined by the thermal conduction loss to the walls so that the expression for the kinetic energy conservation conditions become relatively simple.

In order to obtain simpler expressions it may be assumed that the electrical conduction is uniform across the whole tube section. The arc column then can be assumed to be in a state of local thermal equilibrium (LTE) so that analysis of the column properties depends upon the solution of the normal macroscopic gas kinetic conservation laws applied to the boundary conditions.[25]

Oliver [26] studied the factors influencing the properties and structure of the fuse arc in filled fuses. His experimental results confirmed the fuse arc classification as a wall-stabilized arc, concluding that the axial electric field is inversely proportional to the lumen internal diameter. He found that the wall thickness and the hole size along the arc column are not constant, due to the filler exposed to the arc burning for times which differ, depending on the arc position relative to the electrode root at each time instant.

The fulgurite is relatively larger at the origin of the arc and tapers in both directions to the size of the fuse element. The electric field was found at the center of the arc to be lower than the values measured on the sloping sides of the fulgurite. It was proposed that the arc is confined by an effective stabilized wall after a finite time delay which depends of its length. It was also found [27] that the axial electric field is initially high until a silica molten wall is formed. Based on the previous considerations and neglecting the

anode/cathode falls ,the following arc model for the positive column is proposed: [28, 29]

The basic assumptions are:

- plasma is in thermodynamic equilibrium
- temperatures of light and heavy particles are the same
- all parts of the plasma volume are electrically neutral
- magnetic field effects are neglected
- electric conductivity due to diffusion and convection may be neglected
- electric current of ions is neglected due to their low mobility

The balance between power generation due to the voltage gradient E and power losses and consumption in motionless plasma at constant pressure is described by:

$$\rho \times C_p \times \frac{\partial T}{\partial t} = \text{div.}(K \text{ grad.} T) + \sigma \times E^2 - \varphi$$

where:  $\rho$  is density, T temperature, t time,  $C_p$  specific heat, K thermal conductivity, E voltage gradient,  $\sigma$  electrical conductivity and  $\varphi$  volumetric radiation intensity.

By considering the arc in fuses as plasma in a flat channel, in which the voltage gradient E is constant throughout the whole plasma volume, the equation can be reduced to a one dimensional model.

As the time constant is very small (a few microseconds), a quasistationary approximation of the previous equation can be applied for ac industrial frequency arcs, given by;

$$\frac{\partial}{\partial x} \left( K \times \frac{\partial T}{\partial x} \right) + \sigma \times E^2 - \varphi = 0$$

$$a \geq x \geq -a$$

Subject to the following boundary conditions:

- at channel walls  $x = \pm a$  and  $T = T_1$  (boiling temperature of quartz)
- in channel mid plane  $x = 0$ ,  $\frac{\partial T}{\partial x} = 0$

The equation can be solved numerically by simultaneous iterative approximations to determine the value of voltage gradient  $E$ .

Using this approach, Bizjak et al [29] obtained the numerical solution for various channel thickness (0.2, 0.4 and 1 mm) and pressures (10E5, 10E6 and 10E7 Pa). The power function was obtained from the voltage gradient - electric current characteristics, thus being 0.5 $\pm$ 0.1, which is very similar to the 0.4 value experimentally determined by previous researchers.

The simplest equation for a single arc including the anode and cathode voltage drops, is therefore:

$$V_a = V_{ak} + E \times x(t)$$

where  $V_{ak}$  is the anode and cathode voltage drop,  $E$  is the voltage gradient and  $x(t)$  is the variable column length.

## 2.3 Wall stabilized arc mechanism model

### 2.3.1 Experimental investigation

The following two testing approaches were selected, in order to experimentally investigate the H.B.C. fuse arc mechanism:

## I. Crow-bar Fuse Tests

Test fuse samples under critical current conditions, by by-passing the current in the fuse, using a crow-bar circuit at consecutive time intervals, during the arcing period. The elements were then observed using X-ray technique, obtaining two perpendicular plates from each fuse. Subsequently the relevant samples were disassembled and prepared for microscope studies. The fulgurite was cast in suitable resin then cut at different depths, polished and made ready for observation using a microscope.

### I-1. Samples:

For the assembly of the fuse samples the following conditions were strictly observed:

#### a: Fuse element

The fuse investigation should be kept as simple as possible. A wire fuse element was therefore used. The chosen element material was silver due to its widespread use in semiconductor and high voltage fuses. The length and diameter were chosen in relation to the test circuit and level of arcing energy. The fuse constructions were based on commercial fuse types and the selected voltage was 230 V a.c.

The maximum arcing energy was the value based on the critical current as defined in fuse standards. These requirements gave a fuse element length of 35 mm and 0.6 mm diameter. The silver purity was better than 99.9% (silver 1000) and diameter tolerance less than 0.02 mm. The connection between the fuse element and the knife contacts were made by spot-welding, using a electronically controlled equipment in order to keep welding time and current (the value and wave form) as constant as possible. The filler material chosen was standard fuse quartz sand, purity better than 99% of SiO<sub>2</sub>, free of organic contaminants, with the following chemical composition:

$Fe_2O_3$ .....0.015%  
 $TiO_2$ .....0.001  
 $CaO$ .....0.082  
 $K_2O$ .....0.026  
 $SO_3$ .....0.014  
 $Al_2O_3$ .....0.180  
 $SiO_2$ .....*balance*

Two grain sizes (50 and 80) were used, determined using 425/300  $\mu$  and 300/180  $\mu$ , ASTM standard sieves. The filler was compacted into the fuses using standard vibration equipment. The grain shape can be observed in **Photograph 1**. The vibration was calibrated in frequency and vibrating amplitude in order to obtain the maximum compaction for each grain size, of approx. 1.6 g/mm<sup>3</sup>. Before pouring, the sand was baked at 800 °C for four hours and kept in a dryer.

The fuse design and construction was based on the following requirements:

- Similar to a commercial fuse.
- Easy and safe dismantling.
- Maintenance of good manufacture tolerances.
- Fuse constructions suitable for X-ray and optical fiber observation
- Rated voltage and current appropriate to the fuse element used.

A DIN 43625 (IEC 269) standard (size 00) fuse was adopted, with steatite body, brass knife contacts and silver plated end caps connected by welding. Each cap was fastened to the body using four screws. **Fig 2.1**

#### I-2. Test circuit:

The test rig is shown in **Photograph 2** and the test equivalent circuit is shown in **Fig 2.2**. The electrical energy is obtained from a main 13.2 kV distribution supply transformed down to 230/400 V using two 2 MVA transformers. The make switch installed in the low voltage side is a contactor operated from a d.c. source, giving a scatter in closing angle of less than 2 e° with a rated current of 10 kA. The master switch

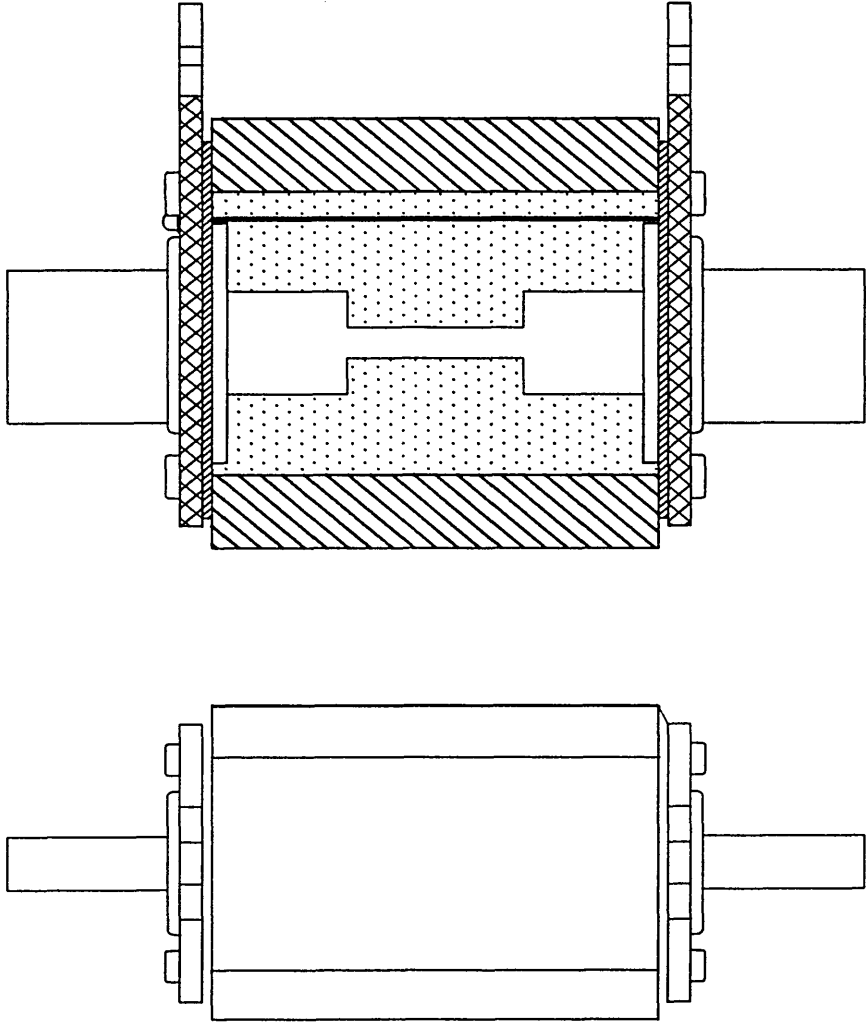
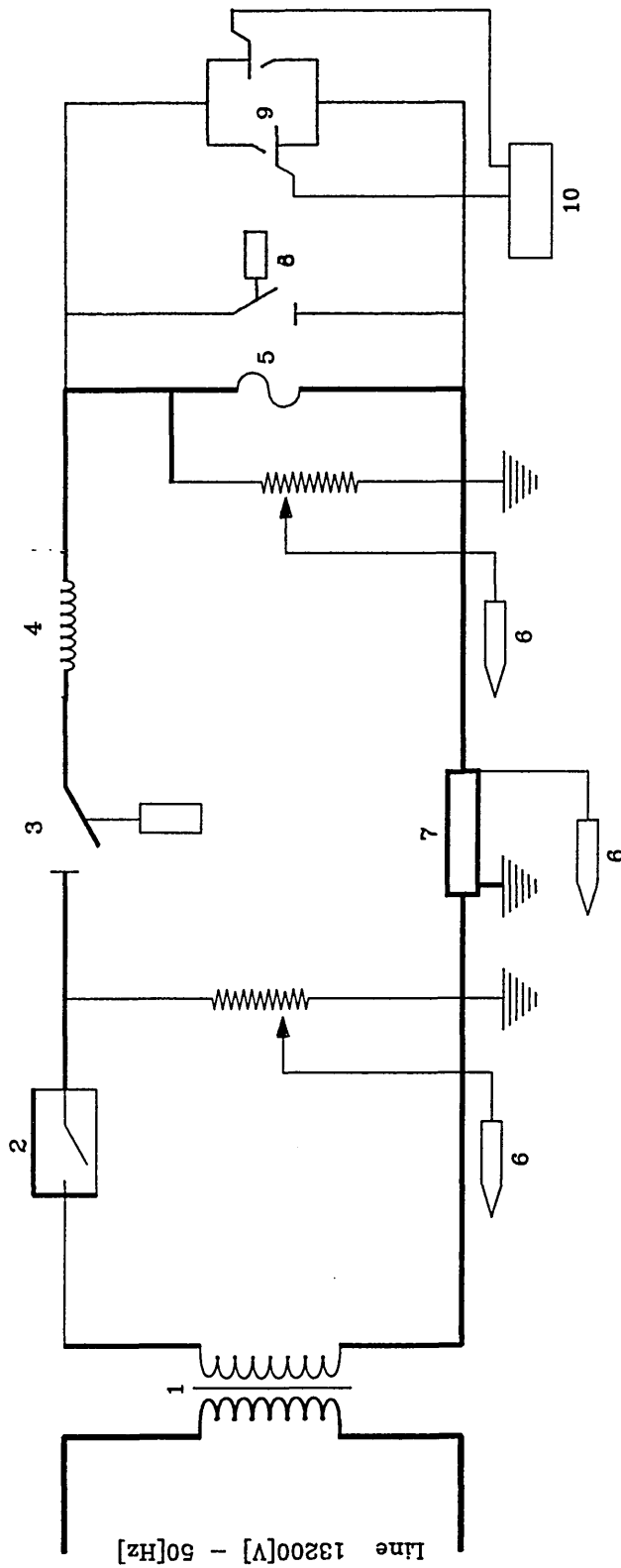


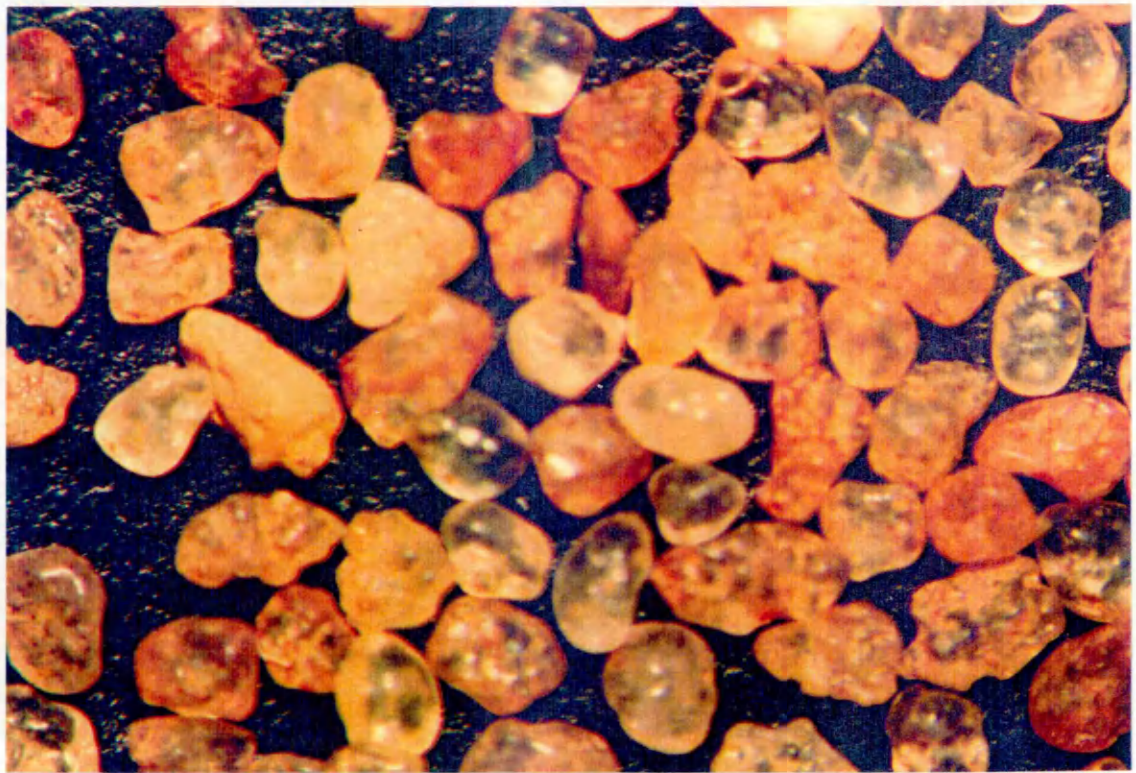
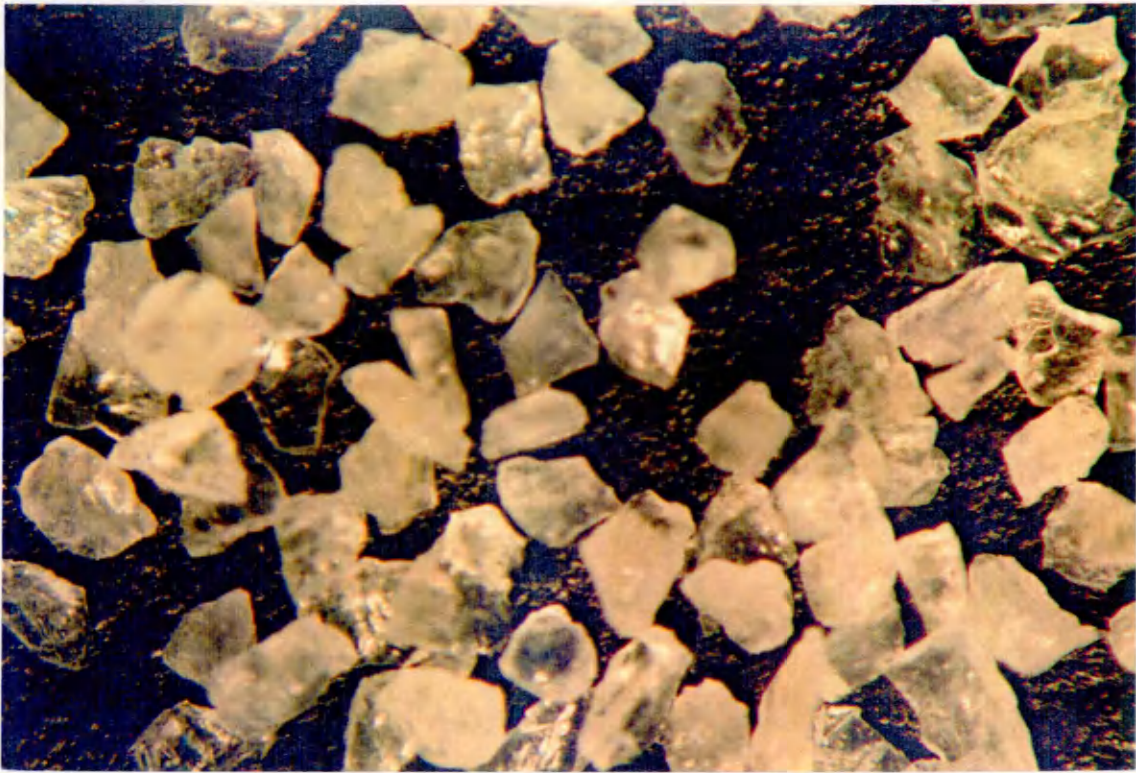
Fig. 2-1 Sample Fuse Construction - Showing  
Notched element



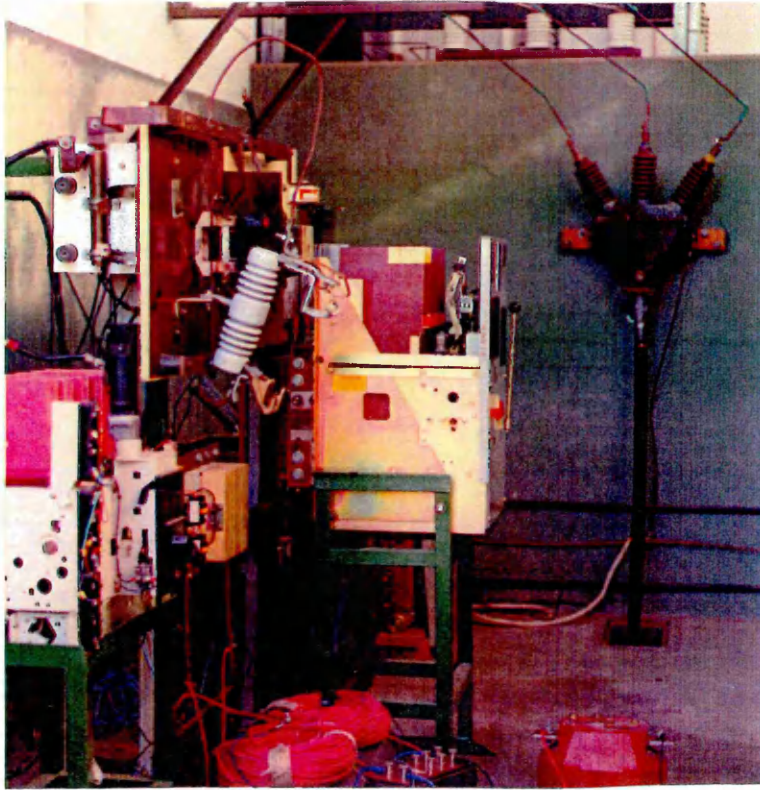
REFERENCES

- |                               |                      |
|-------------------------------|----------------------|
| 1 - TRANSFORMER 13200/410/235 | 6 - OSCILLOSCOPE     |
| 2 - CIRCUIT BREAKER B.T.      | 7 - SHUNT            |
| 3 - MAKING SWITCH             | 8 - MAKING SWITCH    |
| 4 - LOAD                      | 9 - POWER THYRISTORS |
| 5 - TEST FUSE                 | 10 - CROWBAR CONTROL |

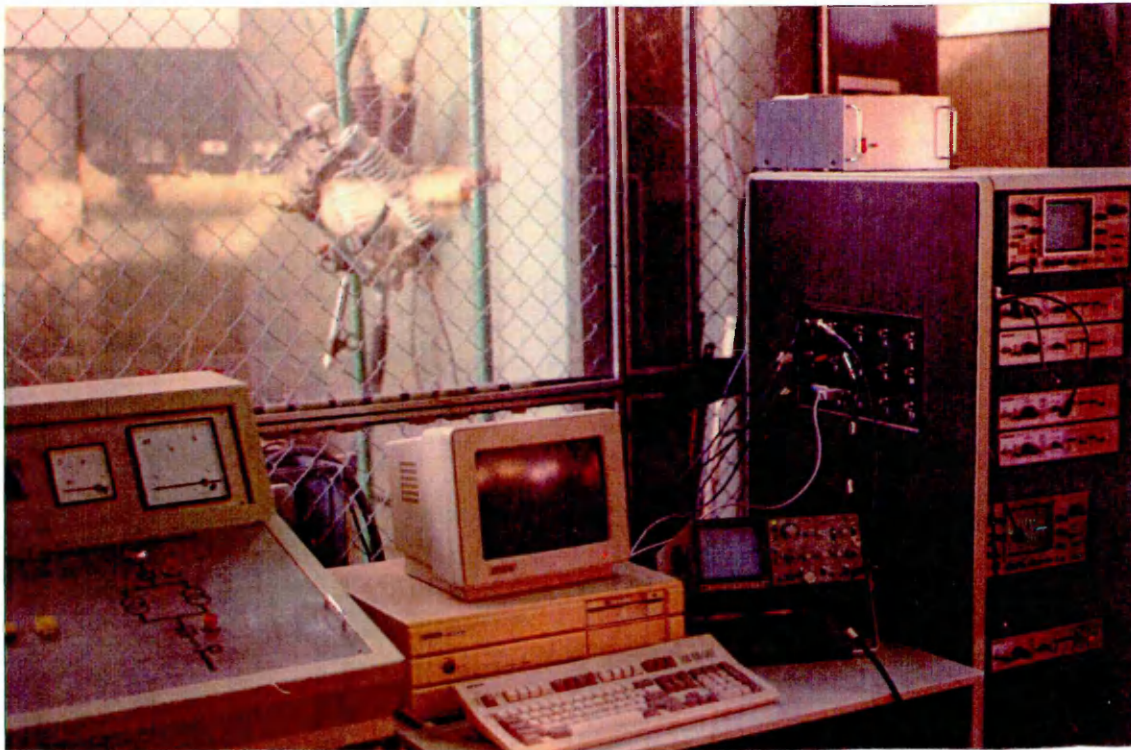
Fig. 2-2 Short-Circuit Test Circuit Arrangement



Photograph 1 - Common grain filler (top) and Fine grain filler (lower)



Photograph 2 - High power test facility



Photograph 3 - Measurement and data recording equipment

is an air circuit breaker of 70 kA breaking capacity and opening time adjustable from 10 ms to several seconds.

The crow-bar system used was formed by anti-parallel connected thyristors, with a parallel contactor acting as back-up. The thyristors are switched by the master controller with a short delay between them. The contactor permits the by-passing of the current from the fuse during arcing.

Three signals were obtained from the test circuit to record the supply voltage, arc voltage and current. Resistive potential dividers were used for the voltage measurements and coaxial shunts were used for measuring the current. The three signals were fed into a digital oscilloscope, which stored the values as 1000 or 2000 samples per channel. The data was subsequently transmitted to a personal computer **Photograph 3**.

The test circuit load was formed by air core inductances and wire-bar resistances, combined to give the prospective current and power factor required for each test.

### I-3. Test Methodology:

Firstly, the resistance measurement of all the samples was made using the volt/amp. method, in order to detect any fuse irregularities. The results were generally very good because less than 1% of fuse samples were rejected.

The next requirement was the determination of the critical current for the sample fuse, using as a guide the values for making angle, power factor and the peak current/RMS current relation (0.95 to 1.06) advised in IEC 269-1; VDE 0636 and BS 88 standards. The test settings were adjusted from the energy results calculated using the personal computer after processing the voltage and current data. A computer program was produced for the calculation of the prearcing  $I^2t$ , arcing  $I^2t$ , arcing energy, prearcing time and arcing time. For example, for the sample having a silver wire fuse element of 0.6 mm in diameter, the critical current was 2540 A for a making angle of 20 e°. The current, fuse voltage and numerical test results are shown in **Fig 2.3** for this critical current condition.

The test series was the incremental application of the critical current to different samples, which involved extending the switching time delay for the crow-bar circuit, in

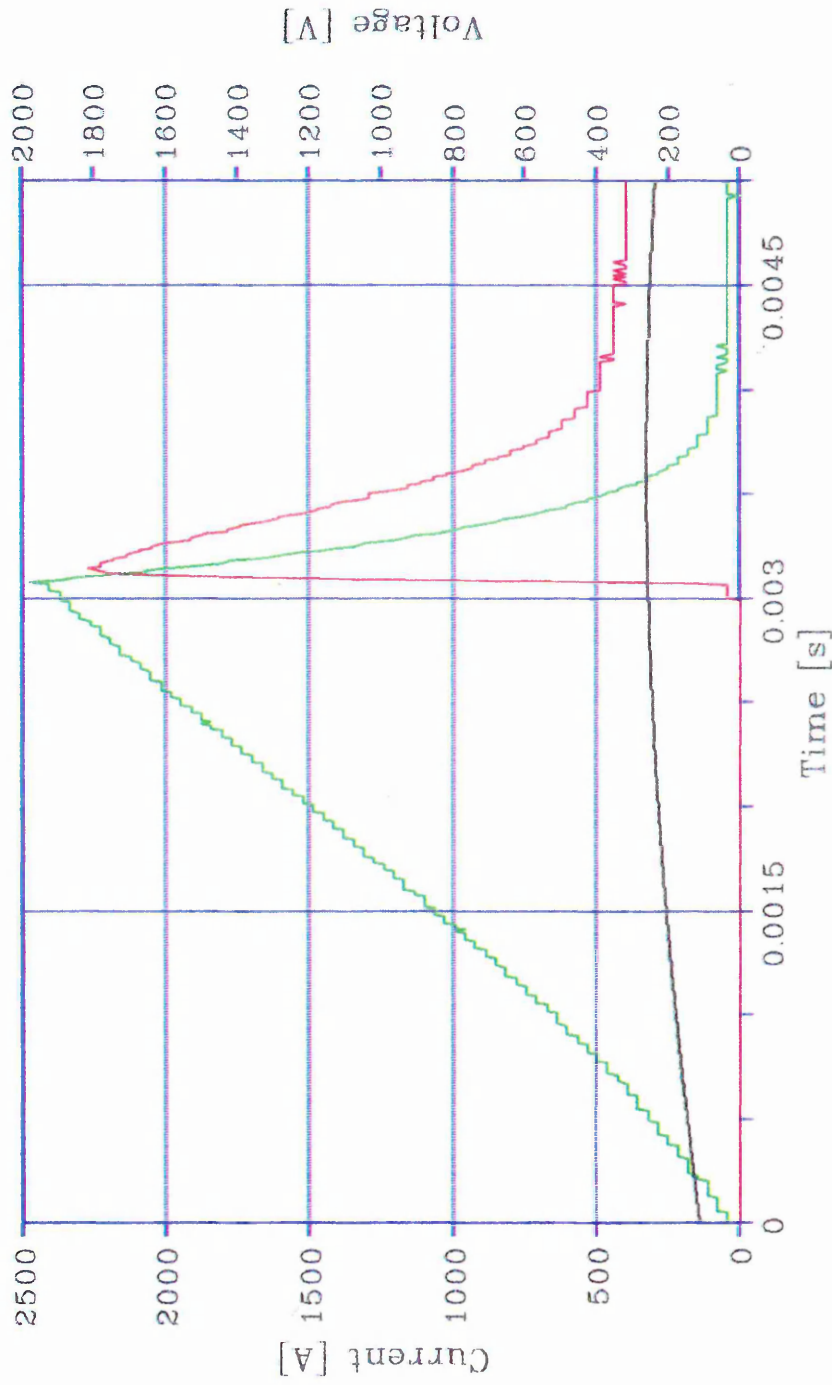


Fig. 2-3 Complete fuse operation for critical current  
 (  $I_{\text{prosp.}} = 2540 \text{ A}$ ,  $\theta = 20^\circ$  )

steps of 0.02 ms. from the end of the prearcing period up to complete current interruption. Not all the test shots were effective because the fuse samples were not exact replicas and the prearcing and arcing time changed by a few tenths of microseconds. Special care however was taken in the sequence for the analysis. Examples of by-passed currents are shown in **Figures 2.4 & 2.5**.

After the fuse samples had been operated, they were X-rayed using a standard industrial equipment ( voltage 110 kV, current 25 mA, exposure time 1 min and focus-film distance 0.75 m). Two perpendicular X-ray plates were taken for each sample, to obtain an image of the whole wire length from each fuse side. An example of two orthogonal views is shown in **Photograph 4**.

All the tested samples were carefully dismantled and the fulgurite formations analyzed using an optical magnifier (x 140 and x 280) in order to obtain basic information and allow the selection of the best samples for the metallographic microscope study. The selected samples were cast in araldite resin and sectioned longitudinally and in a plane orthogonal to that of the fuse wire for examination, having obtained pictures of the most important views. The microscope study was made using magnifications from (x 86) to (x 686), using the dark and bright field technique and changing the filter colors until the best image was obtained. An example is shown in **Photograph 5**.

## II. Optical fiber Fuse Tests

### II-1. Samples:

- Fuse element

The same fuse element was used.

- Filler material:

The same filler and filling techniques were also used.

- Fuse structure:

The fuse structure was slightly changed to allow the installation of optical fiber into the arcing region of sample fuses. The fuse body was a melamine cylinder divided in two, fastened together by two belts. The knives and caps were similar to those used previously, the only difference being that they were glued to the stationary body half.

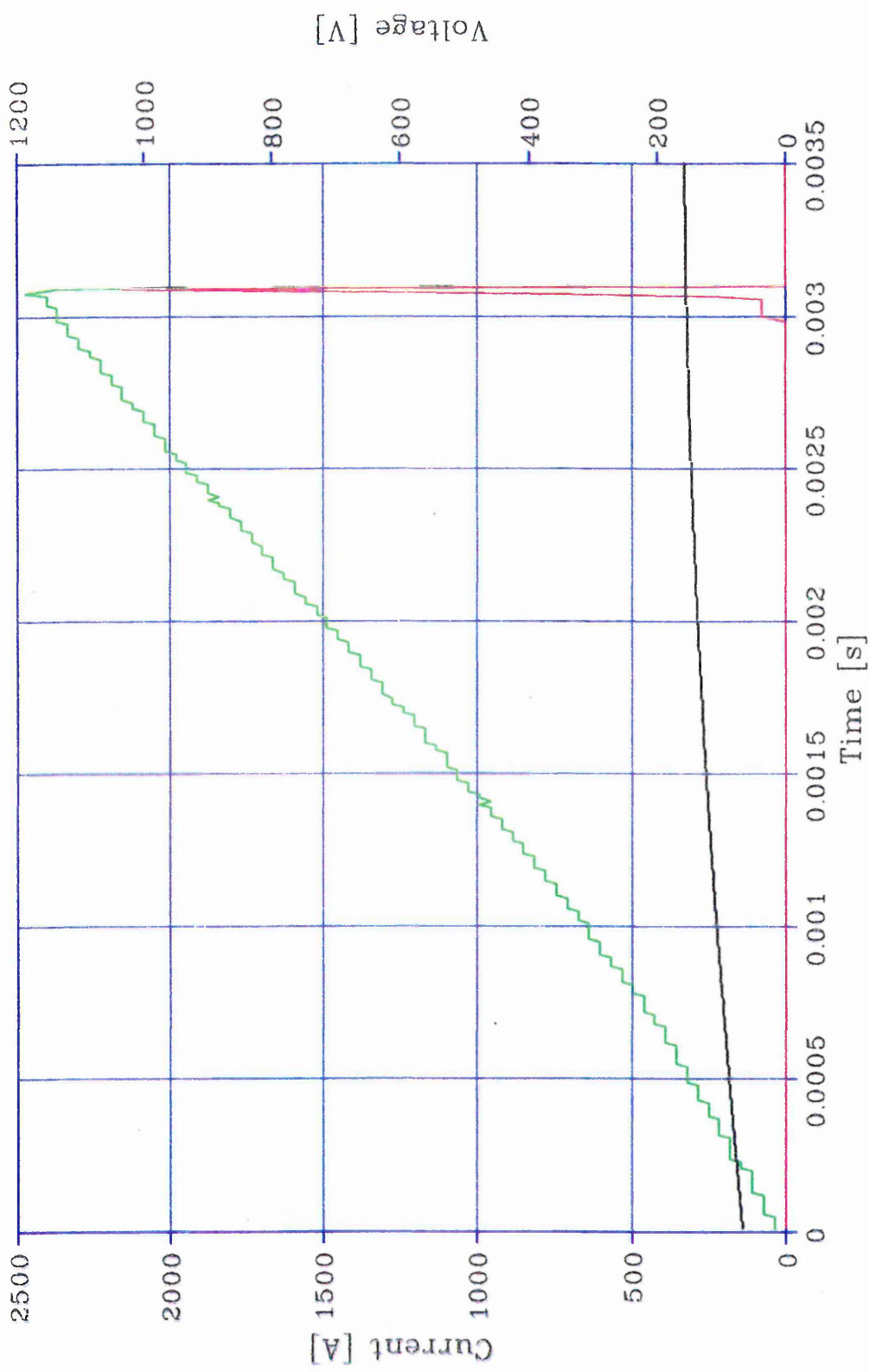


Fig. 2--4 Interrupted Fuse operation before Peak Voltage

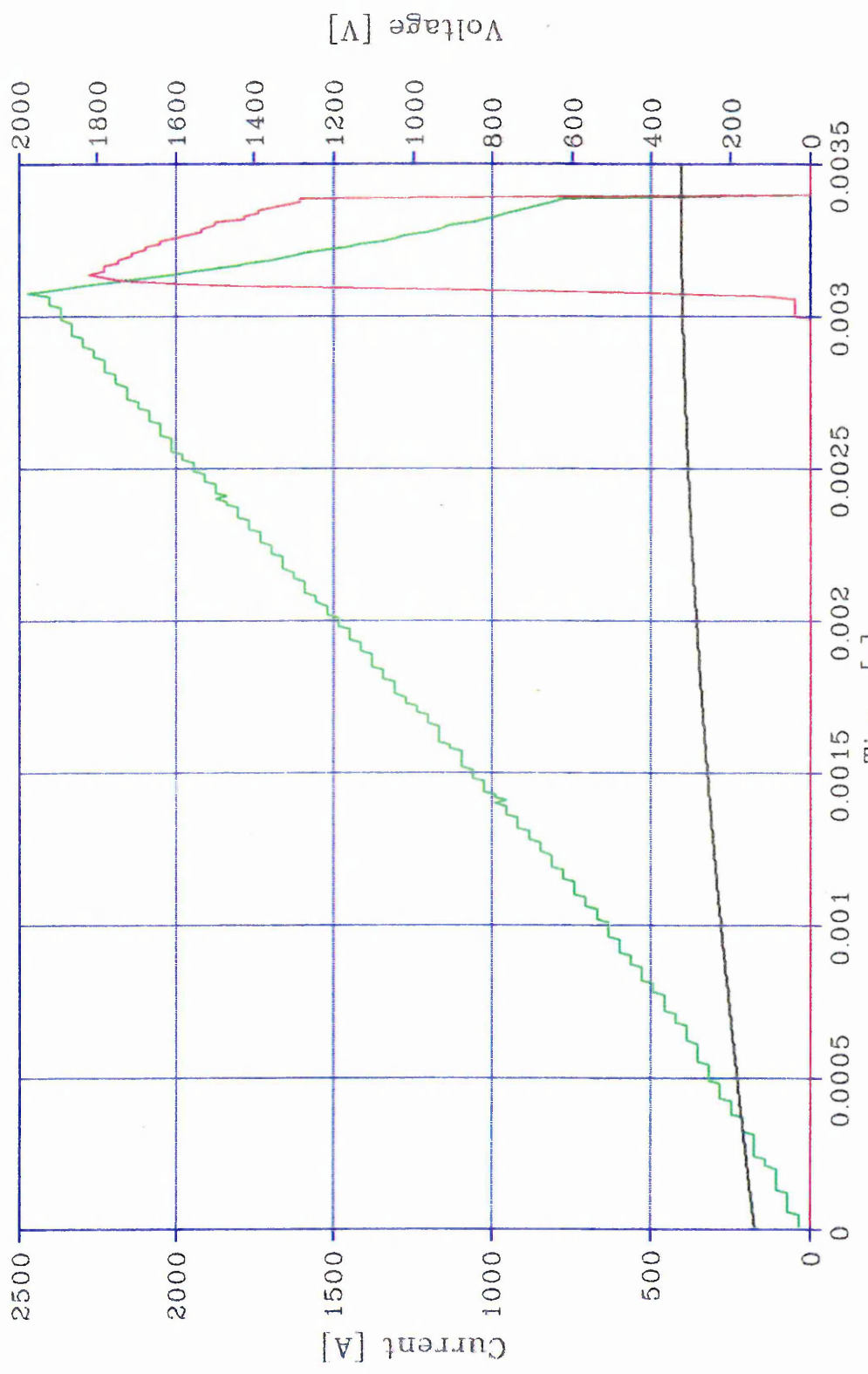
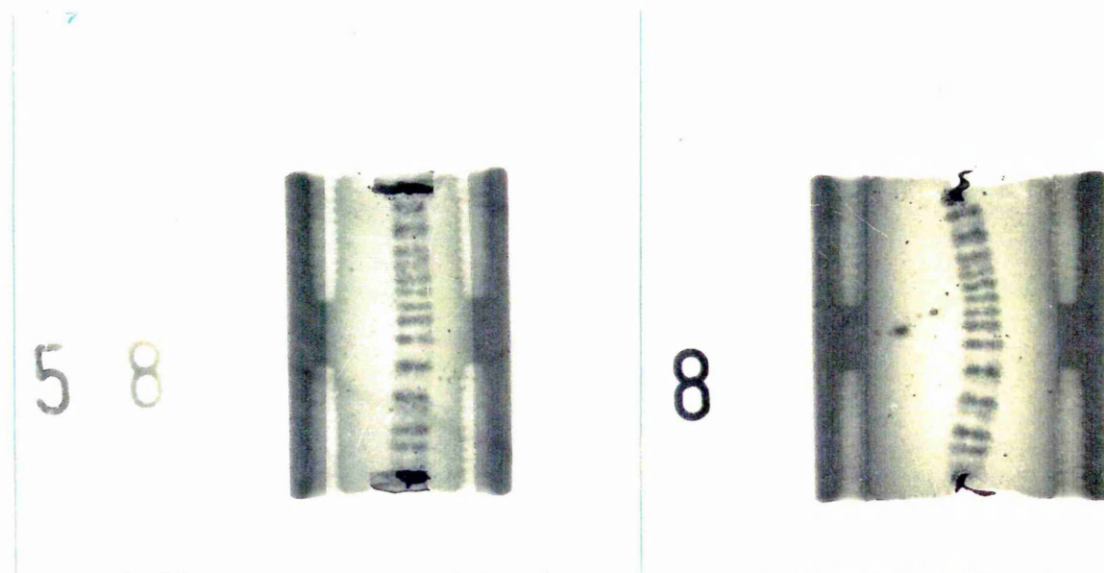
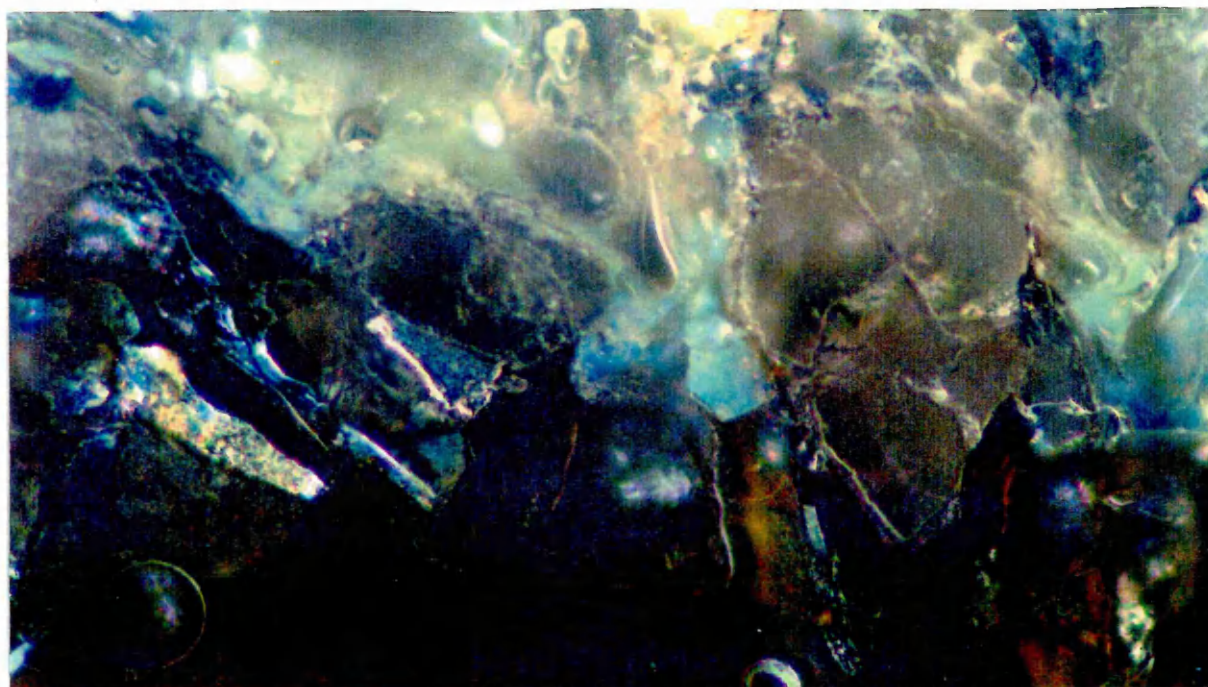


Fig. 2-5 Interrupted Fuse Operation after Peak Voltage



Photograph 4 - Typical front and side X-ray views of operated fuse



Photograph 5 - Magnified image (x 686) of Photograph 13  
(showing unmelted silver deposits in filler)

The free body half contained five ceramic tubes orthogonal to the fuse element and in the same plane, installed facing the wire center and 2.7 mm apart. Holes of 1 mm diameter were made in the body through which 0.5 mm diameter optical fibers were inserted. The rig, **Photograph 6**, enabled precise and safe optical fiber installation. The filler prevented fiber movement. The filler was poured into the fuse body after the fibers have been placed and the vibration was undertaken in a progressive way until suitable compaction was obtained. This operation was done very carefully, since the fibers, being invasive elements, can change the fuse characteristics. The filler compaction, in all cases, was the same as for the first test series.

#### II-2. Test circuit:

The test circuit was practically identical to the circuit used in the first test series. The only difference was that the crow-bar circuit was not applied and the signals for the current, voltage and light transmitted by nine fibers was stored using a data acquisition system with a sampling interval of  $1\mu\text{s}$ . The signals were processed using, as before, a personal computer.

#### II-3. Fiber Optic Test Methodology:

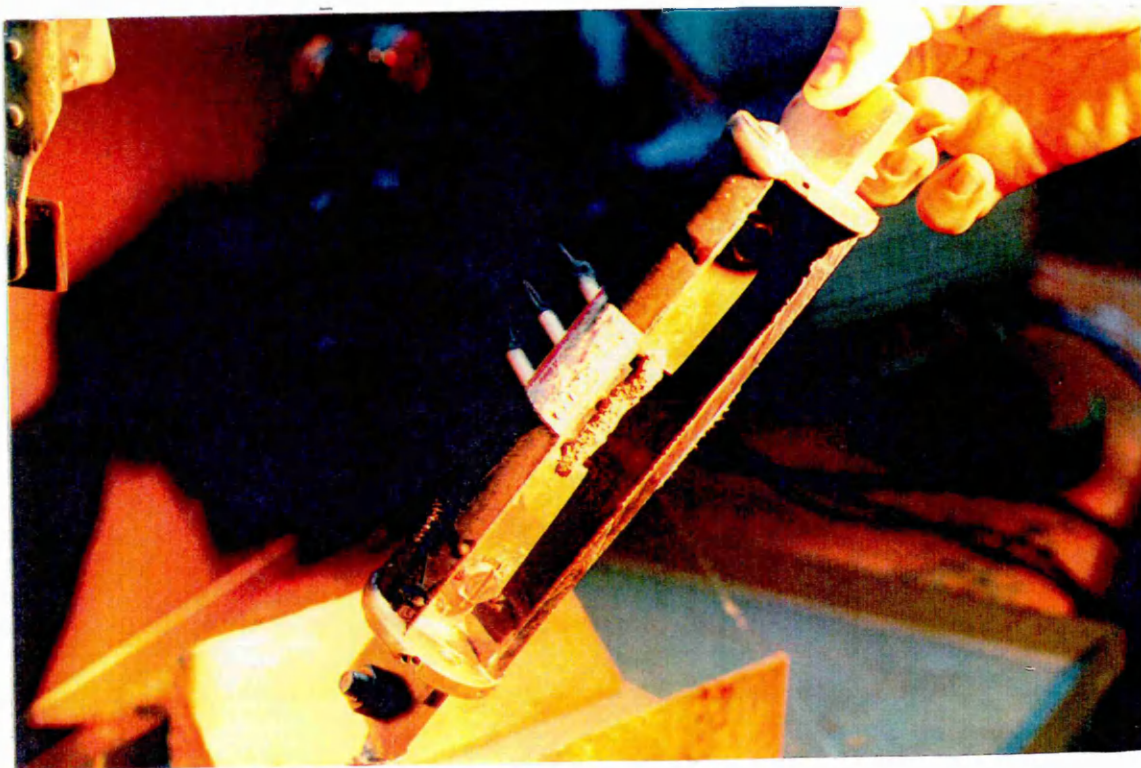
As there was only one fuse construction, it was necessary to assemble, perform resistance measurement, test under critical current, dismantled and repeat the whole procedure for each test shot.

The methodology as previous test, was to the fuse under critical current conditions, for the same current value, making angle and power factor angle as used previously. Several tests were made, with different sampling times to obtain a view of the whole arc phenomena at different filler depths.

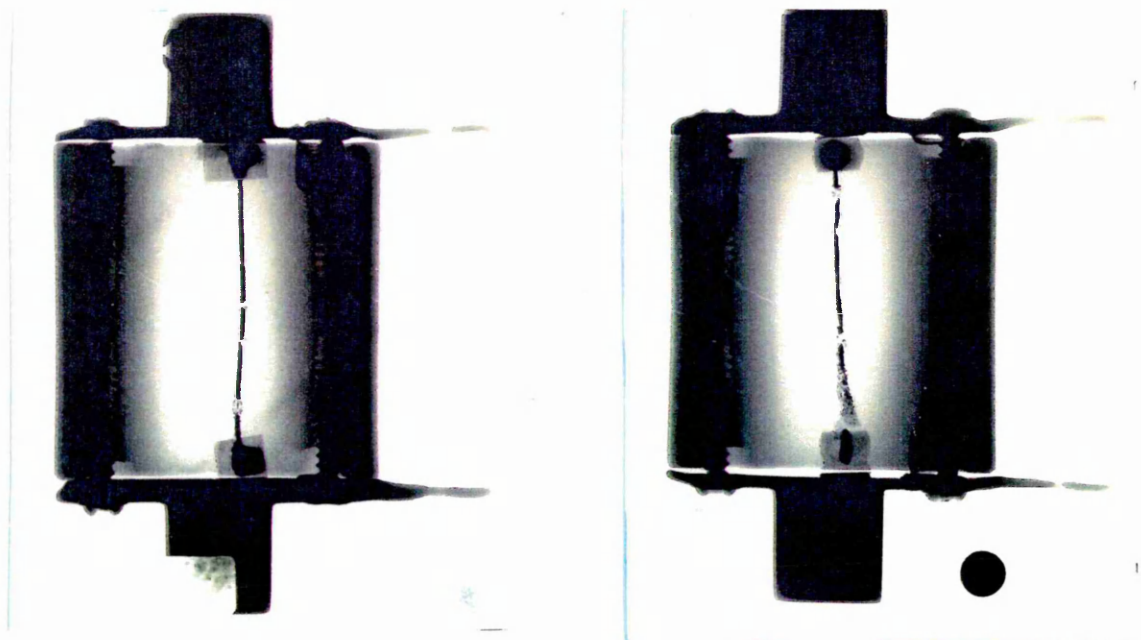
Physical observations :

The following arcing behaviour was observed based on the different experimental methods:

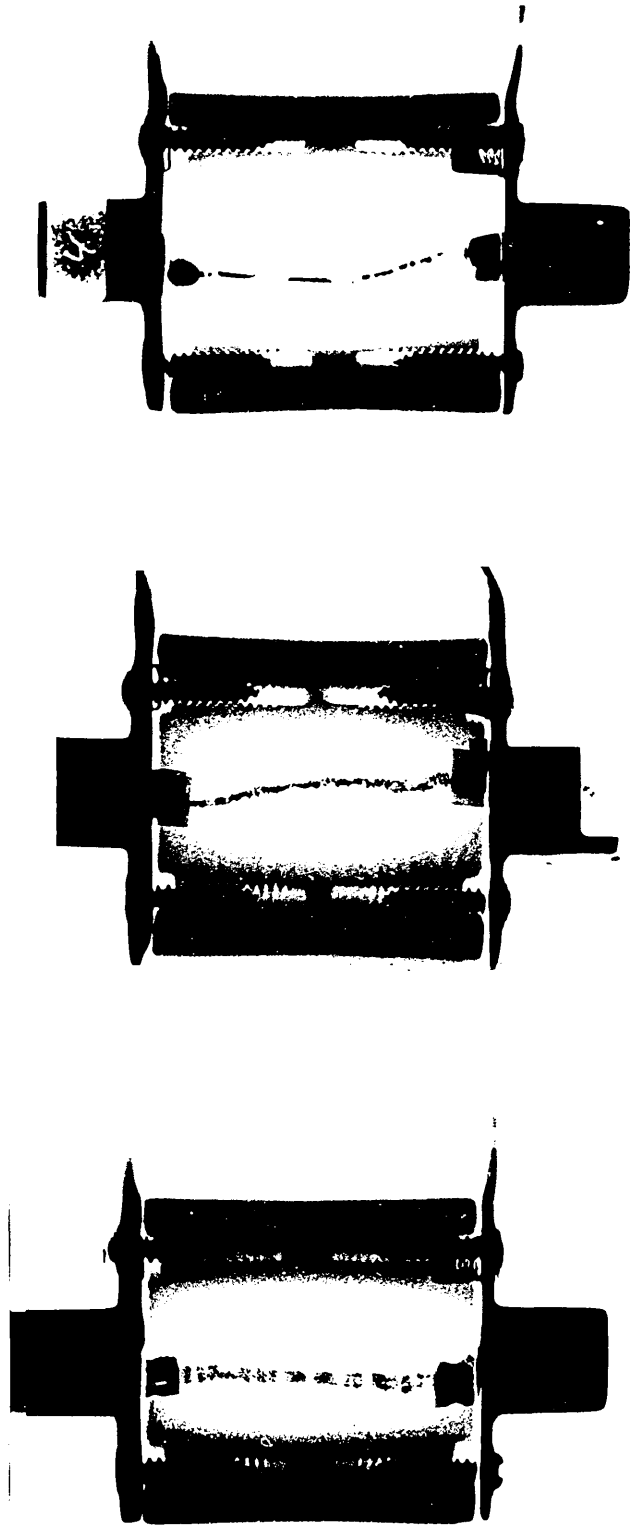
- Crow-bar and X-ray methodologies:
- During the melting period the necks and swollen sections due to pinch-effect and surface tension could be seen, together with some "crown" structures which show that the metal is pushed away from the wire in liquid form. In some parts of the wire it is possible to see a "hair" like form emerging from the wire instead of the "crown" structure. **Photographs 7 & 8**
- At the beginning of the arc period the start of one or several single arcs could be observed **Photograph 9**.
- A short time after an image with a few short and long arcs were observed **Photograph 10**.
- Some instant later it is possible to recognize several short arcs either without any long arc, or with shorter long arcs than before.
- The phenomena continues in this way producing an increasing number of short arcs and some shorter long arcs at the same instant.
- A number of small silver deposits could be seen around a solid cylinder, which seems to be the remains of a previous "crown", where an arc was established **Photograph 11**.
- The number of arcs increases until the maximum voltage peak is reached, which takes place in a very short time, (aprox. 100 to 150  $\mu$ s). Around this voltage level the different arcs begin to coalesce into long arcs.
- Generally speaking, before the arc peak voltage is reached the arcs increase in number and their length increases also but up to a value which seems to be a maximum.
- After the peak arc voltage occurs, the arcs appear to coalesce (although it is impossible to detect from a frozen image of burning vapour). An increase in the lumen diameter is also indicated, which occurs in a short time.



Photograph 6 - Optical fibre fuse assembly

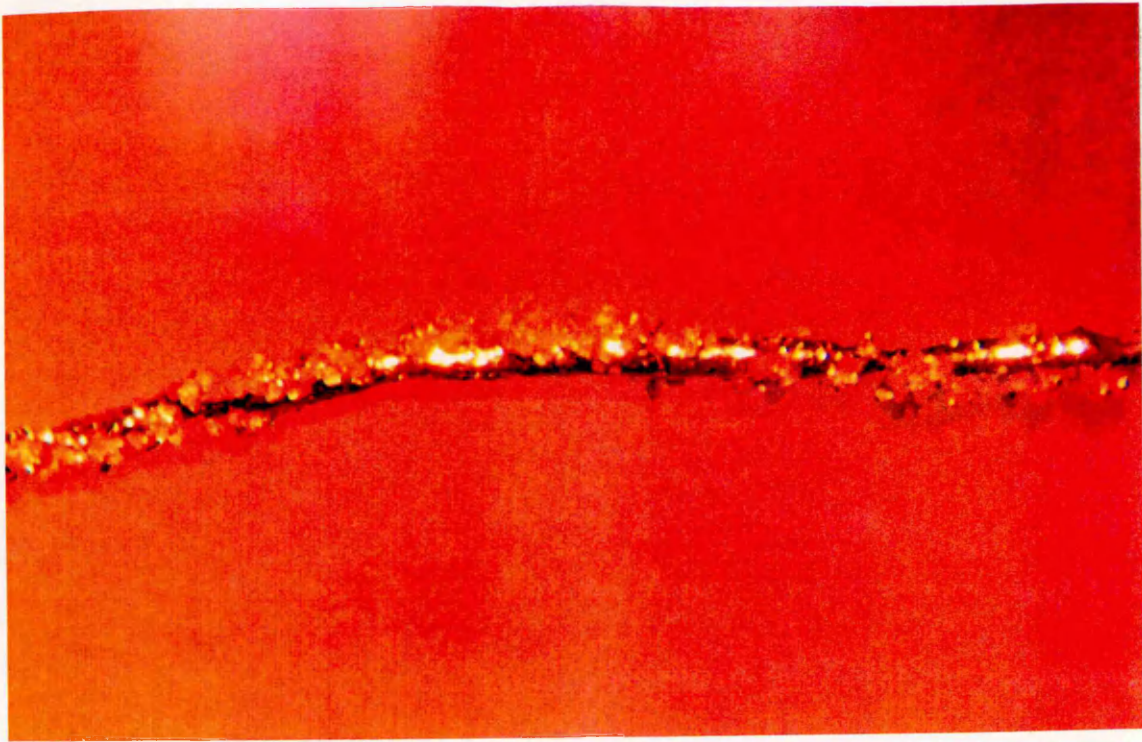


Photograph 7 & 8 - Examples of fuse wire disruption

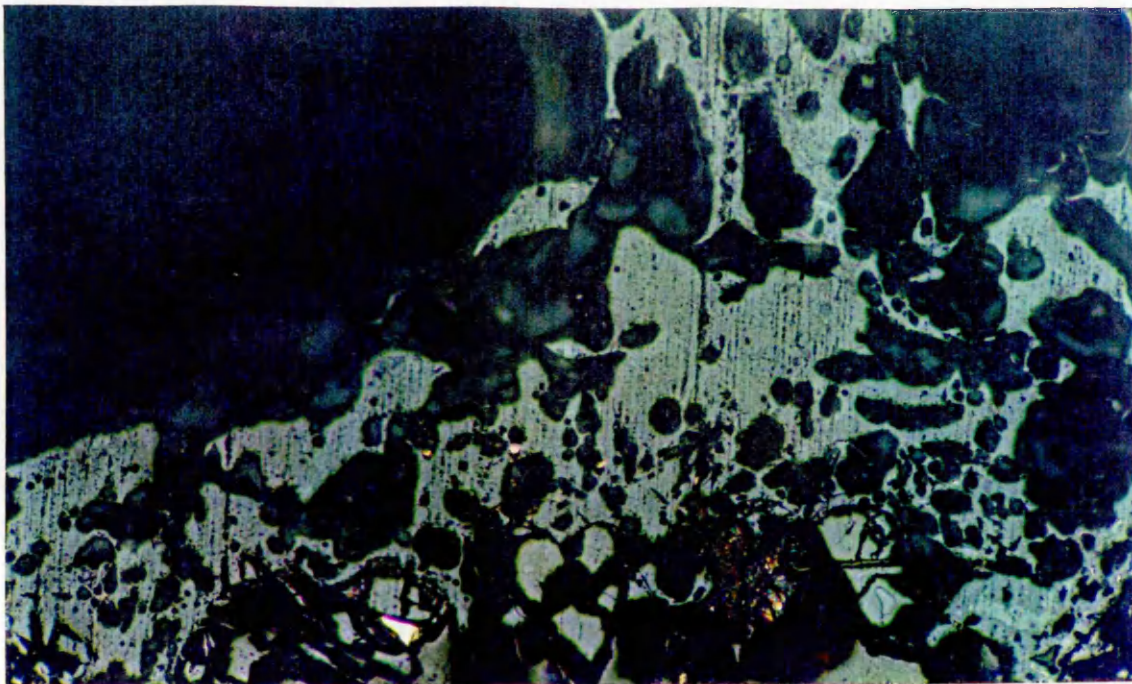


Photographs 9, 10 & 11 - Wire interruption showing long and short arc combinations

- Nothing further of note could be detected from X-ray studies up to the end of the arcing period.
  
- Crow-bar and microscopic methodologies:
  - For all the cases of virtual instantaneous by-passed current, a "quartz signature" over the wire surface could be observed, where the molten grains are attached to the metal and where silver particles are found among the grains.
  - The neck and swollen parts were observed and how their number increased with time. Several of them could be observed before the first arc starts. **Photograph 12**
  - It is impossible with this technique to study arc initiation, because no fulgurite is created in this period. It is therefore necessary for some arc burning to occur to form a suitable physical structure able to withstand dismantling of the fuse
  - The fulgurite has a double-coned shape with circular cross-section. The silver drops could be found only near the arc roots. Where the arc has been burning for a relatively longer time the metal drops were vaporized and pushed-away from the central part.
  - In the area of the first initiated arc, silver particles of irregular forms were observed in zones not reached by the burning arc. **Photograph 13**
  - The fulgurite found after the arc is quenched was formed by a series of alternate uniform modules some differing slightly in length formed by white and dark grey rings. The different length of the bands indicate the areas where the arcs were burning for shorter or longer times respectively.
  
- Optical fiber methodology:
  - When the arc ignites just in front or near the optical fiber end, the arc intensity is directly related to the photo-transistor voltage.
  - No arc extinction (turn-off) was observed during the arcing period, which is in contradiction with the findings of previous workers.[30]



Photograph 12 - Fragments of quartz embedded in molten wire



Photograph 13 - Magnified view of un-melted silver deposits in region of fulgurite lumen (x 343)

- Where several arcs burned at the same time, normally the light emission is not the same for all of them. For example some increase quicker and in a few cases it was observed some arcs produced a decrease in the emitted light. After a short time the emission is of the same level. Fig 2.6 & 2.7.
- The voltage increase is very smooth, thus it is practically impossible to determine when the arcs appeared except for the first one.
- In some of the records it is possible to track some of the arc light emission by looking at the arc voltage value, since when the received light decreases a falling slope is shown in the voltage trace.

The classical explanations for the previous physical arc observations appear to breakdown in this study and several new questions are posed without clear answers.

For example:

- Can a long arc become a short arc ?.
- Can several arcs start together and share the energy ?.
- Can arcs occur at very high speed ?.
- Why should an individual arc length appear initially to be a maximum ?.
- Why should the arc phenomena be complex, since for the fuses, tested under critical conditions and by-passed with the crow-bar circuit, indicated exactly the same step-by- step fulgurite structure ?.
- Why should a sudden jump in the anode-cathode voltage not be detected each time a new arc ignites, or an existing arc is extinguished during the coalescing ?.

These questions had no clear answers except that the results can be replicated consistently .

*It follows, philosophically from the laws of nature, that any mechanism that is capable of replicating itself consistently, has to be, basically, very simple.*

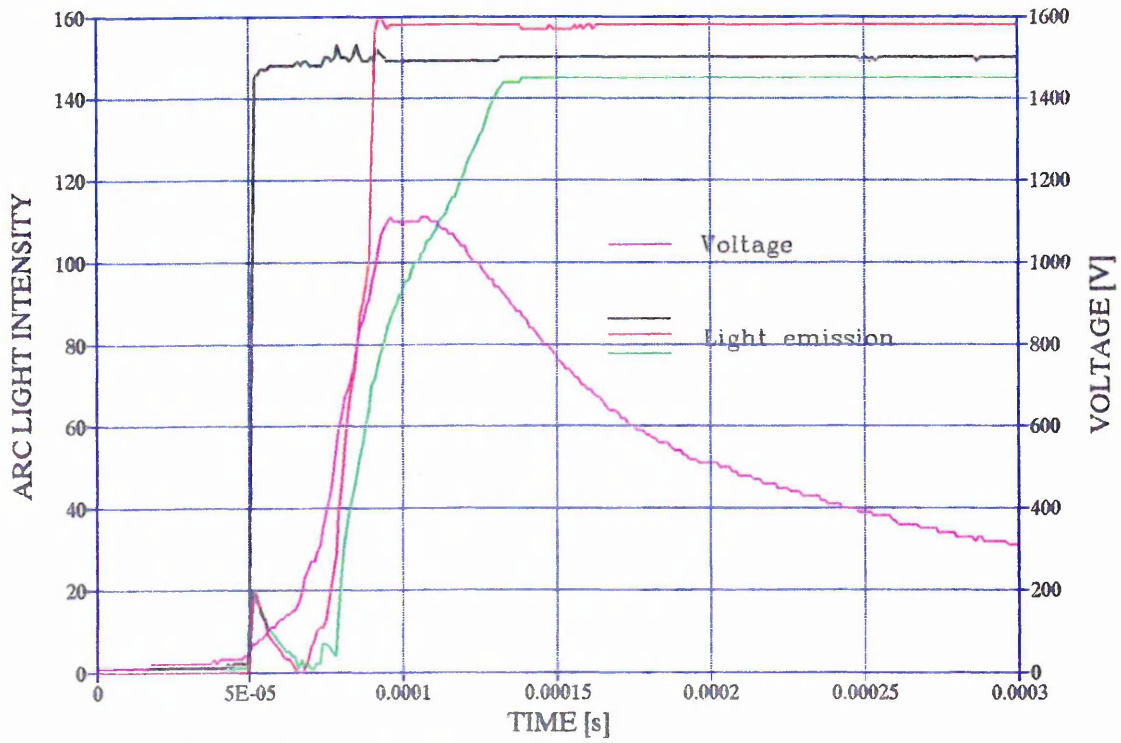


Fig. 2-6 Arc Waveforms from optical measurement system

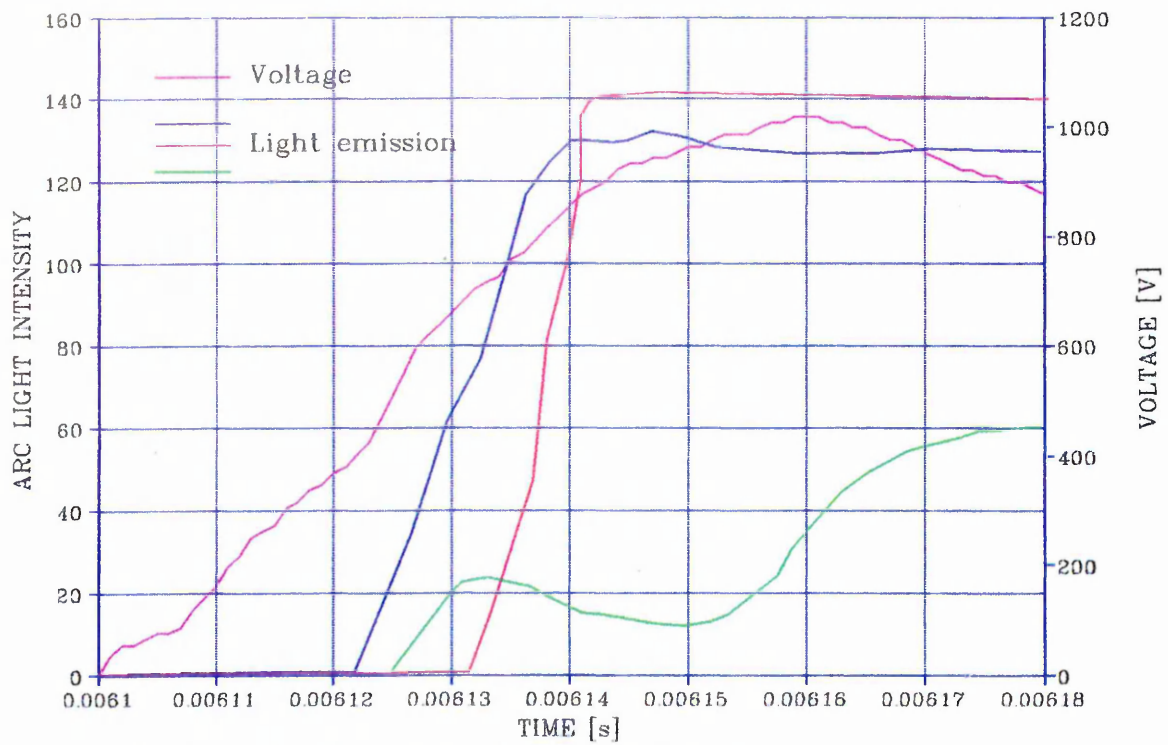


Fig. 2-7 Arc Waveforms from optical measurement system

The aim of our inquiries was to abandon complex models at this point in favour of searching for and recognising simple mechanisms to explain arc formation. This philosophy was applied to the basic arc equations and the arc voltage/time traces. These ideas will now be developed based on the arc voltage versus time trace Fig 2.8.

As the number of arcs can be determined from tests, using the X-Ray plates (Photographs 7 to 11) and fuse voltage oscillograms (Fig. 2.7), it is possible to plot the arc voltage per arc (less the arc-root voltage,  $V_{ak}$ ) against time, Fig 2.9. This figure is important since it shows during the arcing period, up to the maximum voltage instant, that:

- (1) the positive column voltage increases from zero to a maximum value equal to  $V_{ak}$  (the arc root voltage) at each arc initiation.
- (2) the maximum voltage per arc is  $2 \cdot V_{ak}$ , which occurs when  $E \cdot x(t) \rightarrow V_{ak}$ , after which a new arc is formed.
- (3) the maximum arc voltage follows as  $V_{ak \text{ peak}} = 2n V_{ak}$ .
- (4) the time interval between arcs ignitions, up to the maximum value of arc voltage, is a constant.
- (5) the arc voltage value of a wire with "n" arcs is given by the simple expression

$$V_{arc} = n[V_{ak} + V_{ak}(n-2)/n] = 2(n-1)V_{ak}$$

These findings postulate a basic relation for the arc voltage which contradicts with established thinking, as for example:

- The fuse arc voltage is given classically by:

$$V_{arc} = n(V_{ak} + E \cdot x(t)) = n \left\{ V_{ak} + \int_{t_a} (E \cdot dx / dt) \cdot dt \right\}$$

without any limiting values placed on the column voltage  $E \cdot x(t)$ , the column gradient  $E$  or the burn-back rate  $dx / dt$ .

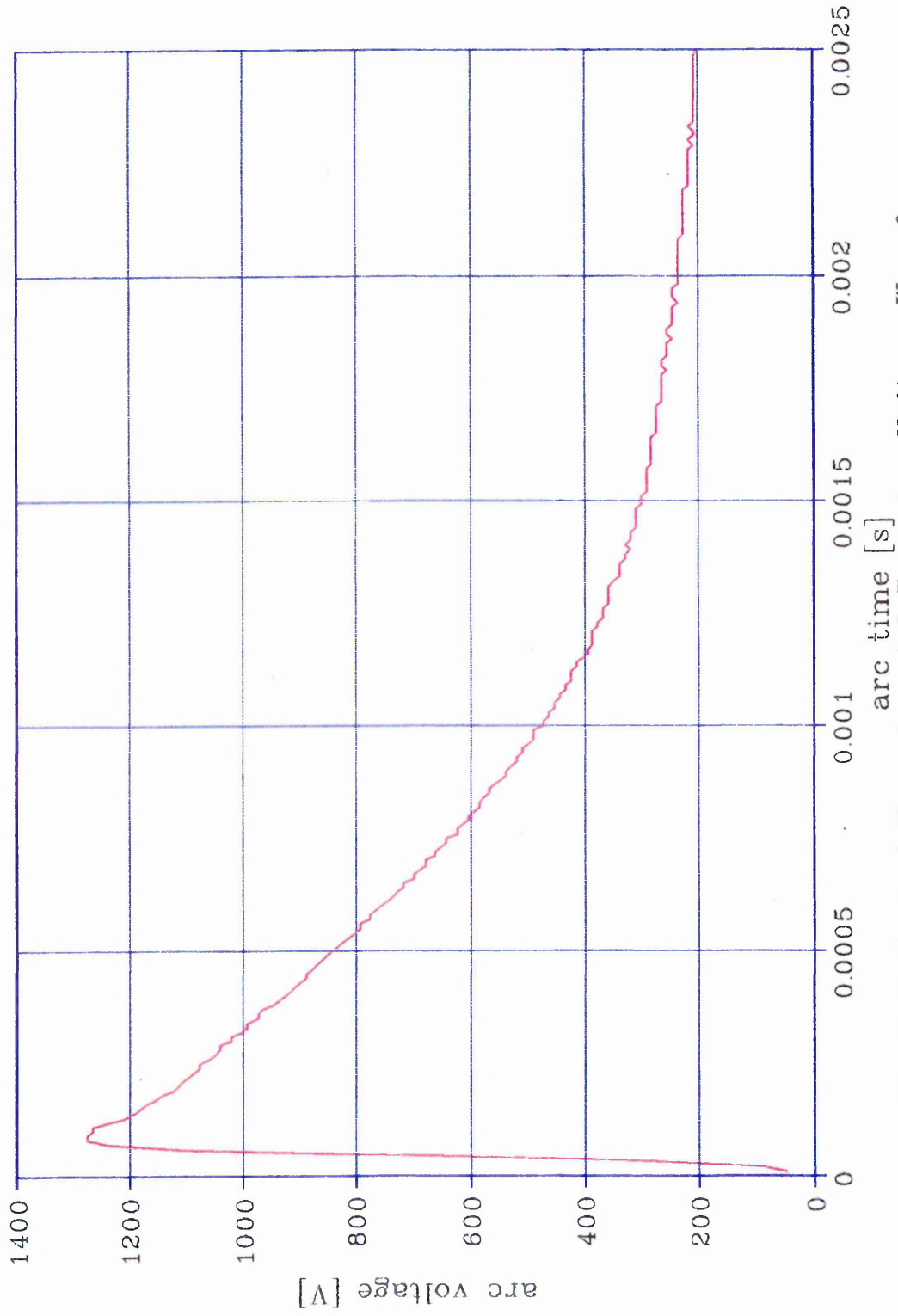


Fig. 2-8 Typical Experimental Fuse Arc Voltage Waveform

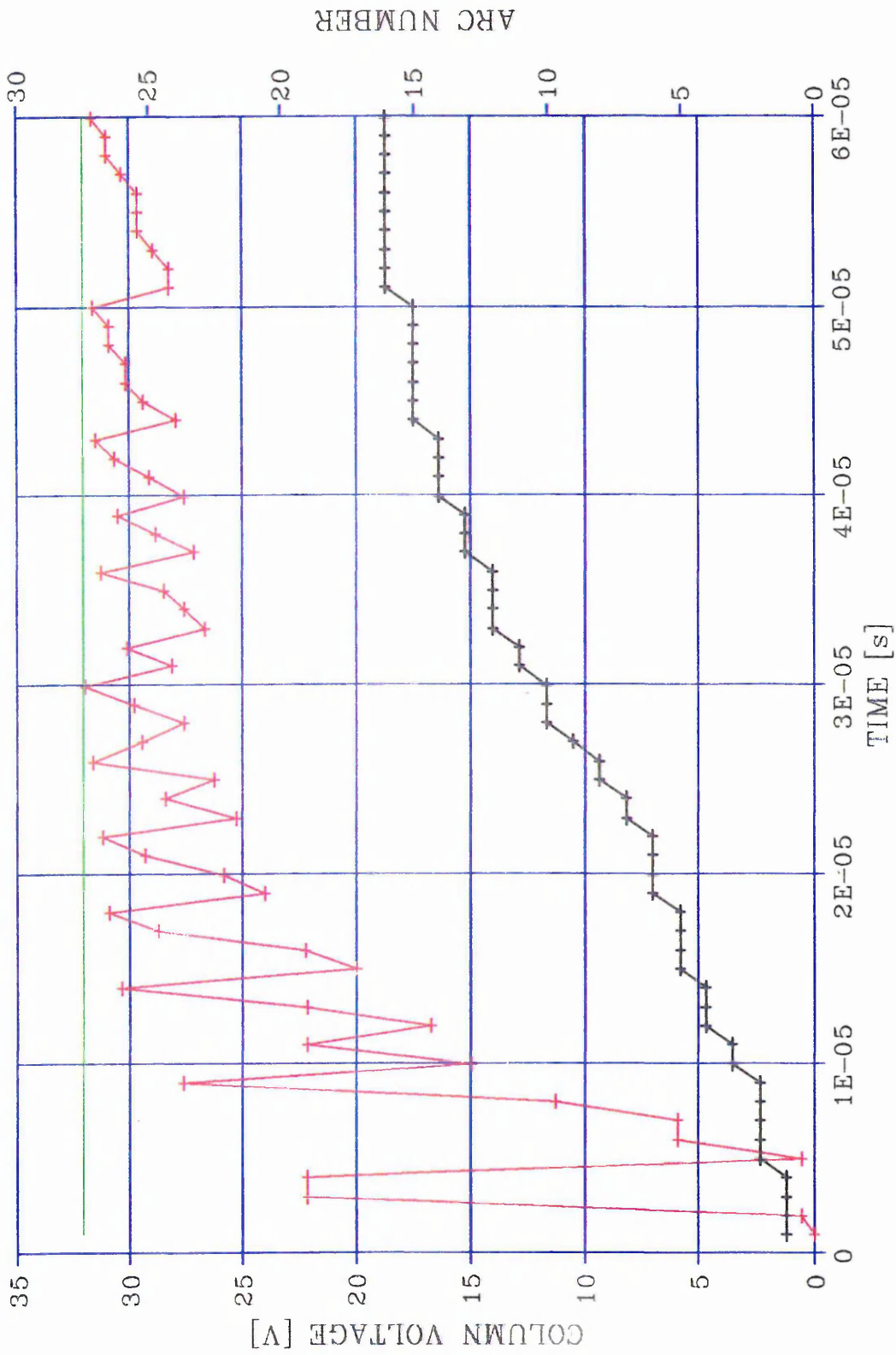


Fig. 2-9 Experimental Column Voltage per Arc

- Also the conventional practical design arc voltage value per constriction is universally considered by fuse designers to be in the range 120-150 V for standard fuse fillers, which is greater than twice the arc-root voltage drop predicted by the model.

### 2.3.2. Arc model for rising arc voltage

Following these postulations additional data is required on the arc-root voltage drop, the maximum arc voltage and the slope or speed of voltage increase for wires.

The first task was to obtain the value of the arc-root voltage. The value was estimated as 32 V from the experiments under the previously specified conditions in relation to fuse element material and dimensions, filler characteristics and critical current. In the presented analysis it is assumed that the arc-root voltage includes the anode and cathode voltage drops.

The second data required is the maximum arc voltage. This is determined using Hibner's equation

$$U_p = k_1 \times I_z \times \sqrt{\frac{i_0}{S_z}}$$

where the value of  $k_1$  is obtained from the experimental data, because it is function of the filler characteristics.

Based upon the proposed arc mechanism, the arcing process is as follows:

After the heating period some part of the fuse wire reaches sufficient temperature to produce an arc due possibly to the classical pinch-effect and surface tension phenomena [3].

As soon as the arc is established the anode and cathode voltage drop occurs, which quickly attains the value of 32 V. This voltage is indicated by the sudden change in the voltage trace jump of 32 V. **Fig 2.7.**

The positive column commences virtually at the same time and begins to increase in length and voltage due to burn-back. The column voltage increases until it reaches the arc-root voltage drop value (32 V). Since the arc voltage is now twice the anode-cathode voltage (64 V), it is postulated that at this instant the arc voltage is sufficient in theory to support two arcs with virtually no positive columns. It is further postulated that the transfer from one arc with a positive column to two arcs with minimal positive columns occurs without change in the total arc voltage. For this to happen the first arc column must either vanish or greatly expand in diameter. It follows that the maximum voltage value for each arc is  $2 \times V_{ak}$  (64 V) which is of the same order as the value measured and adopted by several authors [3, 12]. Physically, for the column to vanish, the arc roots would have to extend across the arc space for this to happen or, alternatively, the vacant arc column space behaves as a capacitor [13] or the column expands in cross-section such that the column voltage reduces virtually to zero.

In any event the situation now is that the two arcs re-establish their positive columns, and the column extension, due to the burn back, recurs, producing an increase of the column voltage at the same rate in both columns. It is therefore postulated that the speed of positive column growth is halved. When the two individual positive columns reach 32 V (the postulated maximum value for a single arc column), a further arc occurs. The positive columns again 'reduce' but for this and subsequent cases does not virtually disappear. This is clear from the traces since after the three arc-root voltage drops have been subtracted, a voltage difference exists and is shared between the arc columns.

For the example described, just before the new arc ignites the total voltage is 128 V i.e. 64 V for each arc, and given three arcs exist, the total arc-root voltage drop is 96 V ( $32V \times 3$ ). At the next ignition the remainder voltage (32 V) is shared i.e. 10.7 V across each positive column. Based on this theory the column voltage of the first arc changes from 0 V to 32 V, then decreases to 0 V and increases again up to 32 V. At the next ignition the column voltage falls to 10.7 V before increasing to 32 V., and for the next ignition the column voltage falls to 16 V rising to 32 V and so on. It follows, based on

this theory, that the positive column voltage decreases without change in the external fuse voltage, the mechanism being just an internal reorganization.

The proposed mechanism for arcing is therefore that the positive columns of each arc extend in length and its voltage increases until the 32 V value is reached such that the column voltage changes in steps 32-0, 32-0, 32-10.7, 32-16, etc. increasing at a lower rate for consecutive arcs after the second arc ignites.

The postulated mechanism is repeated until the maximum number of arcs have been established. At this instant the arc voltage per arc is equal to the sum of the arc-root voltage drop and the column voltage. From a simple mechanistic viewpoint, the rate of the voltage increase (dv/dt) in each arc diminishes as the arc number increases. For example, the dv/dt associated with the first arc will be halved when two arcs are burning, and divided by three when the next (third) arc ignites, and so on. In other words it is postulated that the arc dv/dt, i.e the slope of the wave form Fig. 2.9, is inversely proportional to the number of arcs.

The proposed mechanism produces the following numerical series and formula:

Arc number	Min. column voltage	Total voltage	Arc dv/dt
[n]	[E.x(t)]	[V <sub>arc</sub> ]	[s = initial dv/dt value]
1	0	64	s
2	0	128	s/2
3	10.7	192	s/3
4	16	256	s/4
5	19.2	320	s/5
6	21.3	384	s/6
7	22.9	448	s/7
.	.	.	.
n	V <sub>ak</sub> . (n-2)/n	2.n.V <sub>ak</sub>	s/n
$\hat{n}$	V <sub>ak</sub>	2 $\hat{n}$ V <sub>ak</sub>	0.0

The analytical results are presented in Fig 2.10.

From the X-ray results of the tested fuses, using the crow-bar circuit, it is proposed that before the voltage peak, the positive-column voltage is virtually proportional to the arc length and that the column cross-section remains constant. This means that the column voltage gradient is practically constant during this part of the arc phenomena, these being the conditions of the wall-stabilized arc. This part of the phenomena is represented by the following relations and conditions:

$$(a) V_a = n(V_{ak} + \int_{t_a} (k) dt)$$

$$(b) V_a = n(V_{ak} + k \times t_a)$$

(for  $k = \text{const.}$ )

$$(c) V_a = n(V_{ak} + E \times x(t))$$

$$(d) V_a = n \left( V_{ak} + \int_{t_a} (E \times dx / dt) dt \right)$$

$$(e) V_a = n(V_{ak} + (E \times dx / dt) \times t_a)$$

(for  $E \times dx / dt \neq \text{const.}$ )

from equations (b) and (e)

$$(f) k = E \times dx / dt = \text{const.}$$

where  $n$  = arc number,  $x$  = positive column length,  $dx/dt$  is the burn-back rate,  $E$  the column gradient.

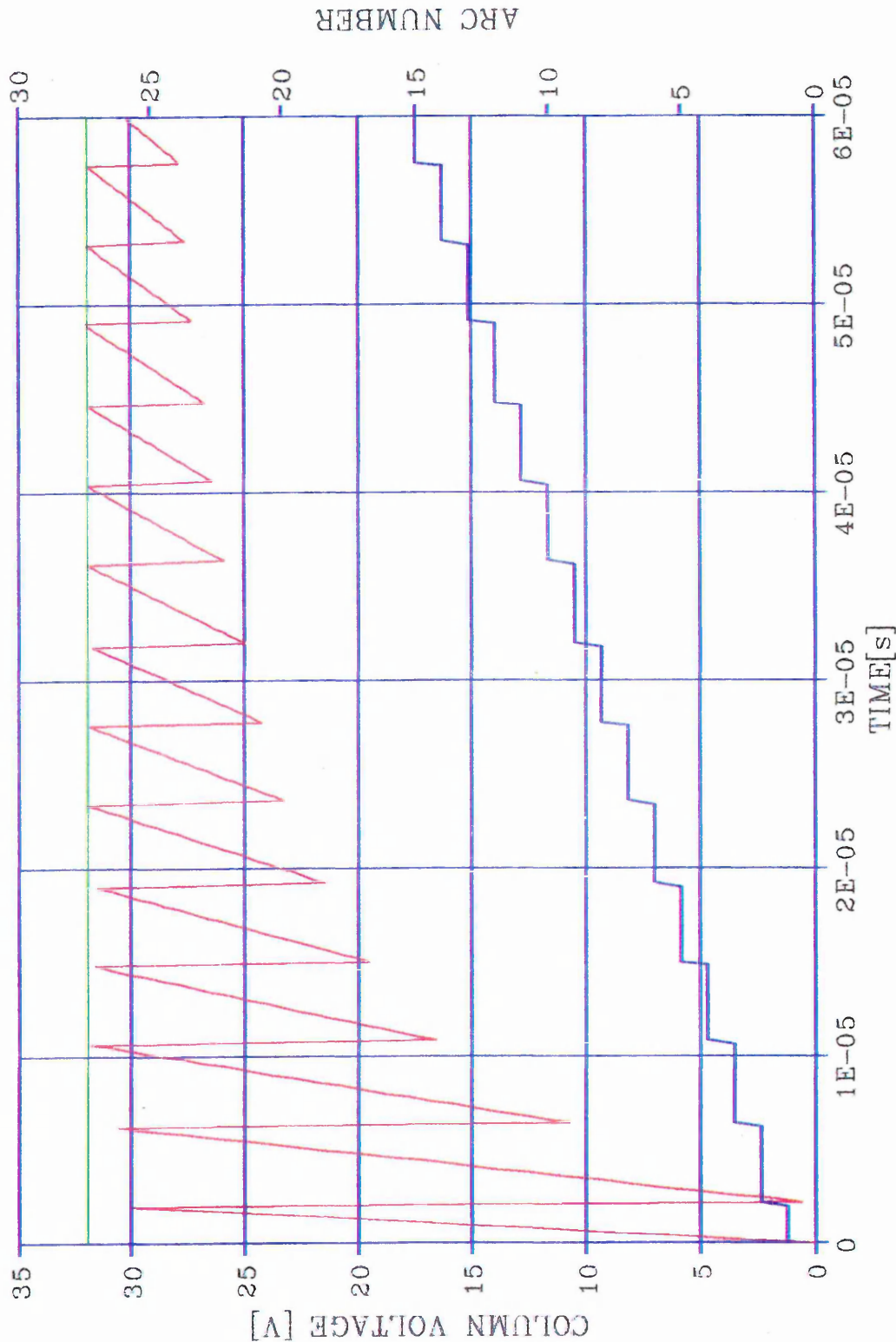


Fig. 2-10 Theoretical Column Voltage per Arc

Subject to conditions (i), (ii), (iii):

$$(i) E \cdot x(t) \max. = V_{ak} \quad \text{or} \quad E \cdot x(t) \leq V_{ak}$$

$$(ii) V_a \leq 2 \cdot n \cdot V_{ak} \quad \text{and} \quad V_a \geq (2 \cdot n - 1) \cdot V_{ak} \quad \text{for } (n = n \max)$$

$$(iii) E \cdot x(t) = V_{ak} \cdot (n-2)/n \quad \text{for } t = t_n$$

(where  $t_n$  is the time at commencement of the  $n^{\text{th}}$  arc)

The application of the proposed postulations gives an arc voltage variation with time following a straight line, because the individual column speed reduction is counter balanced for the increasing arc number or in other words the time interval for the arc mechanism progression is constant. Of course, the voltage conditions are averaged, although each individual arc will be slightly different in dimension and therefore indicate individual behaviour. The general agreement with the experiments results is however very convincing. Fig 2.11 shows the theoretical fuse arc voltage based on relation (b) and the assumption that the  $dv/dt$  for the first arc merging is the same that the  $dv/dt$  of the final arc formation, compared with the corresponding experimental results.

From the experimental-analytical comparison it is concluded that:

- The postulated arc mechanism demonstrates how arcs are formed and the linear increase in the fuse voltage.
- The results are consistent with some previous researchers results.
- The column  $dv/dt$  is constant for the time interval between each arc ignition, which implies that  $E$  and  $dx/dt$  are also constant.

The mathematical relationship for the proposed model is uncommonly simple. The theory has one weak point, which is that the time required for the voltage to reach its peak (or the speed of voltage increase) can not be readily predicted, by the proposed arc mechanism model.

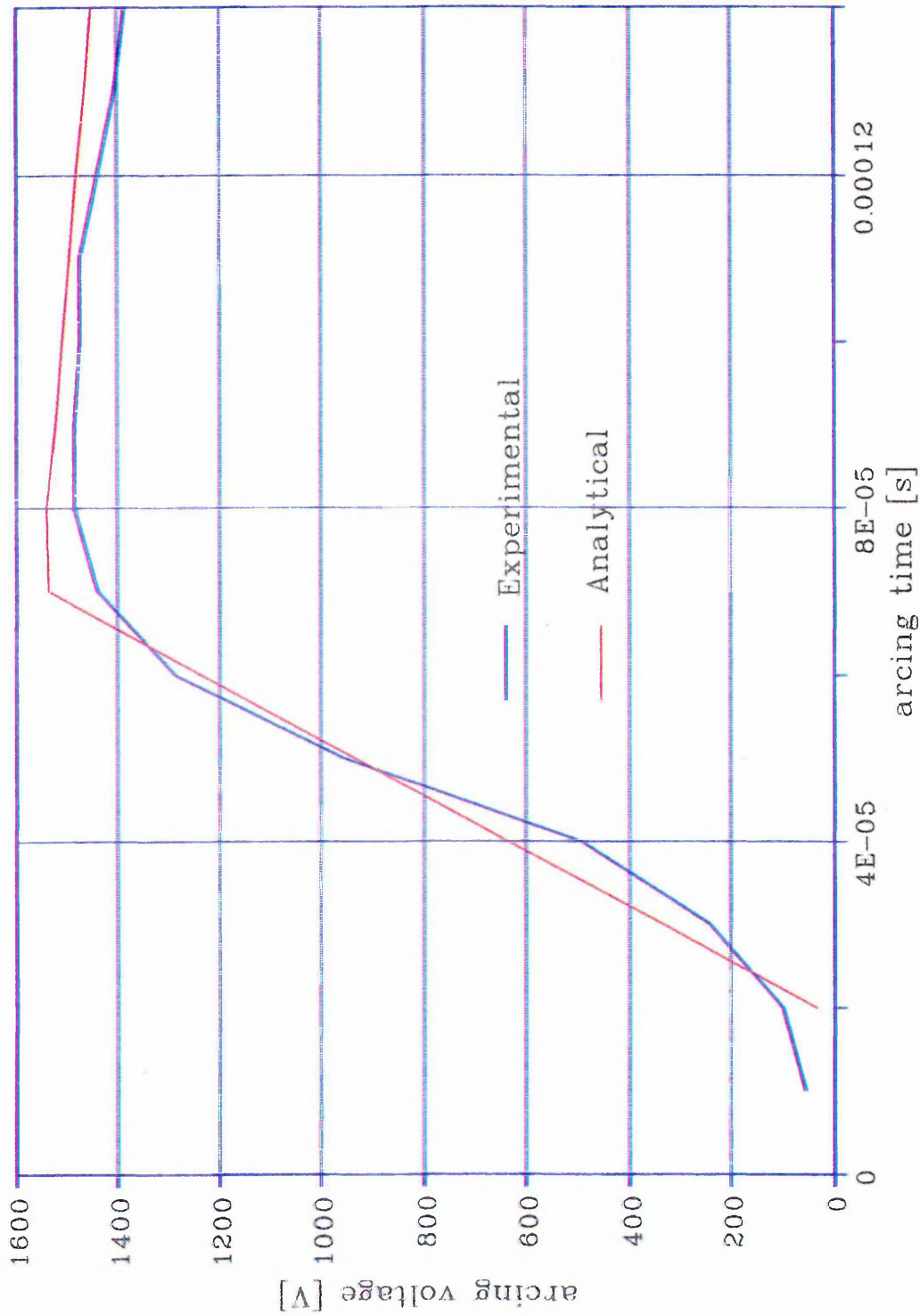


Fig. 2-11 Experimental and Predicted Arc Voltage Traces

### 2.3.3 Basic arc model for falling arc voltage

The same arc mechanism is applied to the arc phenomena subsequent to the occurrence of the arc voltage peak, that is when the arc voltage is decreasing after the peak. Based on the same postulation, the wave form shape for the theoretical arc voltage mechanism, Fig 2.12, can be obtained. This arc voltage shape implies that at the instant the voltage falls the number of arcs is a maximum. The fulgurite length will also be a maximum. The energy balance changes, however, since the voltage is decreasing.

When the arc voltage falls by a value equal to  $V_{ak}$ , then it is postulated that two of the arcs will merge. It is more likely that burn-back continues until two arcs merge, producing an initial fall in the arc voltage equivalent to  $V_{ak}$ . In any event the effect on the arc voltage is the same. There is therefore a loss of an arc root at this instant followed by a reduction of the new column voltage from  $2.V_{ak}$  to  $V_{ak}$ , thus the voltage equivalent to  $2.V_{ak}$  is eventually shared by the remaining arcs. Given that the arc chain length is the length of the fuse wire, then each arc length increases with the time while the arc number is decreasing, but the addition of the partial lengths, or the whole length, is constant. This phenomena results in a column voltage fall whilst the column length increases, which can be explained only if the column diameter decreases at a faster rate than the column length increases. This would occur if the energy losses increased at a faster rate than the energy available from the circuit. This narrowing of the arc column diameter is consistent with arc extinction and wall stabilized conditions and pressure build-up.

If for example wall stabilized conditions breakdown, the pressure reduces the arc increases in diameter and the fuse arcs fail to extinguish by this mechanism, i.e. the fuse is a bad fuse.

As an example the conditions when the number of arcs is changing from 10 to 9 is considered:

- When the ten arcs exist, the individual arc arc-root voltage drop and positive column voltages are both 32 V. The total arc voltage therefore is 640 V.
- When the fuse voltage fall to 576 V i.e.  $(640 - 2.V_{ak})$  the ten positive column voltages falls to 25.6 V each., however with 576 V it is possible for 9 arcs to exist

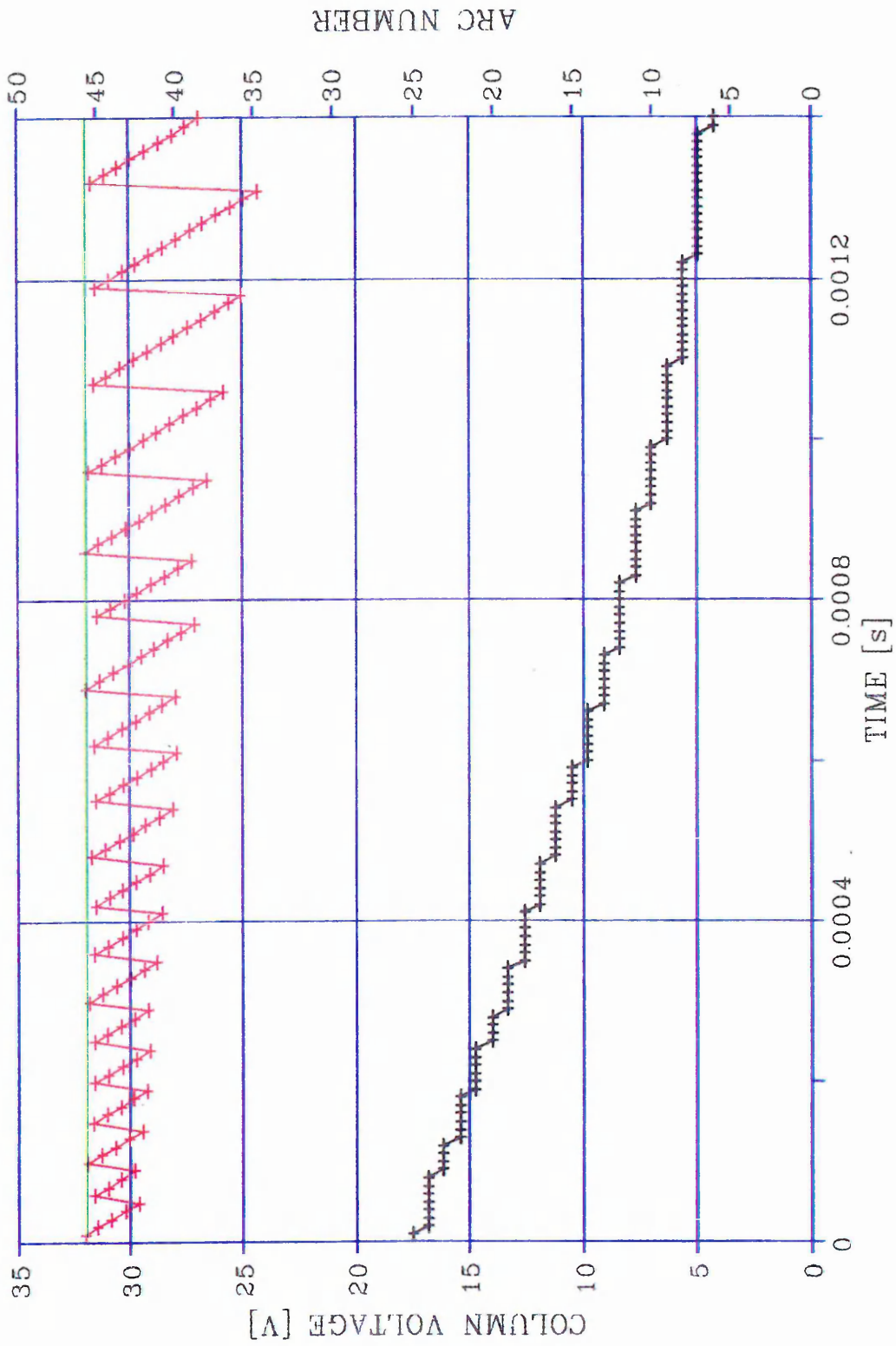


Fig. 2-12 Theoretical Column Voltage per Arc

where, the maximum voltage for each of them 64 V. It follows therefore that two of the previous arcs can coalesce into one.

- The individual arc length will then change from one tenth part of the wire length to one fifth, in other words the arc length will increase by 100 %.
- As the column voltage is decreasing and at the same time the length is increasing, the former consideration that the voltage gradient remains constant no longer applies, since there is no significant burn-back (i.e. equation (b) strictly applies in this case).
- The result of this process is that the decrease in the positive column voltage gradient, causes an increase of the length of the lumen, due to either the ablation of the fulgurite walls or their erosion.

The experimental results **Fig 2-13** show that the proposed mechanism theory is applicable, the main difference with the previous situation is that now the slope of the column voltage is constant for nearly the whole arcing period. From the comparison of figures 2-12 & 2-13, it may be concluded that the proposed theory is soundly based.

The only unexplainable part of the phenomena is that the last and penultimate arcs can not be described by the simple equation.

In **Fig 2-14** a comparison of fuse arc voltage experimental and analytical results is shown, in which the constant value for the slope was estimated from the experimental voltage wave forms. From this comparison, the following conclusions may be established:

- The theory provides an explanations of how the arcs merge.
- The positive column  $dv/dt$  is constant for the whole post-peak arc interval and hence  $E$  is constant.
- The comparison between theory and experimental results is good, the accuracy being between  $\pm 5\%$  (for  $n > 2$ )

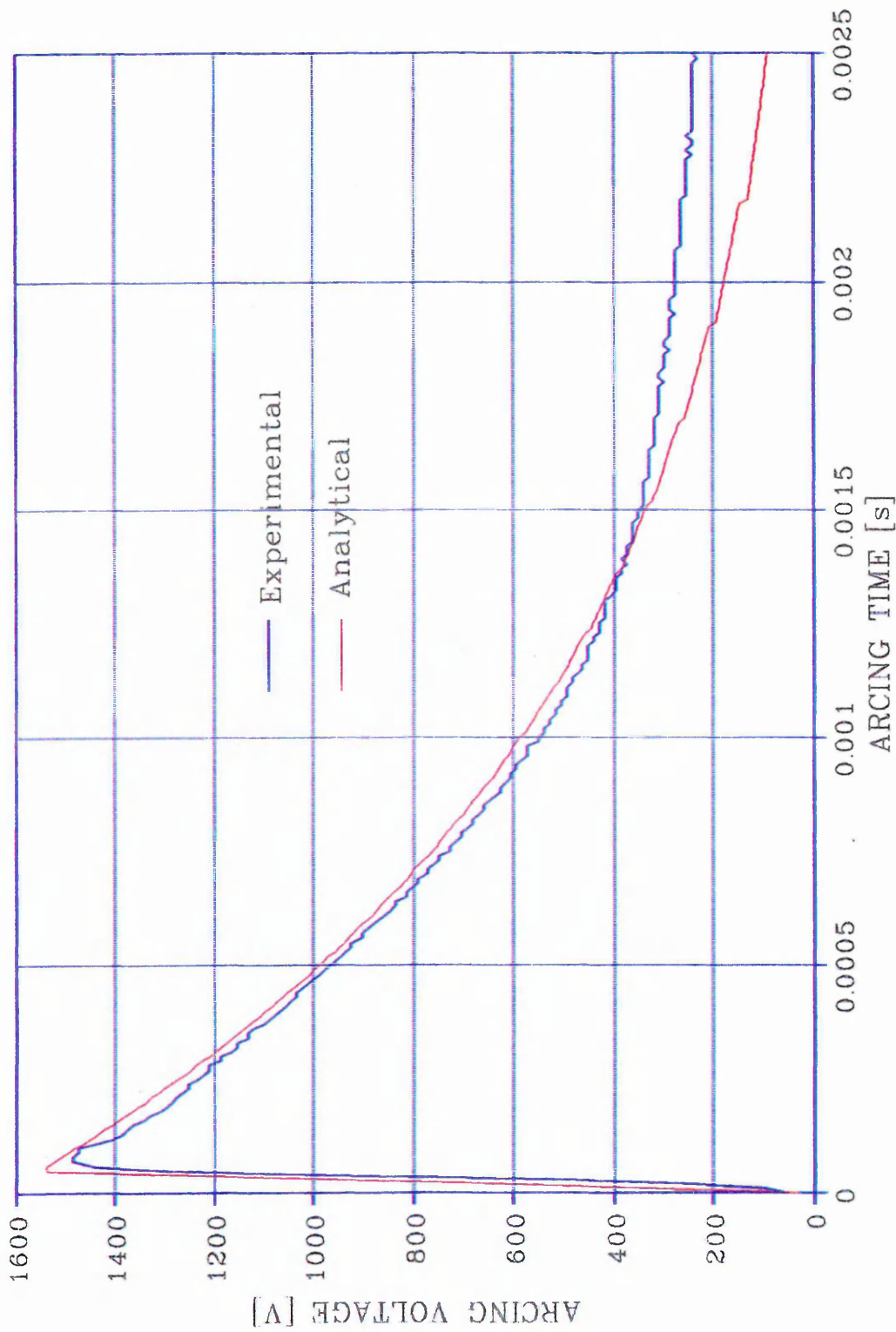


Fig. 2-14 Experimental and Predicted Arc Voltage Traces

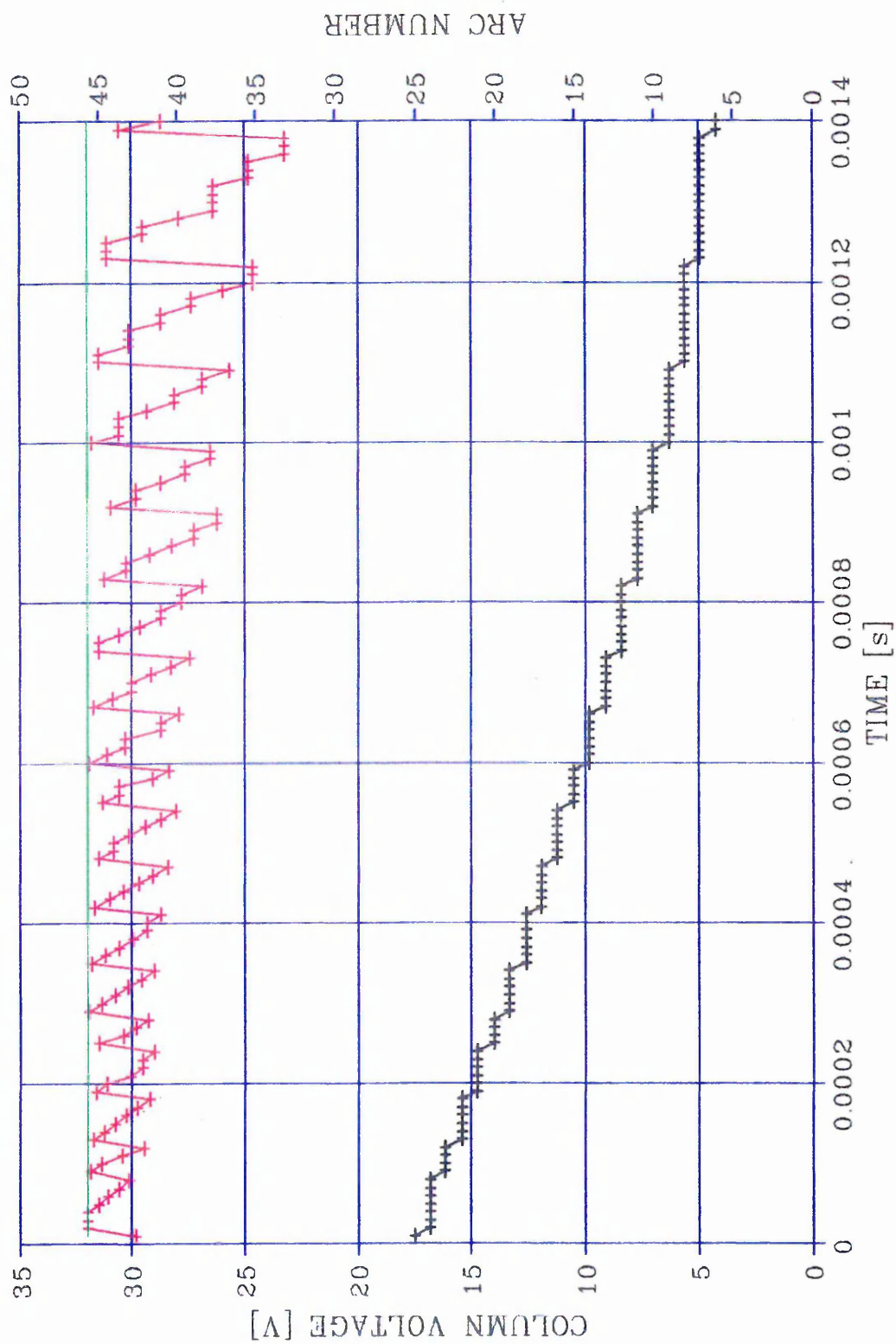


Fig. 2-13 Experimental Column Voltage per Arc

#### 2.3.4 Limitations of basic arc mechanism model

From the preceding explanation and the finite number of tests carried out the limitations of the model were examined and listed in order of significance :

- The model in its simplest form can not be used to predict the arcing behaviour in wires when the number of arcs is less or equal to two.
- In the region of the maximum voltage the analytical values are slightly larger and more peaked than the experimental values. The reason proposed for the difference is that the circuit stored energy is not sufficient to keep the number of arcs burning.
- The model is based on an arc-root voltage drop value, which is assumed to be constant as which must be empirically ascertained. It is considered also that this value depends on the filler and fuse element characteristics.
- Unlike Hibner's equation the model can take account of the filler's influence on the arc voltage if the arc-root voltage fall is known.
- The  $dv/dt$  for the pre-peak arc voltage phenomena is obtained from experimental results, the relation with circuit energy and filler/fuse element characteristics must also be found.
- The post-arc  $dv/dt$  constant must also be determined experimentally.

#### 2.3.5 Evaluation of model for wires in fillers

A test program was conceived in order to study the phenomena to resolve some of the described limitations. As previous studies were conducted for critical current conditions, the test program was basically extended to cover currents from 1400 A to 11000 A (in six ranges 1400A, 2540A, 3990A, 6050A, 8000A and 11000A), with making angle of  $0^\circ$ ,  $20^\circ$ ,  $70^\circ$  and  $90^\circ$ ; keeping constant the former power factor 0.2 , test voltage 230 V and the fuse element diameter, material and length.

The influence of quartz grain size was also studied, by using a very high quality fuse filler, having roundish grains, in two different sizes 40/50 and 50/80 ASTM standard sieves. The samples were assembled using the same DIN 00 standard body, and silver

wire of 0.6 mm and 35 mm in diameter and length, and again utilising the standard filling and measuring procedures.

The test methodology was straightforward. After the prospective current had been calibrated the fuses were operated and the current, system voltage and arc voltage data were stored as before. The next step consisted of the application of the proposed model to the new test conditions. Previously the prearcing period was calculated based upon the concept of  $I^2t$  to being constant. From comparison between the prearcing analytical and experimental behaviour it was determined that it is not necessary to use a more accurate methodology as for example the finite elements technique, due to the short time involved.

For the employment of the proposed model the average arc-root voltage drop was calculated and the number of arcs obtained from the X-ray plates, which gave 49.6 V and 20 arcs respectively. On the other hand the pre-peak and post-peak  $dv/dt$  values were obtained in an empirical way by trial-and-error. On this basis the number of arcs determined agree with the value obtained by the application of the well known equation, for striated wire disintegration:

$$h = 0.555 + 2.08 \cdot d = 1.8 \text{ mm}$$

which gives the number of arcs =  $1 / d = 19.4$  arcs.

The average arc-root voltage drop was 50 % greater than the value previously determined for normal quartz sand, which shows that the filler has an influence on the  $V_{ak}$  value and hence on the arc voltage. The analytical and experimental results are given in Table 1.

In **Figures 2-15 & 2-16** examples of the application of the proposed method are shown, which enable the accuracy of the simulation to be assessed.

It is interesting that no important differences in the postulated arc behaviour were detected when the two sample quartz grain sizes were tested.

Studying the experimental and theoretical results a relationship between the column voltage time and the inductance (or energy stored in the test circuit) was found, **Fig 2-17**. From the analysis of this relationship it can be concluded that the pre-peak  $dv/dt$  is

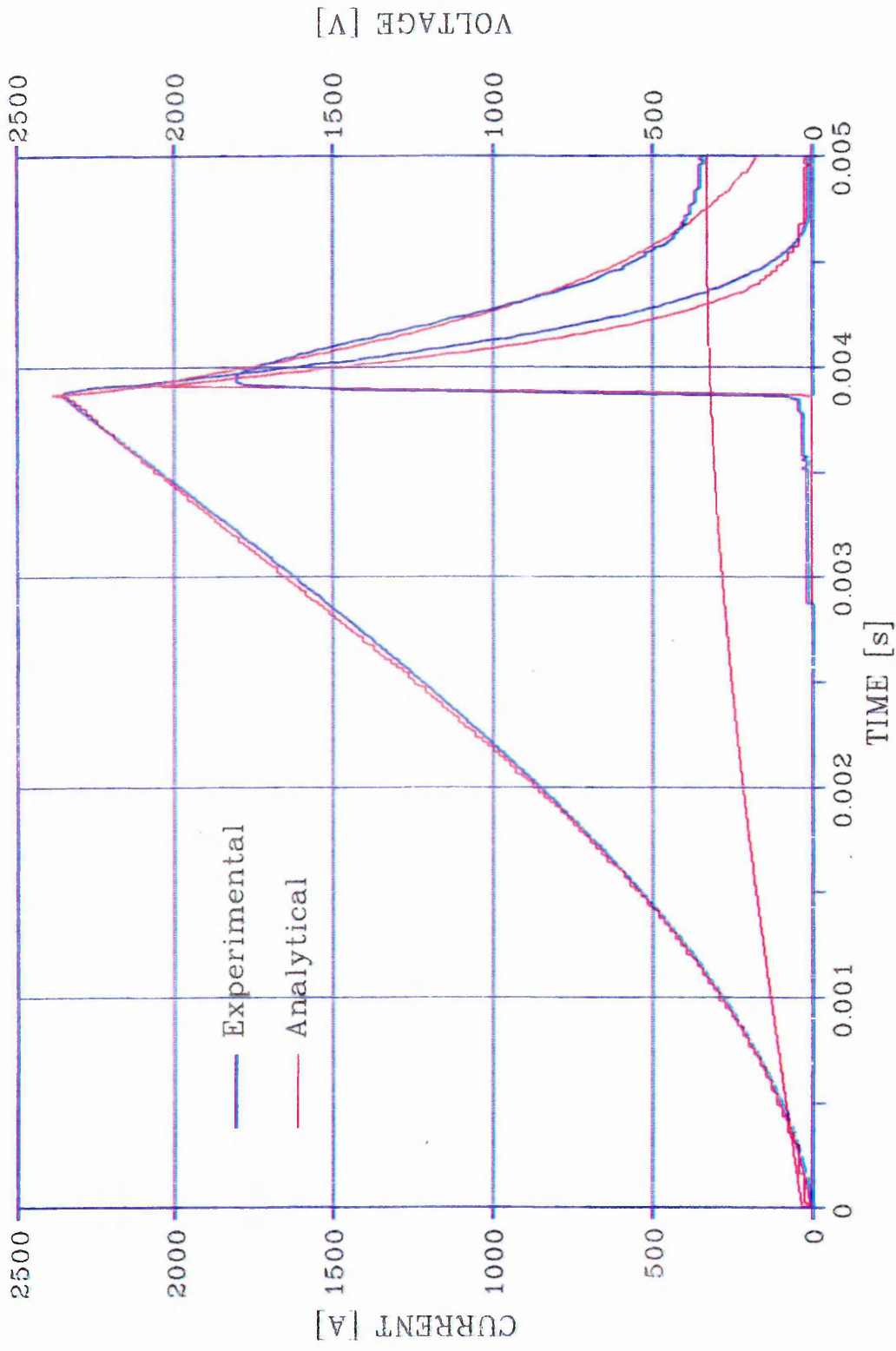


Fig. 2-15 Experimental and Analytical Prediction

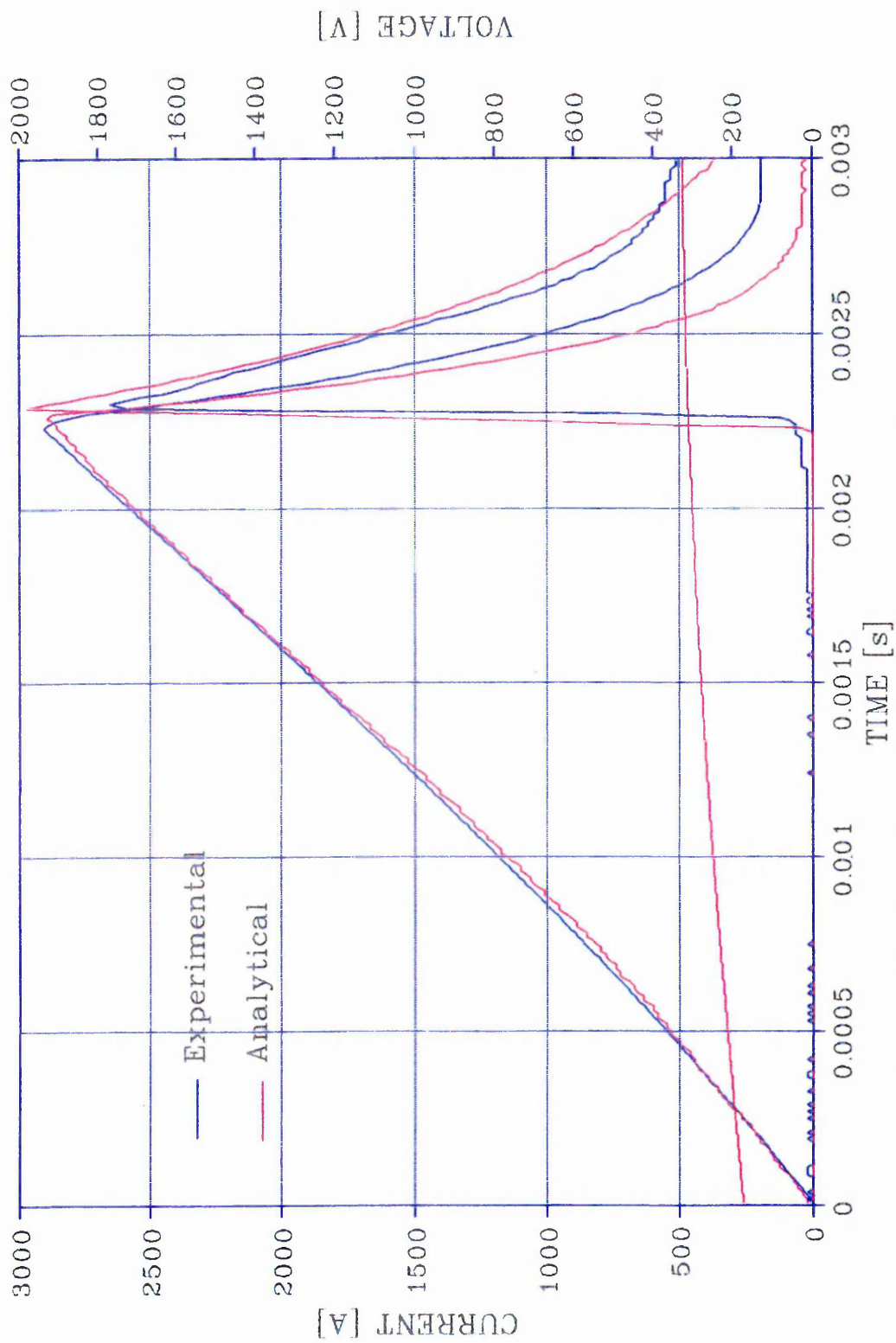


Fig. 2-16 Experimental and Analytical Prediction

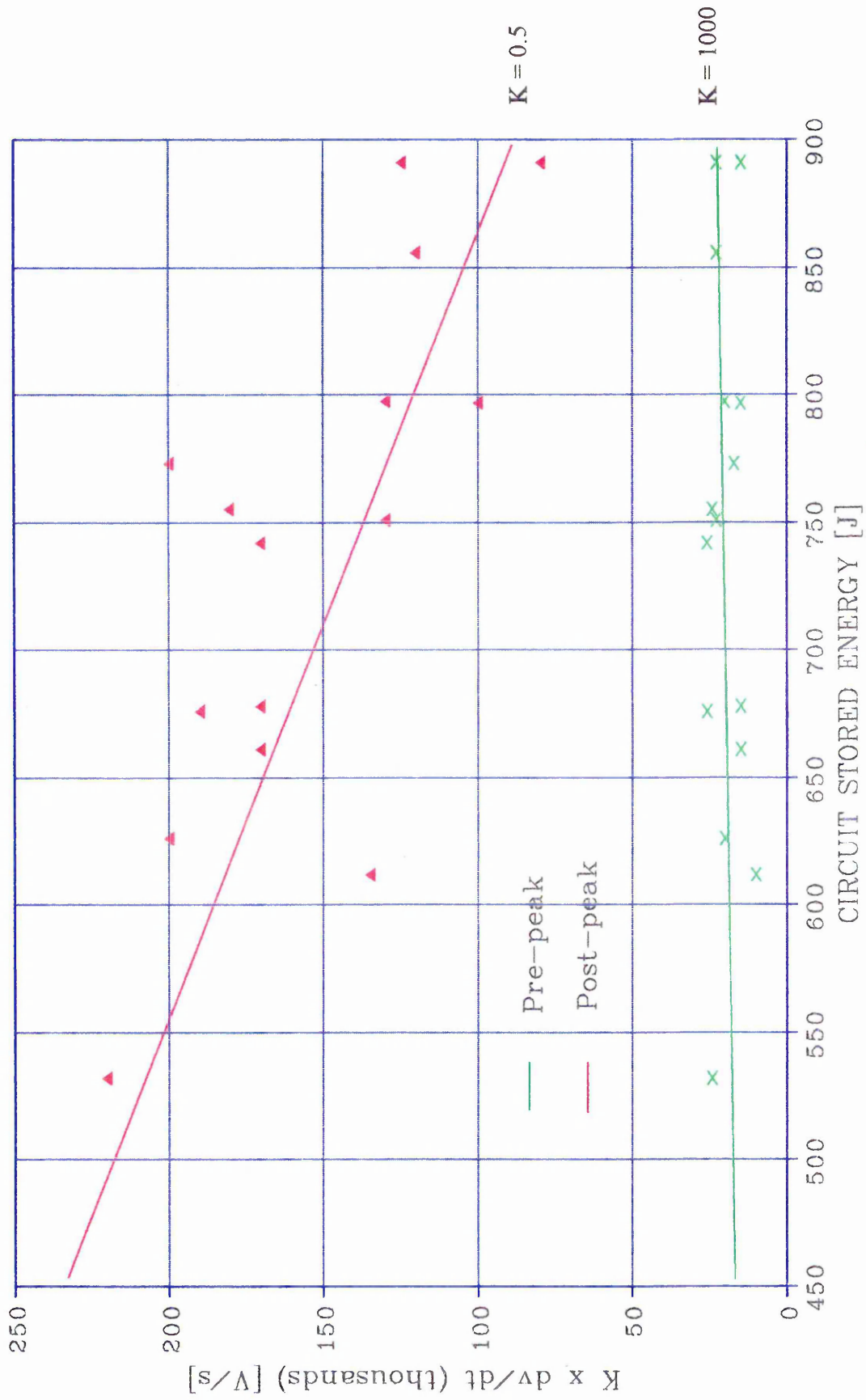


Fig. 2-17  $dv/dt$  as a circuit stored energy function

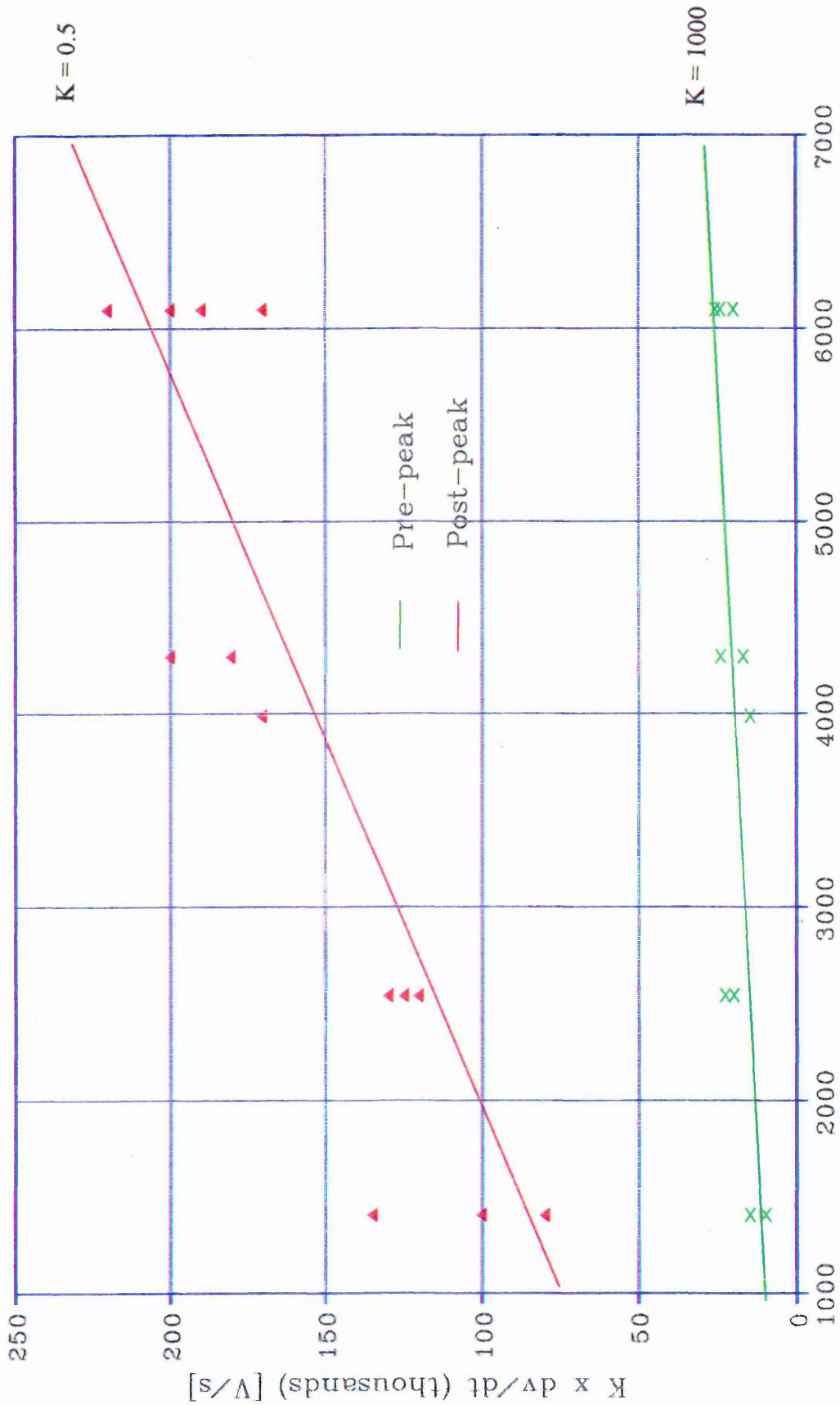


Fig. 2-18  $dv/dt$  as a prospective current function

virtually independent of the energy. On the other hand, the post-peak  $dv/dt$  decreases as the energy increases showing the quenching difficulty when the circuit stored energy increases. The relationship for column voltage as a function of prospective current is given, **Fig 2-18**.

The following conclusions can be drawn from the comparison between the experimental and analytical results for the current and arc voltage using the proposed model :

- A simple arc model mechanism for wire high breaking capacity fuses has been demonstrated to give good results.
- The model is capable of predicting the fuse current and voltage characteristics accurately.
- The model is valuable for explaining the arc mechanism and the experimental observations obtained using crow-bar, X-ray and optical fiber methodologies.
- The arc-root voltage drop and total arc voltage vary as a function of the physical properties of the filler. (grain shape and size)
- The pre-peak and post-peak  $dv/dt$  are functions of the circuit trapped energy or prospective current, the effect on the pre-peak  $dv/dt$  being only marginal.

These explanations allow the idea of an 'ideal fuse' to be introduced and defined for short-circuit current interruption. This definition would be a fuse whose behaviour satisfies the previously described wall stabilised arc conditions precisely, and therefore satisfies the proposed theoretical mechanistic model arc conditions, over the whole of the pre-peak and post-peak arcing periods.

#### 2.4 References

1. Nairne, E.; *Electrical Experiments by Mr. Edward Nairne*; Phil. Trans. Royal Soc., vol. LXIV, pp. 79-89, London, 1774.
2. Kleen, W.; *Über der Durchgang der Elektrizität durch metallische Haardrahte (On the passage of electricity through fine metallic wires)*; Ann. Phys., Vol. II, pp. 579-605, Lpz., 1931.
3. Baxter H.W.; *Electric Fuses*; Edward Arnold, London, 1950.
4. Carne, E.B.; *A mechanism for the fuse pre-arcing period*; AIEE Trans., Vol. 72, pp. 593-599, August 1953.

5. Nasilowski, J.; The process of short circuit opening by a fuse with single wire fuse element and explanation of some phenomena observed during its operation; First Int. Conf. on Swit. Arc Phen., Lodz, 1970.
6. Vermij, L.; Electrical Behaviour of Fuse Elements; Thesis, Eindhoven University, The Netherlands, May 1969.
7. Ossowicki, J.; Attempt at Systematic Arrangement of Mechanisms of Wire Fuse Elements Disintegration at overload; First Int. Conf. on Swit. Arc Phen., Lodz, 1970.
8. Lipski, T. Furdal, A.; New observations on the formation of unduloids on wires; Proc. IEE, Vol. 117, n° 12, December 1970.
9. Zimny, P.; On the magneto-thermo-viscous-elastic mechanism of unduloids formation on wires; Second Int. Conf. on Swit. Arc Phen., pp. 241-246, Lodz, 1973.
10. Lipski, T.: Why unduloids do not always appear?; Third Int. Conf. on Swit. Arc Phen., pp. 305-310, Lodz, 1977.
11. Turner, H.W.; Third Int. Conf. on Swit. Arc Phen., Post Conference Materials, pp. 183-184, Lodz, 1977.
12. Dolegowski, M.; Voltages in Single Short Arcs in Sand-filled Fuselinks and Elements with One Neck; First Int. Conf. on Swit. Arc Phen., pp 219-225, Lodz, 1970.
13. Wright, A. Beaumont, K.J.; Analysis of high-breaking-capacity fuselink arcing phenomena; Proc. IEE, vol. 123, n° 3, pp. 252-258, March 1976.
14. Lipski, T.; Correspondence on Analysis of high-breaking-capacity fuselink arcing phenomena; Proc. IEE, Vol. 123, n° 12, December 1976.
15. Mikulecky, H.W.; Current-Limiting Fuse with Full-Range Clearing Ability; IEEE Trans. on PAS, Vol. PAS-84, n° 12, pp. 1107-1116, December 1965.
16. Hibner, J.; The Voltage of Single Disrupt in a Chain of Arc Intervals by Short-circuit Disintegration of Strip Fuse Elements of Fuses; First Int. Conf. on Swit. Arc Phen., pp. 226-231, Lodz, 1970.
17. Hibner, J.; Calculation of overvoltage peak-values when breaking short-circuits by means of multi-strip fuses; Second Int. Conf. on Swit. Arc Phen., pp. 269-274, Lodz, 1973.
18. Lipski, T.; Application of the arc-pinch-forces-interaction theory to the calculation of striation modulus of the strip H.B.C. fuses; Second Int. Conf. on Elec. Fuses and their App.; pp.52-59, Trondheim, 1984.
19. Jakubiuk, K.; Electrothermal fuse-element disintegrating mechanism by short-circuit currents; Fourth Int. Conf. on Elec. Fuses and their App.; pp.226-230, Nottingham, 1991.
20. Dolegowski, M.; Geschwindigkeit der verlängerung des lischbogens bei den streifensicherungen mit sandlosch-mittel (Speed of increase in length of arc for sand-filled strip fuses); Second Int. Conf. on Swit. Arc Phen., pp. 275-282, Lodz, 1973.
21. Arai, S.; Deformation and disruption of silver wires; First Int. Conf. on Elec. Fuses and their App.; pp.50-58, Liverpool, 1976.
22. Hibner, J.; The operation joule-integral calculation of current-limiting fuses by the resistance method; Third Int. Conf. on Swit. Arc Phen., pp. 293-299, Lodz, 1977.
23. Lipski, T.; Post conference materials.Third Int. Conf. on Swit. Arc Phen., pp.184-187, Lodz, 1977.
24. Hibner, J.;Post conference materials.Third Int. Conf. on Swit. Arc Phen., pp.193-195, Lodz, 1977.
25. Edels, H. Fenlon, F.H.; Theory of a filled-tube thermal arc column; Brit. J. Appl. Phys., Vol. 16, pp. 219-230, 1965.
26. Oliver, R.; The elementary structure of the cartridge fuse arc; Third Int. Conf. on Swit. Arc Phen., pp. 310-314, Lodz, 1977.

27. Ranjan, R. Barrault, M.R.; Axial electric-field measurements of d.c. arcs in current-limiting fuses; IEE Proc., vol. 127, Pt. C, n° 3, pp. 199-202, May 1980.
28. Bizjak, M. et al; Evaluation of stationary characteristics of arc burning in a narrow quartz channel; Ljubljana University, Internal report, Yugoslavia, 1986.
29. Bizjak, M. et al; Characteristics of Arc in Melting Fuse Element filled with Quartz Sand; 6th. Medit. Elec.Conf. IEEE, pp.1493-1496, Ljubljana, 1991.
30. Barrow, D.; Evaluation of arcing parameters in High Breaking Capacity Fuses; PhD Thesis, Nottingham University, October 1988.

## Chapter 3 : Arc models for practical fuse links.

### 3.1 Evaluation of arc model for practical HBC fuses

The good accuracy obtained using the proposed arc model developed for single wire fuse elements is extended to the study of element shapes which approximates to those used in practical industrial semiconductor type fuses.

The fuse construction used in this study was the DIN 00 standard type previously employed. The assembly and filling methodologies were also the same.

The power circuit, data acquisition and recording equipments together with the test procedure were also not modified and X-ray plates were obtained in the same way. The crow-bar circuit and fiber optic system were not used in this study.

#### 3.1.1 Fuse elements types and arc quenching media

The arc mechanism model was applied to the following basic fuse elements types:

- single uniform strip
- single notched strip:
  - long notch
  - medium notch
  - short notch

---

*"It should be noted that aspects of these studies have been omitted from this chapter owing to patent limitations regarding premature disclosure"*

- parallel single elements:

two uniform wires

two uniform strips

All the samples were manufactured from silver of the same purity as the wire fuse elements studied. The dimensions of the strip were specially prepared in order to preserve the same characteristics as that of the wire. For example the strip was made the same length (35 mm). The cross-section was approximately the same i.e. 3.2 mm width and 0.0813 mm thickness (wire cross-section 0.283 mm<sup>2</sup> was slightly larger than the strip cross-section 0.260 mm<sup>2</sup>).

The selected arc quenching materials used were compacted silica sand and bound filler.

### 3.2 Evaluation of arc model for compacted filler

#### 3.2.1 Single strip fuse element:

The filler used in the fuse samples was the same as previous i.e. roundish silica grain size determined by 40/50 and 50/80 ASTM standard sieves.

The tests were performed using a similar test circuit and procedures. The subsequent analytical study based on the proposed arc model was also the same. Tests were undertaken for four currents each with a different making angle. Two quartz grain sizes were tested giving a total number of 32 tests for each element.

The comparison of experimental results between strip and wire fuse elements, accepting variations due to manufacturing tolerances of different samples and consistency of the data acquisition setting's, indicates the following :

- Slight differences between the prearcing behaviour (specific energy, peak current and time) were found due to the small discrepancy of the wire and strip fuse element cross-sections. **Figures 3.1 & 3.2.**
- Insignificant differences between the results using fine or coarse quartz sand were detected. The main discrepancy can be seen in the final part of the arc extinction period **Fig 3.3**, being longer when fine sand is used. This behaviour is similar to that previously found in wire fuse elements.
- The peak voltage with coarse quartz sand was on average 5 % greater than for the corresponding values obtained using the fine filler. This was the same as found for wires.
- The number of arcs obtained from the observation of fulgurite by X-ray plates was identical to that of wires. The average being 20.

The great similarity between the wire and strip fuse element results confirms that the proposed model should be equally applicable for strip elements. This hypothesis was investigated by applying the same criteria developed for the arc mechanism in wires.

First the anode-voltage drop was maintained constant at 49.6 V and the maximum number of arcs was kept the same i.e. 20. The pre-peak and post-peak  $dv/dt$  values were determined empirically as previous.

The current and arc-voltage wave forms based on the analytical and experimental results for a single strip fuse element, under different current and making angle conditions, are shown in **Figures 3.4 & 3.5** and in **Tables 1 & 2**, (Appendix 1) from which comparison can be made.

From the experimental and theoretical results the relationship between the column voltage/ time and or energy stored in the test circuit, was found to be similar to that determined for wire fuse elements. **Fig 3.6.**

The relationship expressed in terms of prospective current is also shown in **Fig. 3.7** .

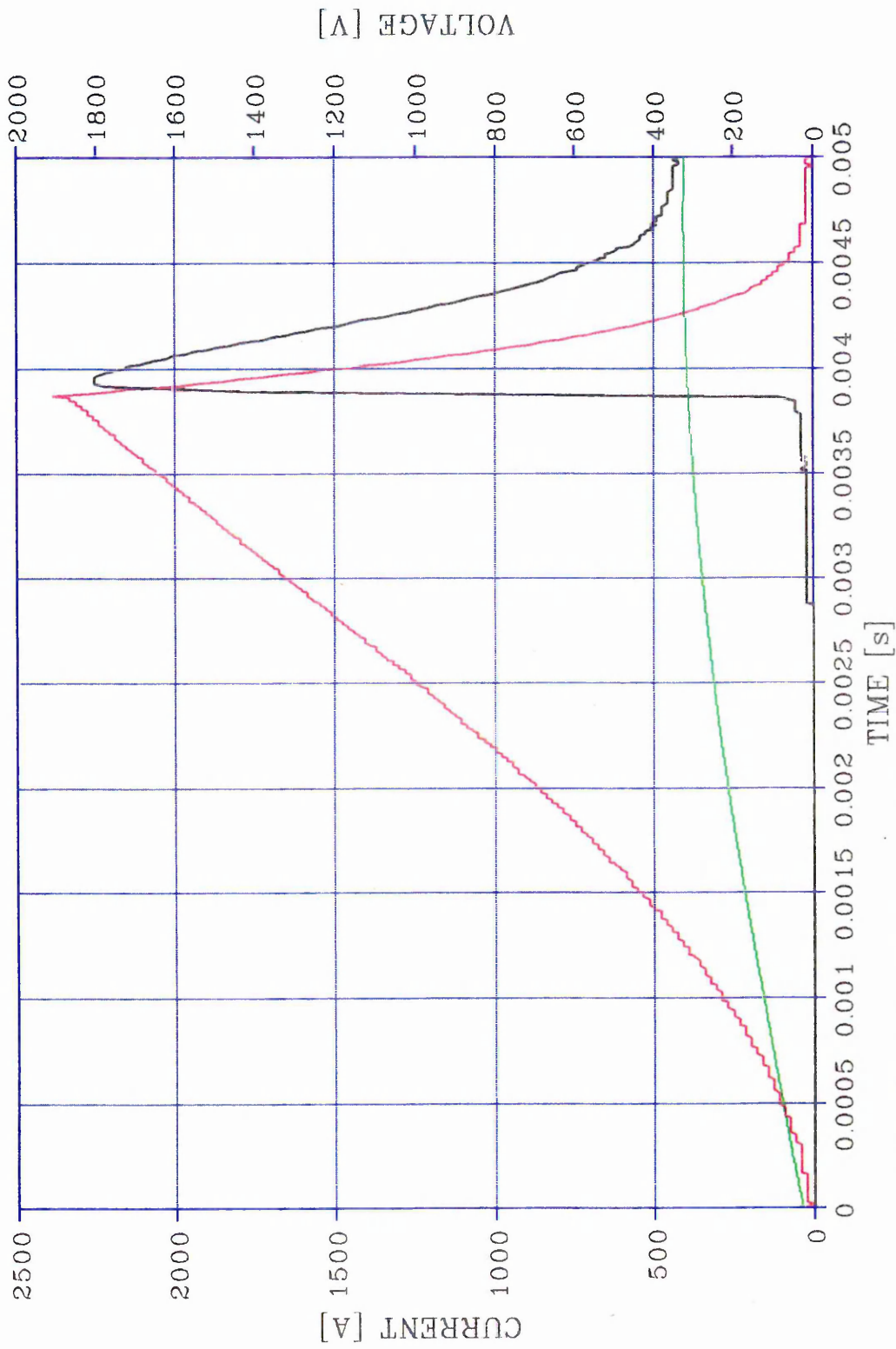


Fig. 3-1 Short-Circuit Test Voltage and Current Waveforms  
for Wires ( $I_{pros} = 2540$  A,  $\theta = 5^\circ$ )

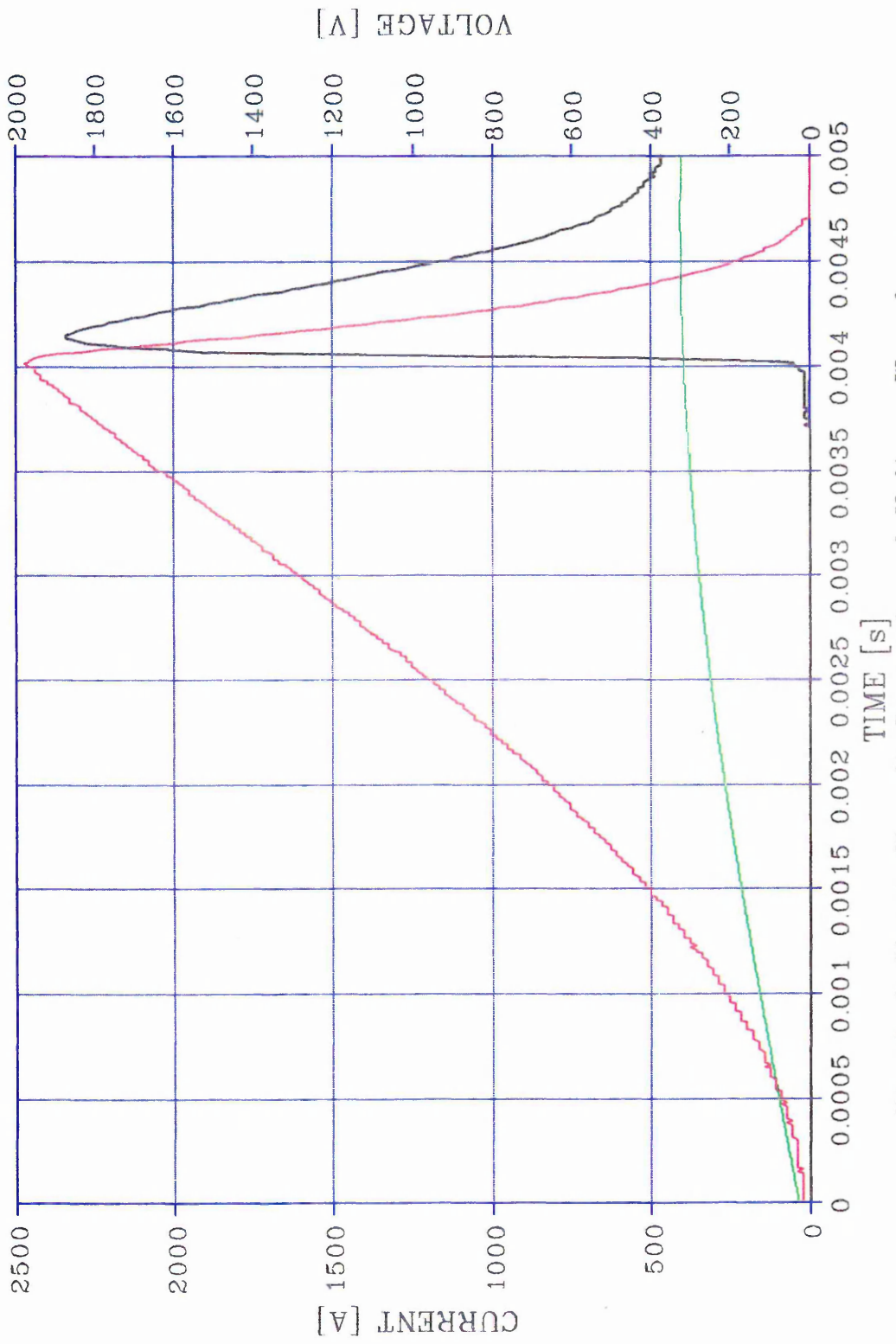


Fig. 3-2 Short-Circuit Current and Voltage Waveforms for Uniform Strip (I<sub>prosp.</sub> = 2450 A, Theta = 5°)

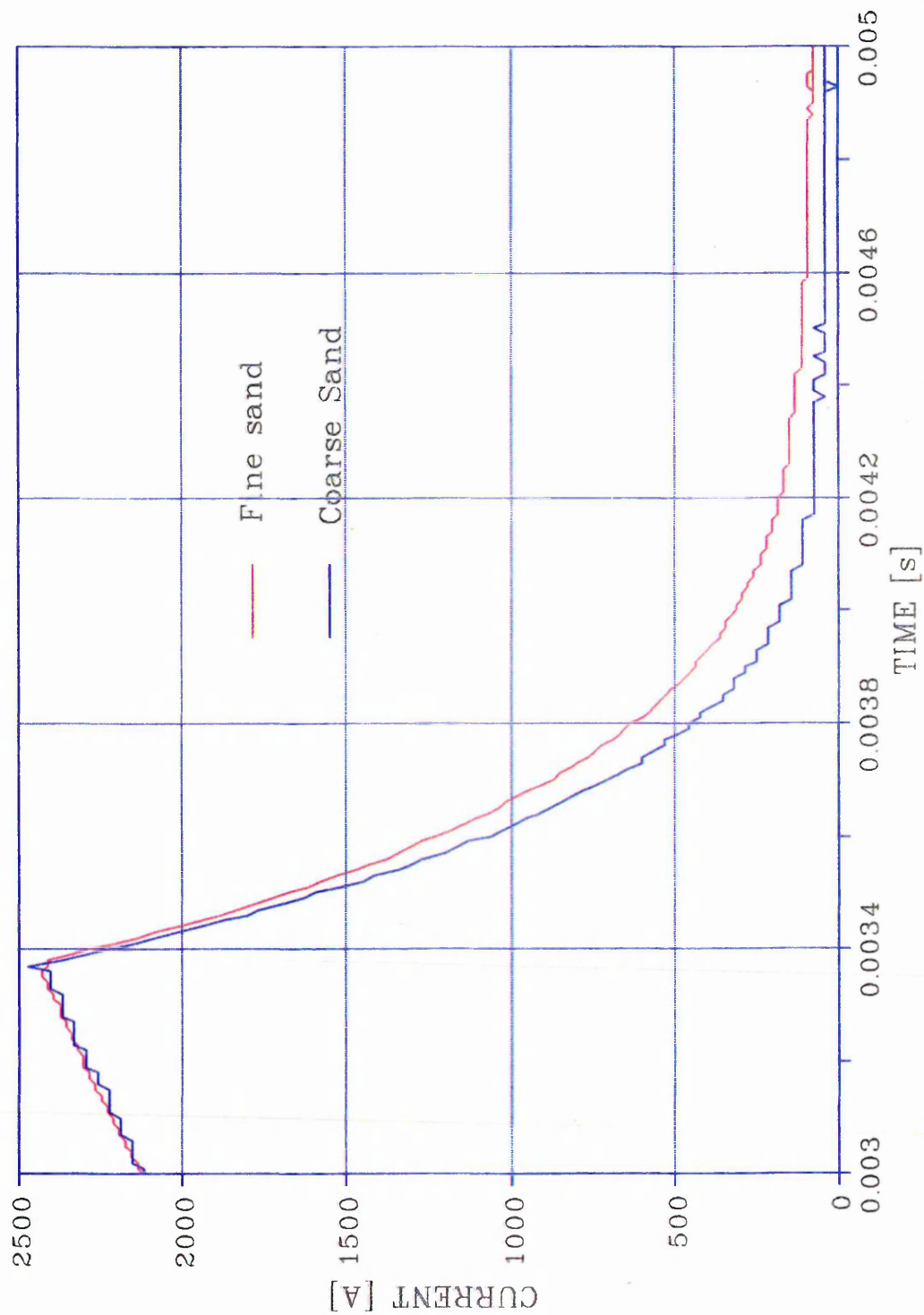


Fig. 3-3 Experimental Short-Circuit Current for Uniform Strip Element using fine and coarse sand filler

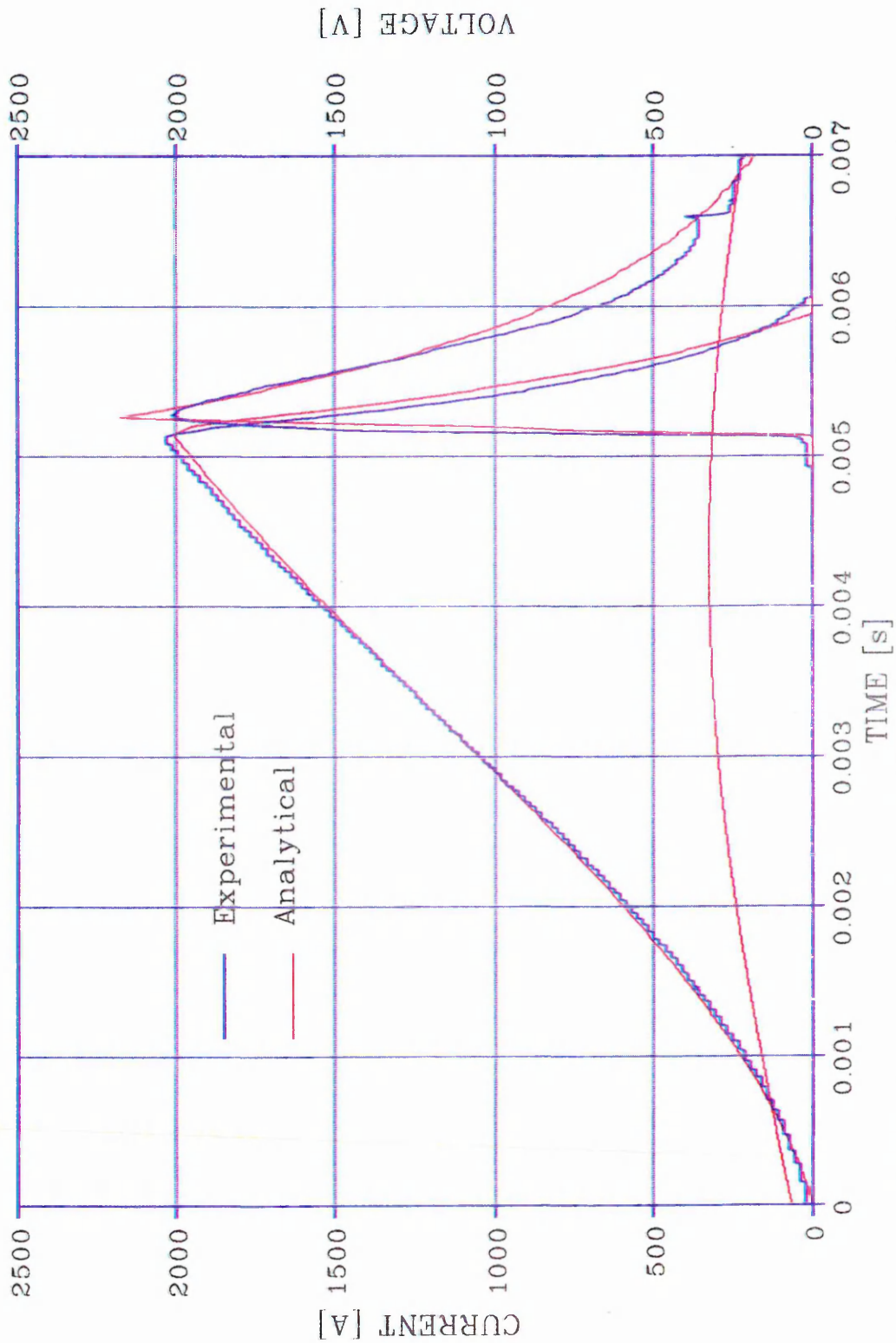


Fig. 3-4 Experimental and Analytical Short-Circuit Current and Voltage Waveforms for Uniform Strip Element ( $I_{\text{prosp.}} = 1404 \text{ A}$ ,  $\text{Theta} = 12^\circ$ )

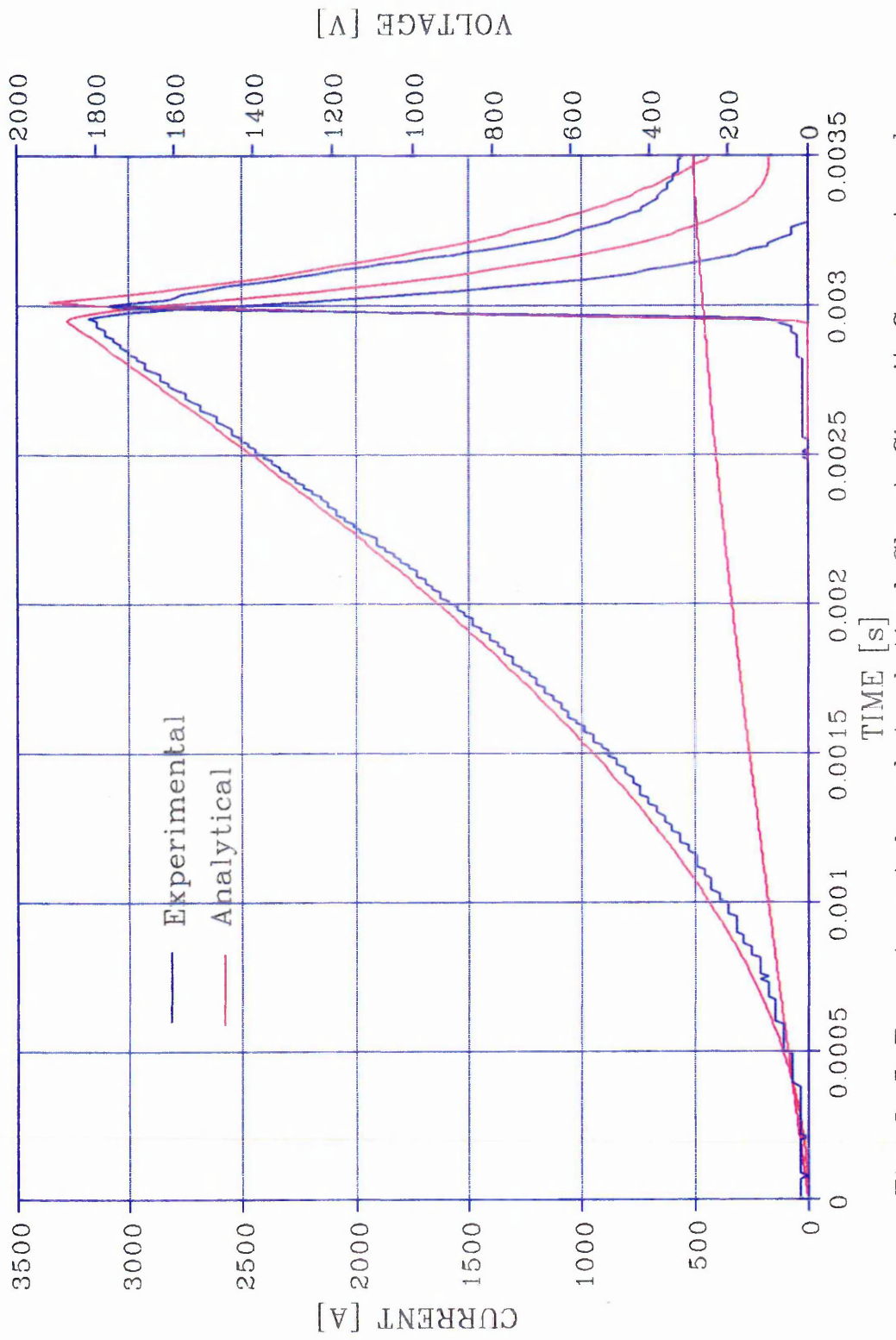


Fig. 3-5 Experimental and Analytical Short-Circuit Current and Voltage Waveforms for Uniform Strip Elements ( $I_{\text{prosp.}} = 6100 \text{ A}$ ,  $\text{Theta} = 0^\circ$ )

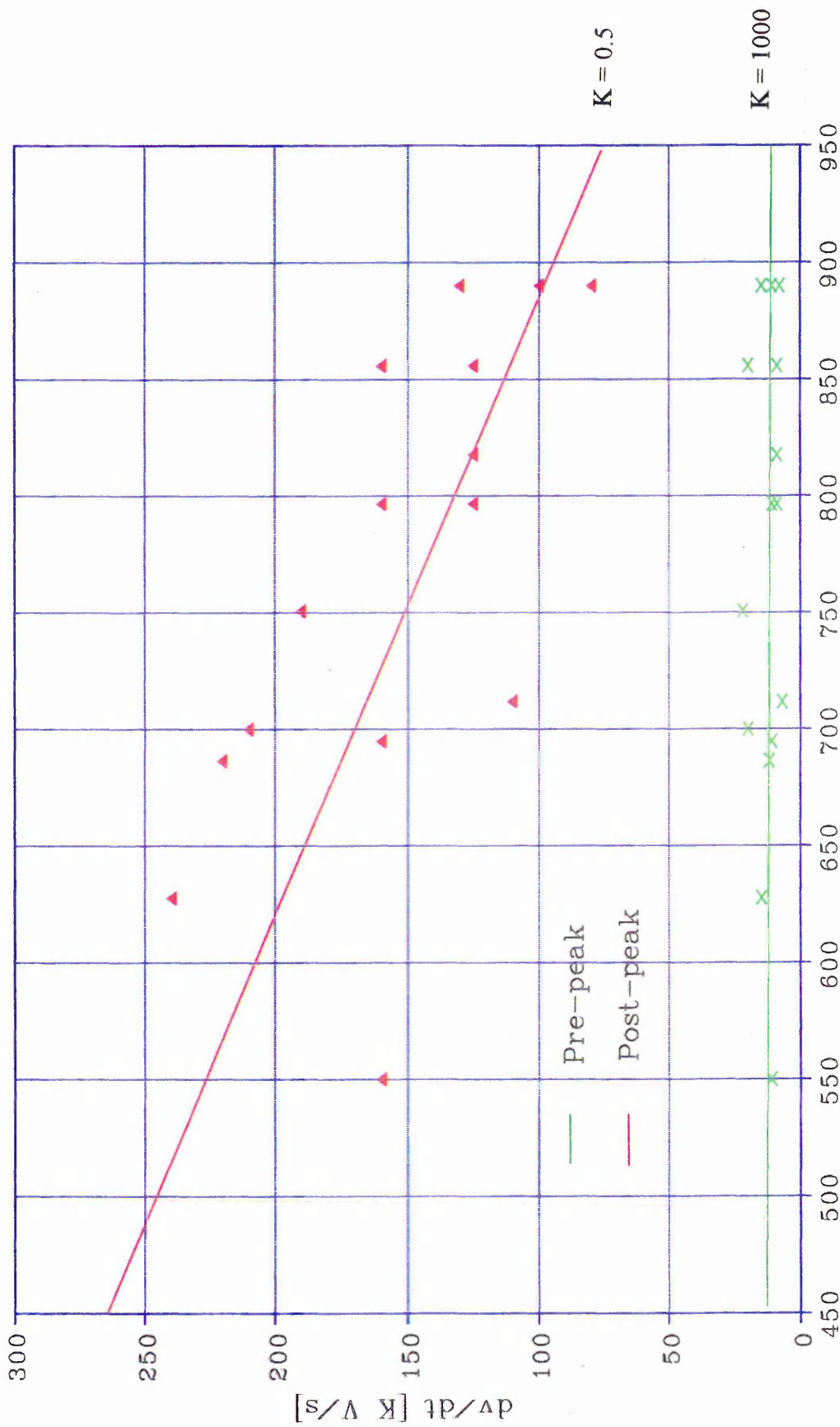


Fig. 3-6 Relationship between  $dv/dt$  and Circuit Stored Energy for Uniform Strip Elements

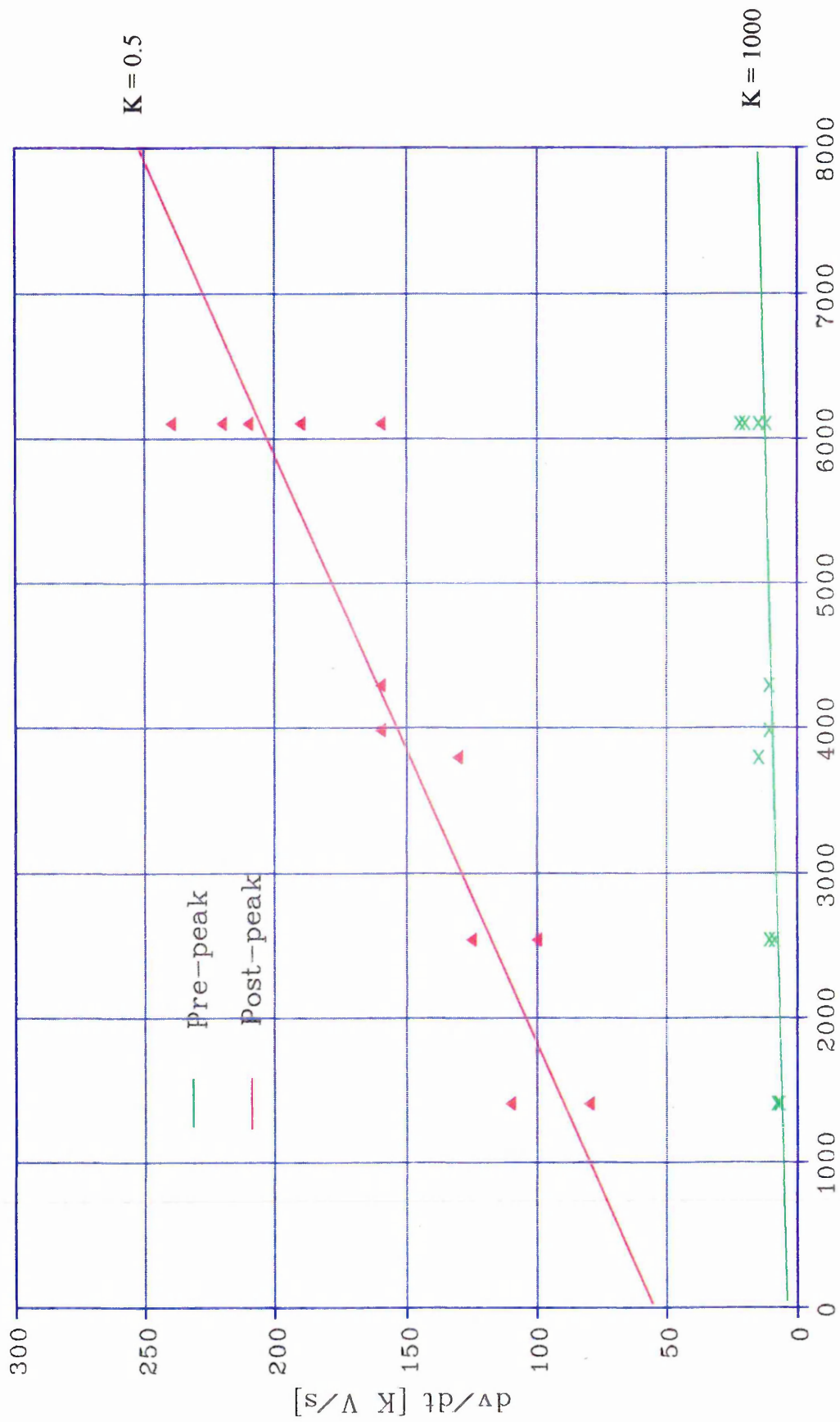


Fig. 3-7 Relationship between  $dv/dt$  and Prospective Current for Uniform Strip Elements

The study resulted in the following findings:

- The number of arcs and the arc-root voltage drop were identical to the values determined for wire.
- On average the pre-peak and post-peak  $dv/dt$  values are similar to the corresponding measurements for wire. The pre-peak values for strip are slightly lower and the post-peak values are slightly greater.
- The applicability of the model, was satisfactory for strip when the number of arcs is greater than two, this being the same as for wires.
- The same relationship between  $dv/dt$ , pre-peak and post-peak voltage and the circuit stored energy was found for strip fuse element and wires.

The essential conclusion is that the arc mechanistic behaviour discovered for single wires is the same as found for uniform single strip.

### 3.2.2 Single notched strip fuse element:

In this study the same strip element was used with a single notch mid-way along its length. The constriction was 1.5 mm in width and of three selected lengths: a long notch 20 mm, a medium notch 10 mm and a short notch 0.7 mm. The same fuse construction and types of quartz sand were used. Each test series was undertaken at five different current values, four making angles and the two grain sizes, giving a total of 40 samples tested for each notch type.

From the results obtained the following findings were indicated:

### 3.2.2.1 Long notch arcs (20 mm)

Following the described procedure, the number of arcs were determined from the fulgurite deposits. The voltage per arc was calculated using the total number of arcs and the maximum arc voltage determined from the voltage wave form. The  $dv/dt$  values for the pre-peak and post-peak intervals were determined empirically as previously.

The current and voltage wave forms presented important differences in comparison with the previous cases. For example the post-peak current **Fig. 3.8** shows a change in the slope and the voltage has the sharp peak compared with the uniform fuse element but now the peak value is followed by a kink in the arc voltage trace. This kink is explained in the following analysis.

The arc phenomena starts in the same way as in uniform fuse elements, i.e. one arc after another, increasing the positive column voltage until a new arc can be created and so on. The limitation presented with the 20 mm notch length is that this length is not sufficient to support the necessary number of arcs for the value of the supply test voltage and inductive stored energy. It follows that the additional arcs must be established in the fuse element shoulder, where the dimensions are different, hence the current density and the volumetric energy are nearly a half of the values of that within the notch. This lack of arcs can be seen in the pre-peak section of the arc voltage trace but more clearly in the post-peak periods. This dual mechanism can be analysed using the proposed model in the following way.

Two mechanisms are working at the same time, increasing the arc number in the notch and simultaneously in the shoulder. Each mechanism will have their own slopes. Arcing will commence in the notch although melting of the shoulder can occur during arcing in the notch. The shoulder zone produces new arcs also after arc coalescence has taken place in the notch. It seems that this phenomena does not occur frequently with very long notches unless the supply voltage is very high.

The above explanation results in four  $dv/dt$  values, two for the pre-peak and two for the post-peak periods.

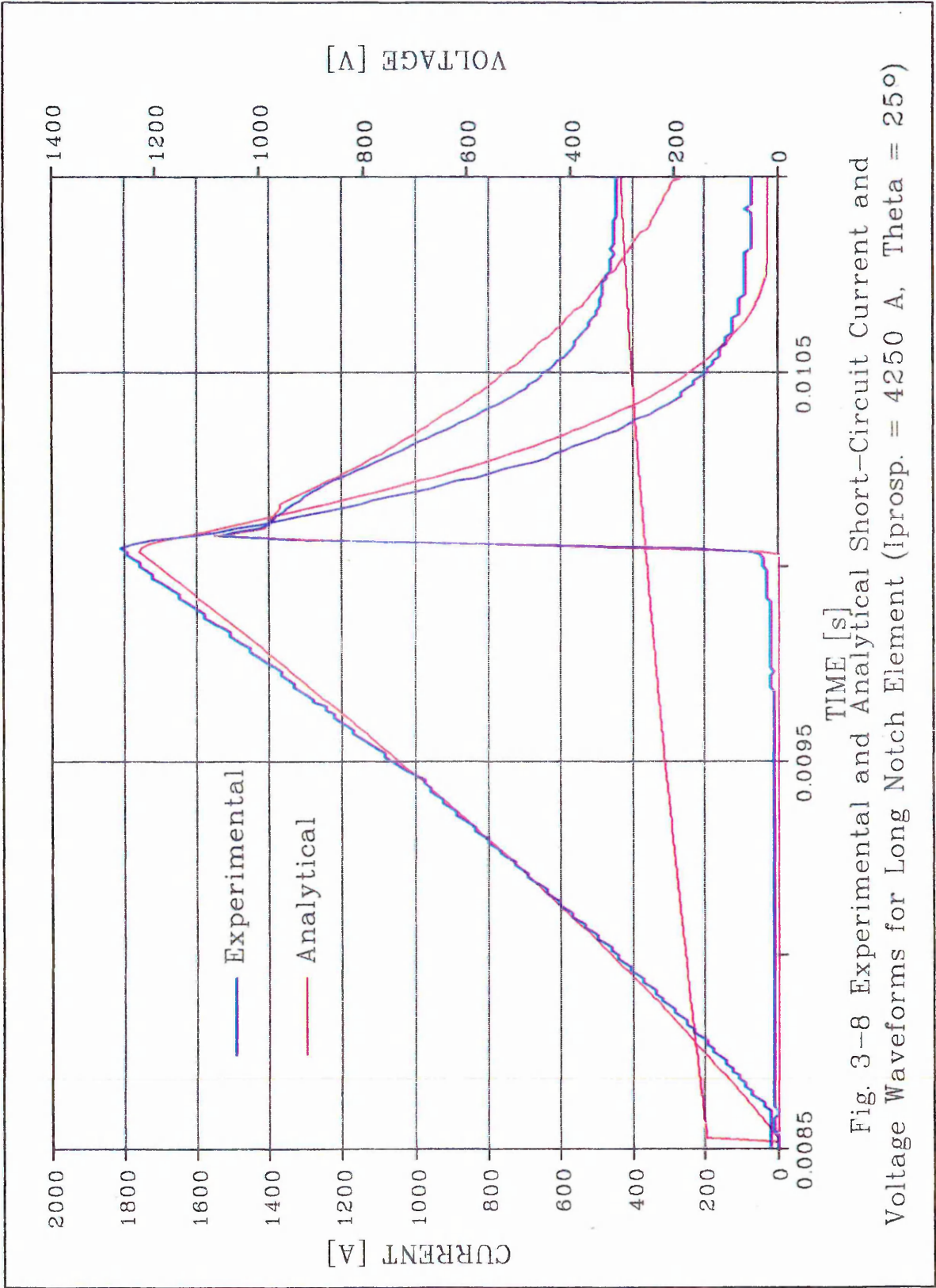


Fig. 3-8 Experimental and Analytical Short-Circuit Current and Voltage Waveforms for Long Notch Element (I<sub>prosp.</sub> = 4250 A, Theta = 25°)

The number of arcs is also complex because there are three values, notch maximum, shoulder maximum and a minimum one which is reached when the notch post-peak voltage intersects the shoulder pre-peak value.

The numerical results of the simulation can be seen in **Table 3** (appendix 1), and two examples of the application are shown in **Figures 3.8** and **3.9**.

The values of  $dv/dt$  for pre-peak and post-peak applicable to the notch and shoulder are a function of the prospective current are shown **Fig 3.10**.

The slope of the  $dv/dt$  lines doubles compared with the slopes for the uniform cross-section which confirms that the  $dv/dt$  dependence is related with the current density.

From the study of long notches can be concluded:

- The average number of arcs are 11, 9 and 9. The value equal to 11 which is directly related to the notch length, indicates the same relationship as for uniform wire or strip. ( $20 \text{ mm} / 11 \text{ arcs} = 1.82 \text{ mm per arc}$  compared with  $35 \text{ mm} / 20 \text{ arcs} = 1.75 \text{ mm per arc}$ ).
- All the pre and post-peak  $dv/dt$  values for notch and shoulder are a direct function of the prospective current density, the relationships being very similar to those for strip and wires.
- It is possible to detect the double mechanism from the arc voltage wave form.
- The discovered arc mechanism model has therefore been found to be applicable for single long notched fuse elements.

#### 3.2.2.2. Medium notch arcs (10 mm)

The same fuse construction procedures were repeated for this study. Testing the medium notched fuse element was also undertaken in the same way as previously described, with similar currents and making angles. The number of arcs was obtained from X-ray photography. The maximum voltage value was obtained from oscillograms and the voltage per arc was estimated as discussed previously. The pre-peak and post-peak  $dv/dt$  values were determined empirically.

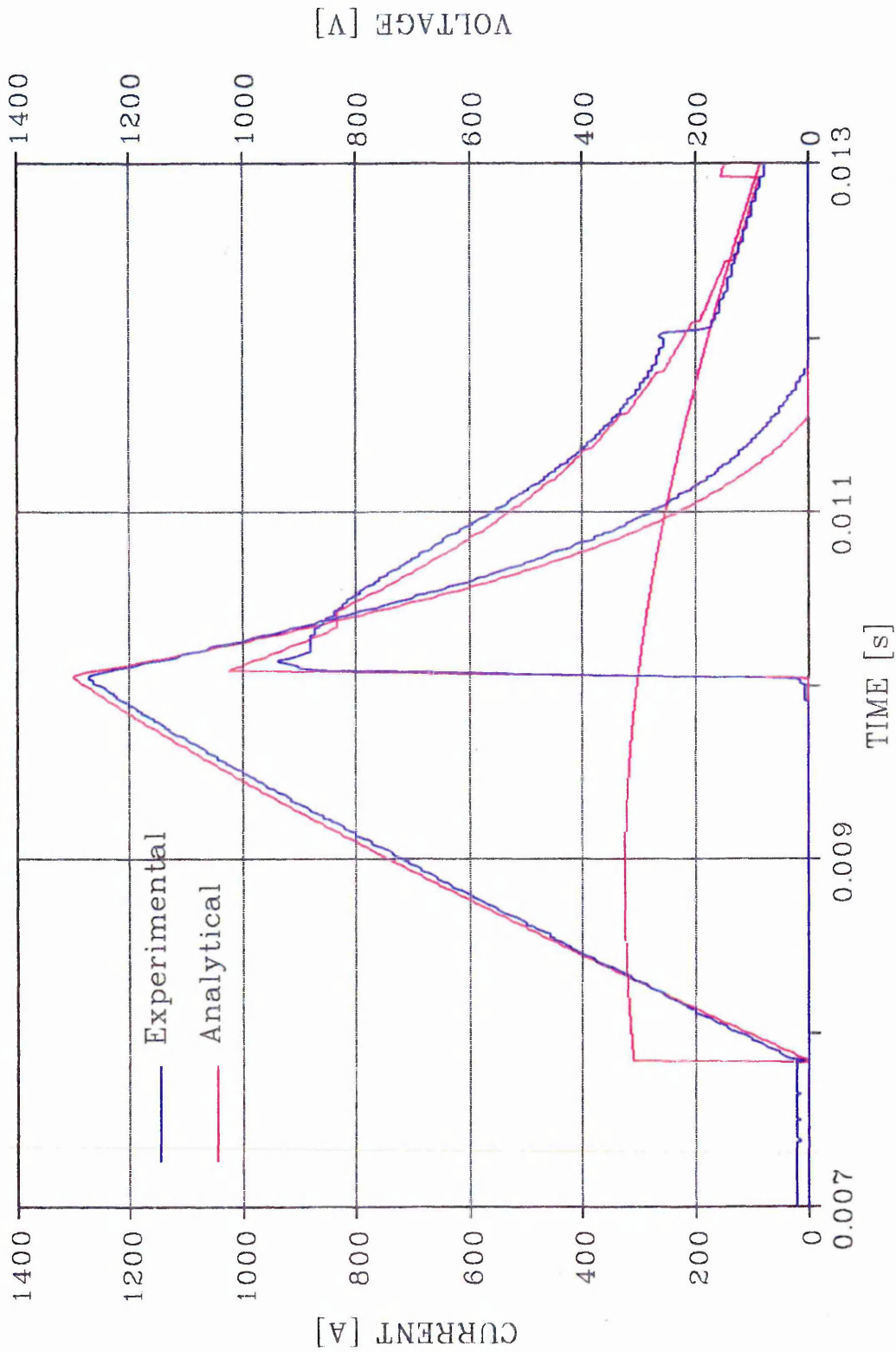


Fig. 3-9 Experimental and Analytical Short-Circuit Current and Voltage Waveforms for Long Notch Elements ( $I_{\text{prosp.}} = 1435 \text{ A}$ ,  $\Theta = 72^\circ$ )

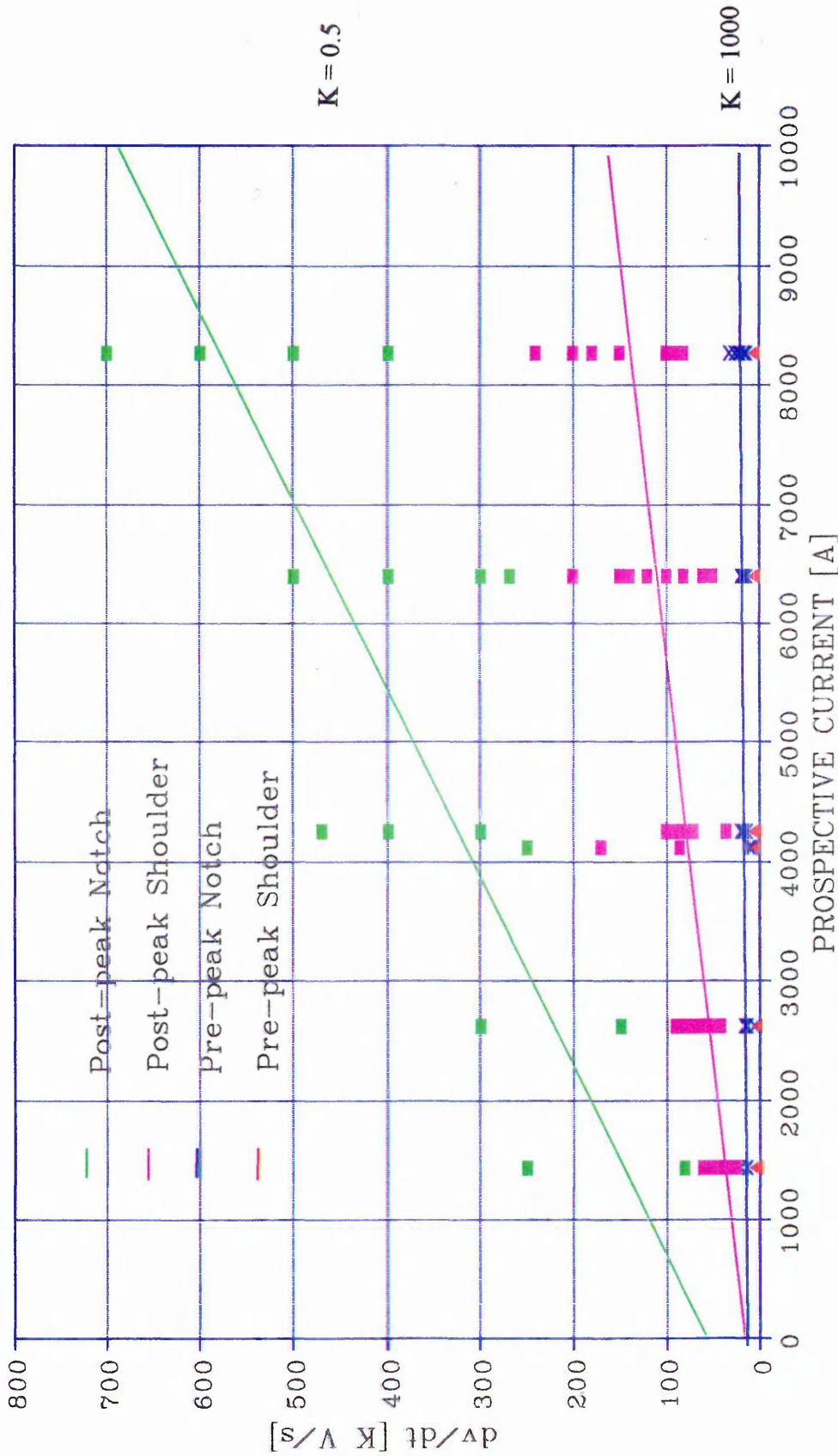


Fig. 3-10 Relationship between  $dv/dt$  and Prospective Current for Pre-peak and Post-peak Interruption in Notch and Shoulder Sections of Long Notch Elements

For this case the voltage and current wave forms **Fig 3.11, 3.12** differ significantly in shape compared with single strip fuse elements. The previously observed hump is particularly noticeable and very important. Since its maximum value is normally greater than the first peak, i.e. the double mechanism is magnified in medium notched fuses.

This can be explained since the notch length was 10 mm, the necessary number of arcs for its voltage is not enough. The additional arcs, as before, must be produced in the shoulder very early on in the arcing period, continuing with the creation of new arcs much later than when arc coalescence has taken place in the notch. As for long notches the additional arcs in the shoulder will produce lower current densities and volumetric energy.

The average number of arcs estimated from the peak voltage values using the previously determined 49.6 V per arc, was 6. This gives a relation for the notch length/number of arcs of 1.66. An average of 1.74 mm per arc being the value calculated from comparison with the wire, strip and long notch relationships.

**Table 4** (Appendix 1) gives the values based on the application of the proposed methodology to this type of fuse element.

**Figure 3.13** shows the relationship between the pre-peak and post-peak  $dv/dt$  values as a function of the prospective current and inductive stored energy.

The following conclusions can be made from the experiments and calculations:

- The average number of arcs for notch, shoulder and junction between notch post-peak and shoulder pre-peak were 6, 6 and 5 respectively, which is consistent with the value of approximately 1.74 mm per arc..
- The pre-peak and post-peak  $dv/dt$  values for notch and shoulder appear to be a direct function of the prospective current density.
- A double arc mechanism clearly occurs and is present on all the voltage wave forms.
- The proposed arc model is therefore applicable for single medium notched fuse elements with no modifications.

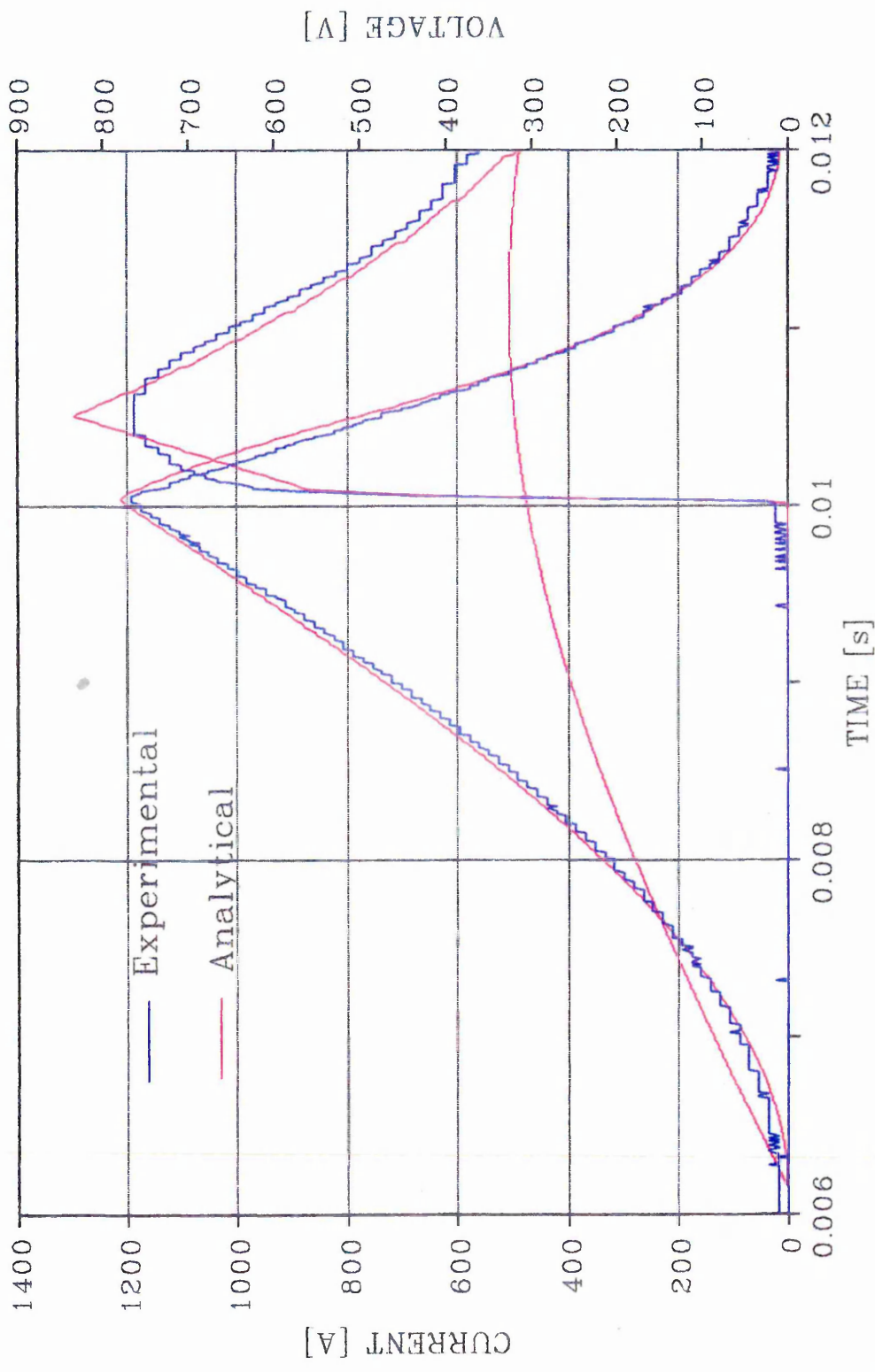


Fig. 3-11 Experimental and Analytical Short-Circuit Current and Voltage Waveforms for Medium Notch Elements (I<sub>prop.</sub> = 1435, Theta = 0°)

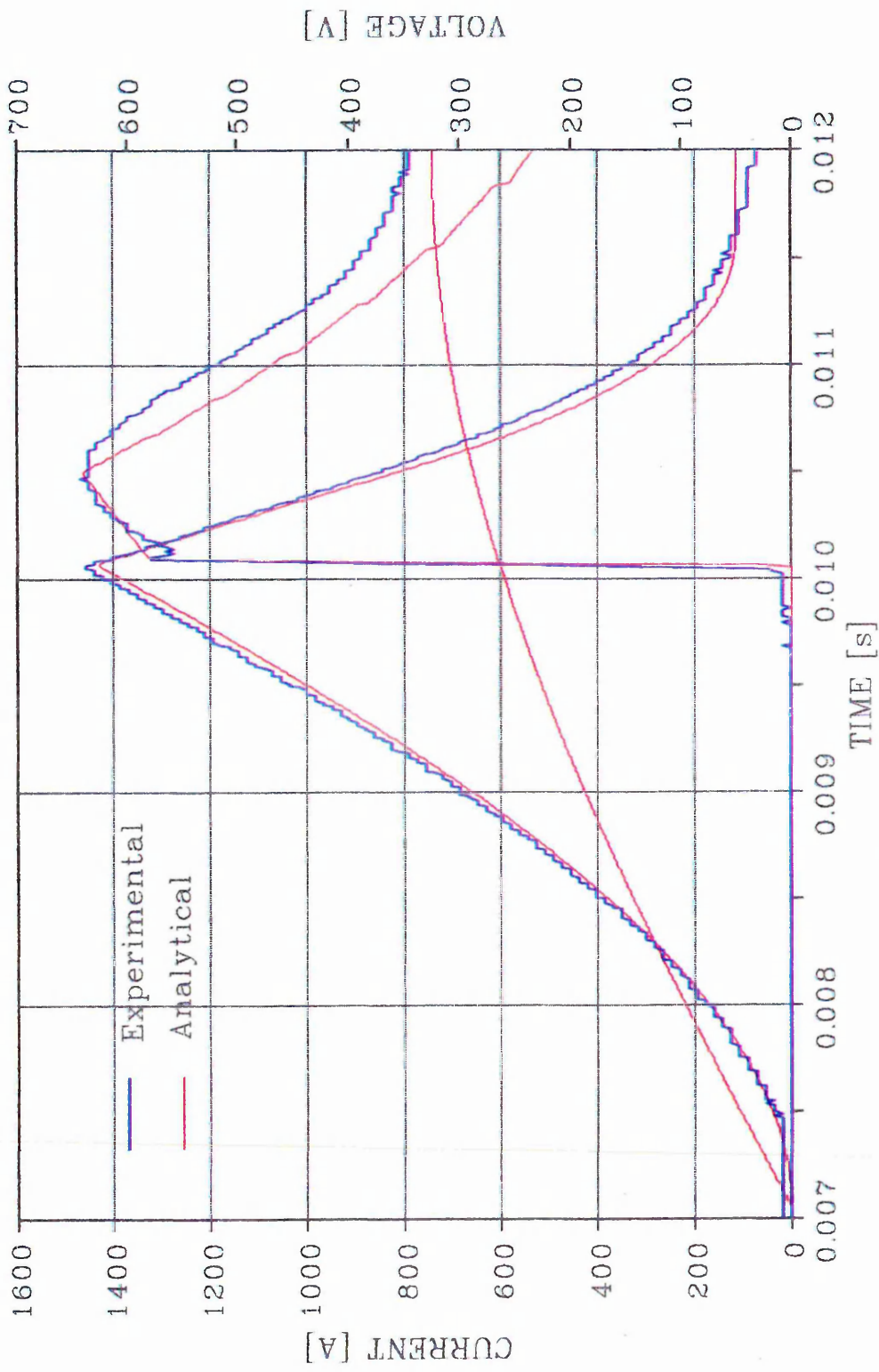


Fig. 3-12 Experimental and Analytical Short-Circuit Current and Voltage Waveforms for Medium Notch Element ( $I_{\text{prosp.}} = 2560$ ,  $\text{Theta} = 0^\circ$ )

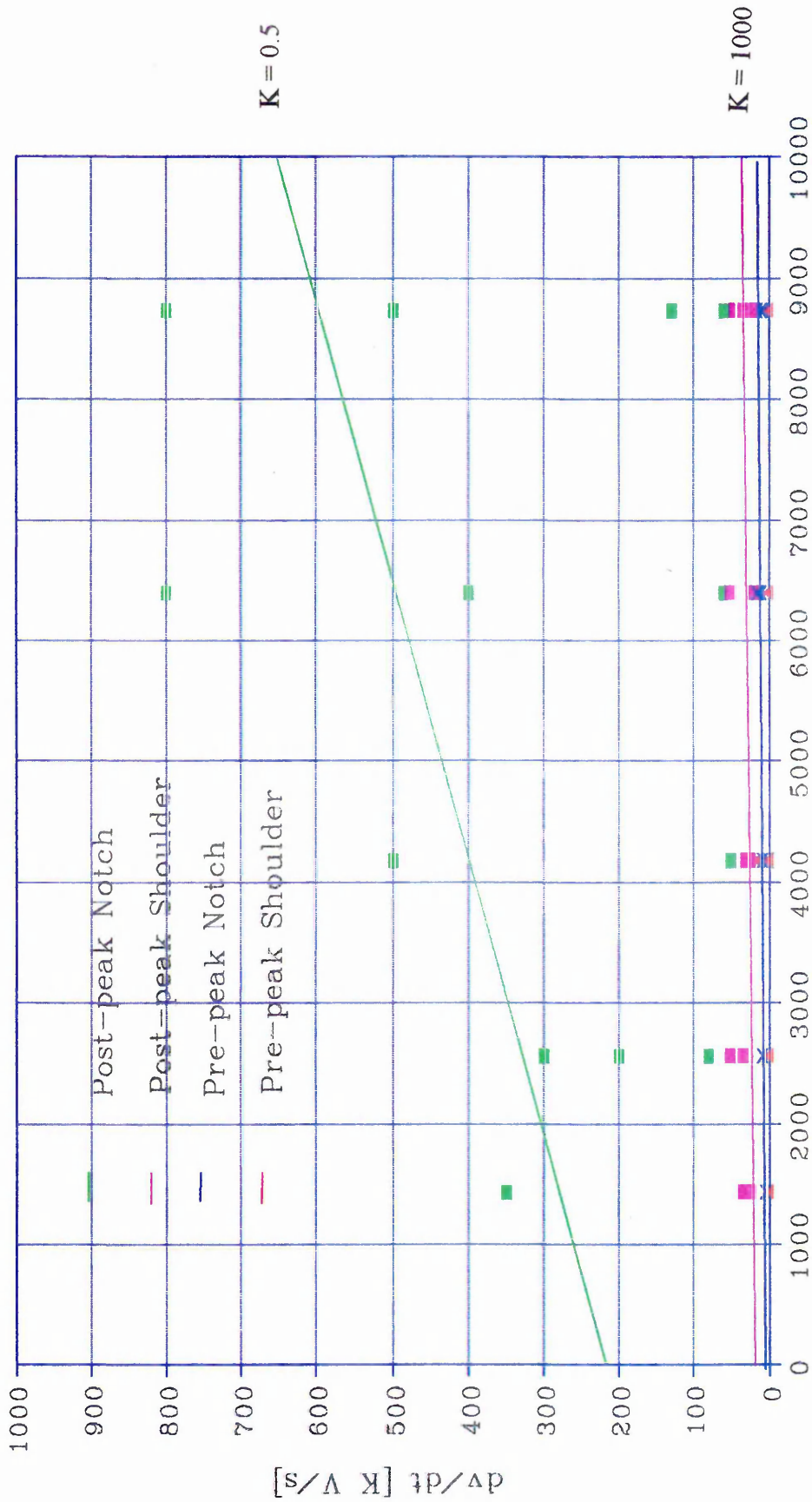


Fig. 3-13 Relationship between  $dv/dt$  and Prospective Current over Pre-peak and Post-peak Periods for Medium Notch Elements

### 3.2.2.3 Short notch arcs

The previous results using long and medium notched fuse elements show a similar tendency which can be explained by the stabilised arc model and discovered arc mechanism.

To confirm that the model was sound it was decided to investigate the behaviour in a fuse element having as short a notch as possible. The idea was to create a single arc.

The tests were done using the same equipment and under critical current conditions, adjusting the oscilloscope amplitude and time base in order to read very low voltage values.

The results of the explained methodology can be observed in **Figure 3.14**, where a selection of the most typical voltage values are shown.

From the graph the following facts can be deduced:

- There are clearly two different voltage slopes, which corresponds to the notch and shoulder.
- The transition between the slopes can be estimated as nearly 90 V.
- The  $dv/dt$  values determined from the graph are  $383 \text{ E}04 \text{ V/s}$  for the notch and  $63.2 \text{ E}04 \text{ V/s}$  for the shoulder, the relationship between them is very different than the cross-section ratio.

The observations indicate that at the instant at which the change in slope is detected more than one arc is burning, i.e. probably two of them have been created. The effect of the shoulder/notch ratio therefore does not apply due to the arc squeezing phenomena.

### 3.3. Evaluation of model for varying filler media

To be able to extend the application of the proposed model to more practical situations, it was decided to apply the model to a semiconductor fuse. One of the most important characteristics of this type of fuse is that the arcing energy control for which

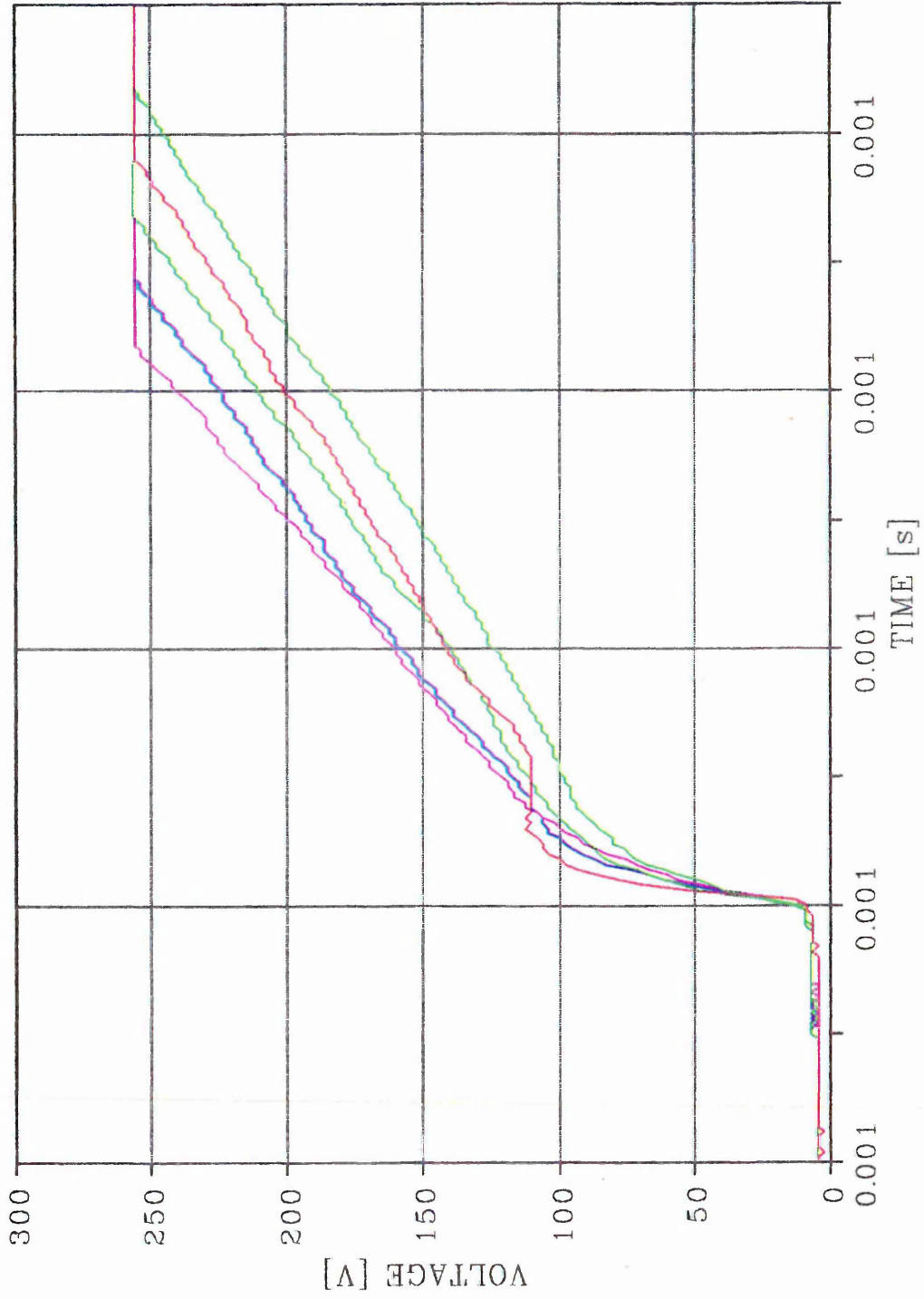


Fig. 3-14 Initial Arc Voltage Waveforms for Short Notch Elements  
 (I<sub>prosp.</sub> = 2370 A, Theta = 20°)

several sophisticated improvements have been introduced, the most effective perhaps being the use of solid filler.

A set of experiments and simulations on samples similar to the simplest model was performed on the DIN 00 structure with wire and uniform strip fuse element but with solid filler. The tests were extended to long, medium and short notched fuse elements immersed in solid filler.

The quartz sand used were the two previous roundish grain sizes ASTM 40/50 and 50/80, compacted into the fuses in the standard way. The binding agent used in this study was water glass, introduced in drop form into the compacted filler by gravity (the fuse and room temperatures were very important to get the desired result), until a predetermined liquid volume occupied the inter-grain spaces. The fuse was rotated periodically during one hour and later baked for two hours at 160 ° C in an electric oven. Several dummy fuses were filled and baked with the samples in order to verify the state of the whole batch by examining the dummies at the different time intervals.

Seven different types of samples were analysed, in this research study as indicated:

- wire, fine sand, bound.
- wire, coarse sand, bound.
- strip, fine sand, bound.
- strip, coarse sand, bound.
- strip, long notch, fine sand, bound.
- strip, medium notch, fine sand, bound.
- strip, short notch, fine sand, bound.

Each of these seven types were tested in the same power circuit, for the prospective currents 1400A, 2540A, 3990A, 6050A, with two making angles 25 e° and 90 e°.

The normal procedure was followed, for the simulation i.e. number of arcs were determined from the X-ray plates (when possible), and pre and post-peak  $dv/dt$  were obtained empirically.

(a) Comparison between the uniform fuse elements in compacted and solid filler, Table 5, indicate that:

- The maximum voltage using solid filler is on average 1.80 times the equivalent value for the normal filler.
- The number of arcs determined from the X-ray plates is the same, i.e. 20.
- As a consequence the positive column voltage and arc-root voltage drop should have the same relationship as with the unbound quartz sand, i.e. the arc-root drop must be near to 89.3 V. This result confirms the previously cited fact that the arc-root voltage drop is function of the filler.
- The speed of voltage increase and decrease with solid filler is greater than the values obtained with unbound sand.

From the application of the proposed model the following relationships can be calculated:

- The  $dv/dt$  for the pre-peak period is 1.9 times the values for compacted filler.
- The  $dv/dt$  during the post-peak interval is 2.4 times the values for normal filler.

Figures 3.15 and 3.16 show examples of wire and strip solid filler fuse behaviours are shown.

The basic conclusion that can be drawn from the comparison is that the simulation gives satisfactory results and that the  $dv/dt$  for the pre-peak and post-peak periods are filler dependent. The number of arcs, however, do **not** depend on the filler.

(b) The study of the results using notched fuse elements in bound fine filler and the comparison with the unbound sand follows:

- The double hump voltage mechanism was not observed either in long notched fuse elements or in medium notch ones, the arc behaviour being similar to that for a uniform cross-section. This is so because the number of arcs in the notch generated

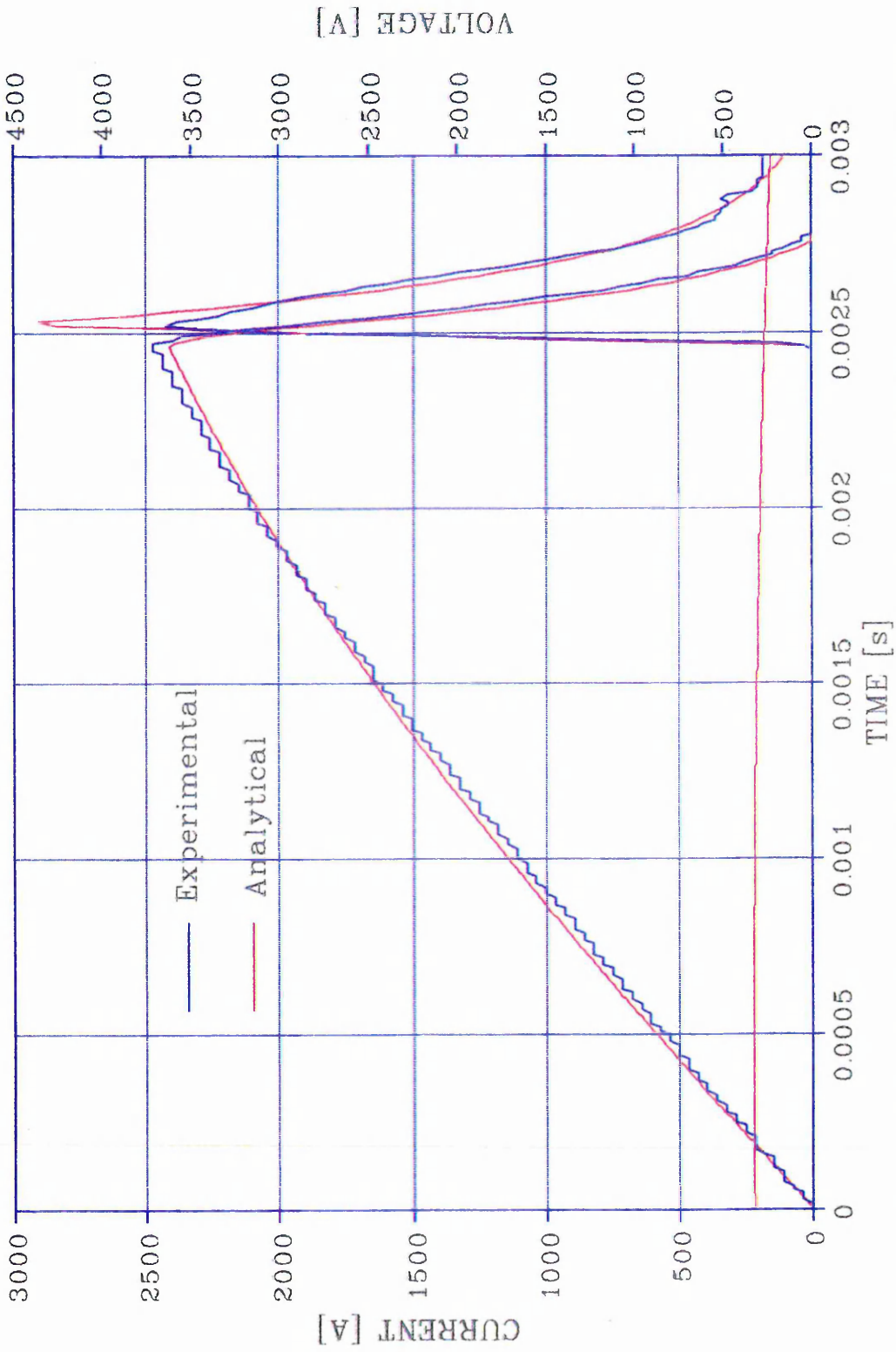


Fig. 3-15 Experimental and Analytical Short-Circuit Current and Voltage for Waires in Bound Filler (I<sub>prosp.</sub> = 2540 A, Theta = 82°)

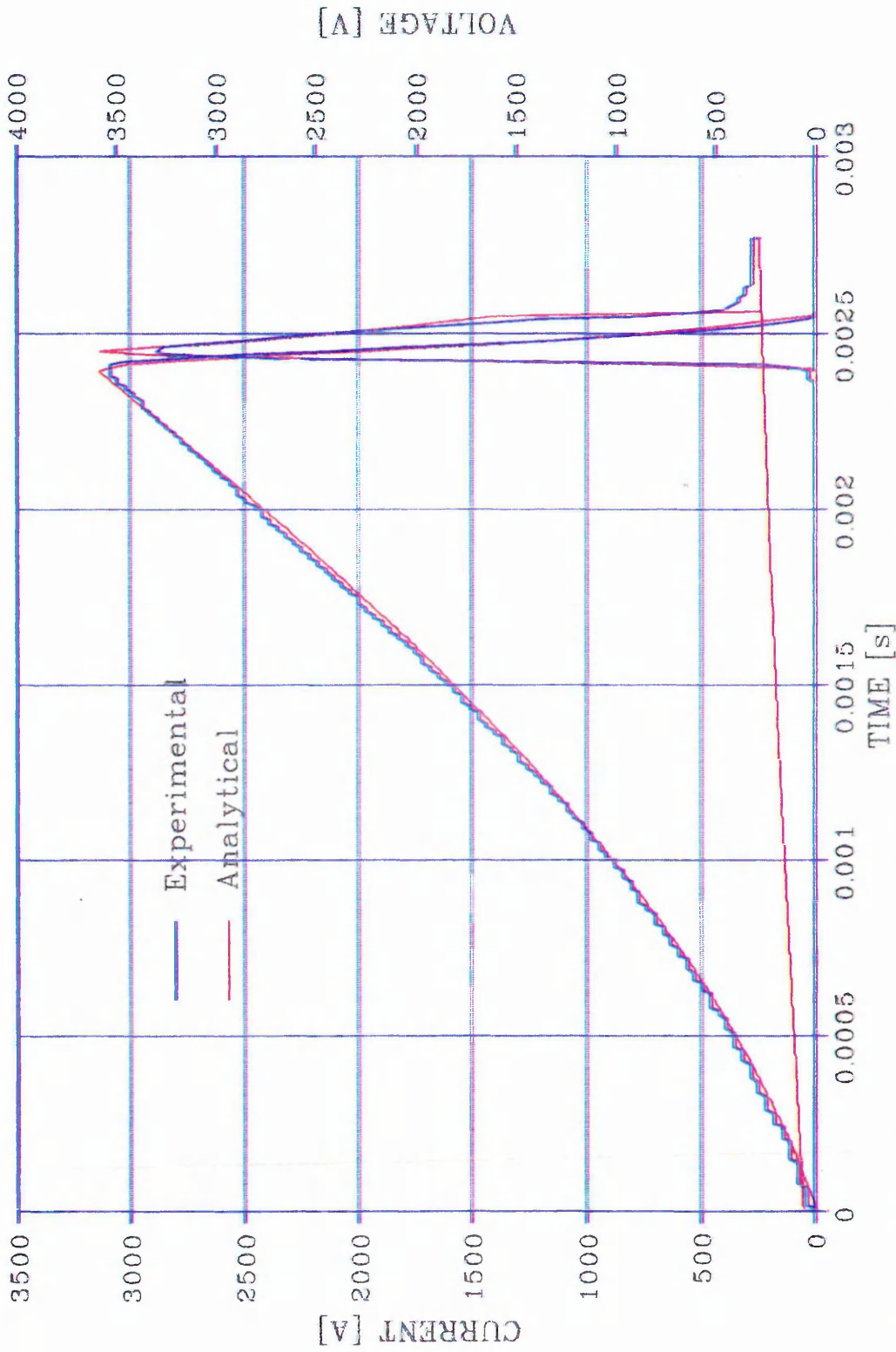


Fig. 3-16 Experimental and Analytical Short-Circuit Current and Voltage Waveforms for Uniform Strip Element in Bound Filler  
 (I<sub>prosp.</sub> = 5930 A, Theta = 11°)

sufficient voltage in bound filler and, hence, arc burning did not occur in the shoulder.

- The  $dv/dt$  pre-peak values were now very noticeable, being nearly 4 to 6 times the corresponding values for free sand.
- The  $dv/dt$  values for the post-peak period were 50 % greater than the corresponding values for normal filler.

The analytical and experimental results are listed in **Tables 6 and 7** (Appendix 1) for long and medium notch strip elements respectively. Furthermore the proposed arc model also can be applied when  $dv/dt$  values are available.

### 3.4 Evaluation of simple parallel elements

For industrial fuses it is usual to use complex fuse elements having several parallel branches in practice. It was therefore considered necessary to evaluate the proposed model for parallel elements. Since it is advisable that the increasing of complexity should be done step by step, the fuse element types selected for this part were two parallel wires and two parallel strips (without any notch), of similar dimensions to those used previously and immersed in the same two round grain unbound fillers.

The test program was unchanged, except that the current was doubled in comparison with the previous test in order to keep the element current density the same as that for the former experiments and so allowing direct comparisons to be made.

The prospective currents and making angle were 2800A, 5080A, 7980A, 12100A, 25 e° and 90 e°. The simulation methodology did not change, the 49.6 V arc-root voltage drop was also used. The number of arcs was 20, similar to that which was applied in single wire and single strip. This idea was confirmed from the study of the X-ray plates. The  $dv/dt$  for pre-peak and post-peak voltages were determined by the same empirical procedure.

The results are listed in **Table 8** (Appendix 1). **Fig 3.17** shows the experimental and typical analytical wave forms.

The following conclusions can be drawn from the test series:

- As expected the voltage wave forms did not change significantly in shape from those of other tests.
- The current was equivalent, the same wave forms times a factor of 2, maintaining prearcing and arcing times constant.
- The number of arcs is constant when the fuse element length is unchanged.
- The dv/dt values were also very similar (the post-peak values are slightly greater, 5% on average) to the previous amounts when the comparison was done using the current density as the common factor. This latter finding confirms that there is a relation between the dv/dt and the circuit energy per fuse element volume, because the  $\frac{1}{2} L i_0^2$  is doubled at the same time as the fuse element volume and is similarly described.
- The arc and wave form behaviour were the same with the two quartz grain sizes used.
- The simple arc mechanism gives very good results for simple paralleled fuse elements.

It follows that the results confirmed that the proposed model is also applicable for simple paralleled fuse elements.

### 3.5 Complex notched shaped elements (round and rhomboid holes)

The results obtained using very simple fuse elements, uniform cross-section and single square notch, promotes the idea of extending the application of the proposed model to more complex elements, for example ribbon with round, square, rhomboid and ellipsoid holes or notches.

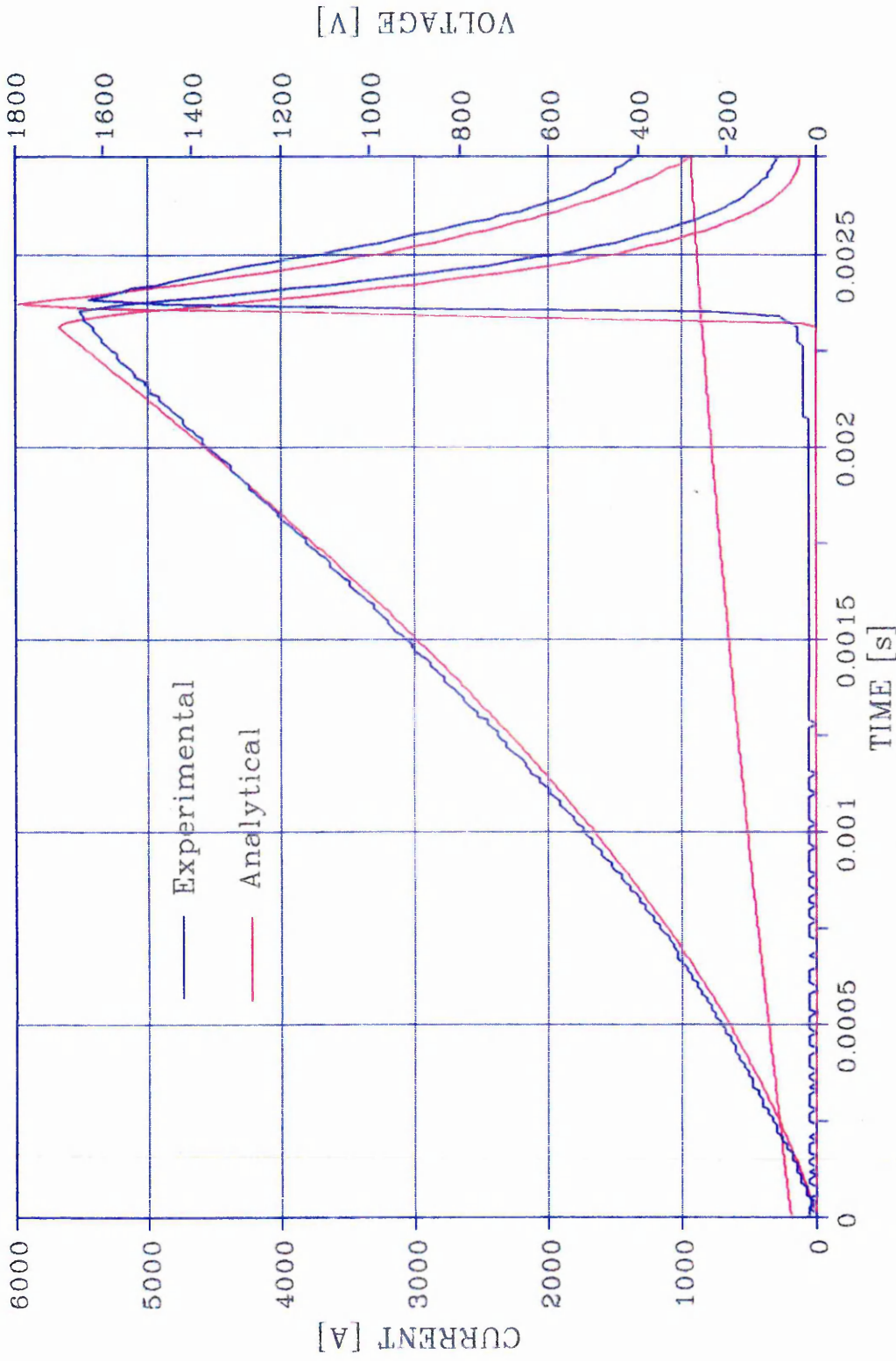


Fig. 3-17 Experimental and Analytical Short-Circuit Current and Voltage Waveforms for Two Parallel Ware Elements in Fire Grain Filler  
 ( $I_{prosp.} = 11584$  A,  $\theta = 10^\circ$ )

It is postulated that the model would be appropriate for the simulation of notches of progressive (regular or irregular) increase in cross-section, obtaining the corresponding  $dv/dt$  for each cross-section based on the current density.

In this way, it should perhaps be possible to design the fuse element notch to obtain a desired arc voltage wave-form.

The values for the arc-root voltage drops for bound and unbound filler gave increases of the order of 1.9 which is in good agreement with the available limited results of other researchers. [2]

The results obtained by Lipski and Ossowicki, where the arc peak voltage was assumed to be the same for free or bound quartz sand, differ with the values obtained in the present research. The peak voltage predictions using the proposed arc model, however agree with the application of an equation presented in the same paper. [3]

When the filler used is different from the types described, the arc-root voltage drop for only one arc should be experimentally determined by a test using an element with a very short constriction.

#### 4.1.2. Determination of the pre-peak $dv/dt$ parametric values

The parametric values for pre-peak  $dv/dt$  and post-peak  $dv/dt$  are functions of the element cross-section and prospective current density or circuit trapped volumetric energy. The determination of these parameters is straightforward given the test circuit parameters and element parameters.

In Fig 4.1 a summary of all the experimentally determined  $dv/dt$  values (using free high quality sand) is shown as a function of prospective current density, on which equations are based and variations were calculated. Fig 4.2 is similar to the previous figure but for solid filler. It is straightforward also to establish relations for the same  $dv/dt$  dependence using free quartz sand presented by other researchers.

From Fig 4.1 the average pre-peak  $dv/dt$  value is calculated as  $13.5 \text{ E}06 \text{ V/s}$ . This value is not current density dependent. These results were for a fuse element length and the average number of arcs of 35 mm and 20 respectively, giving an average arc length of 1.74 mm. This length includes the arc roots and the positive column. If it is assumed that the arc roots length is negligible [4] then the maximum column length during the pre-peak period would be 1.74 mm.

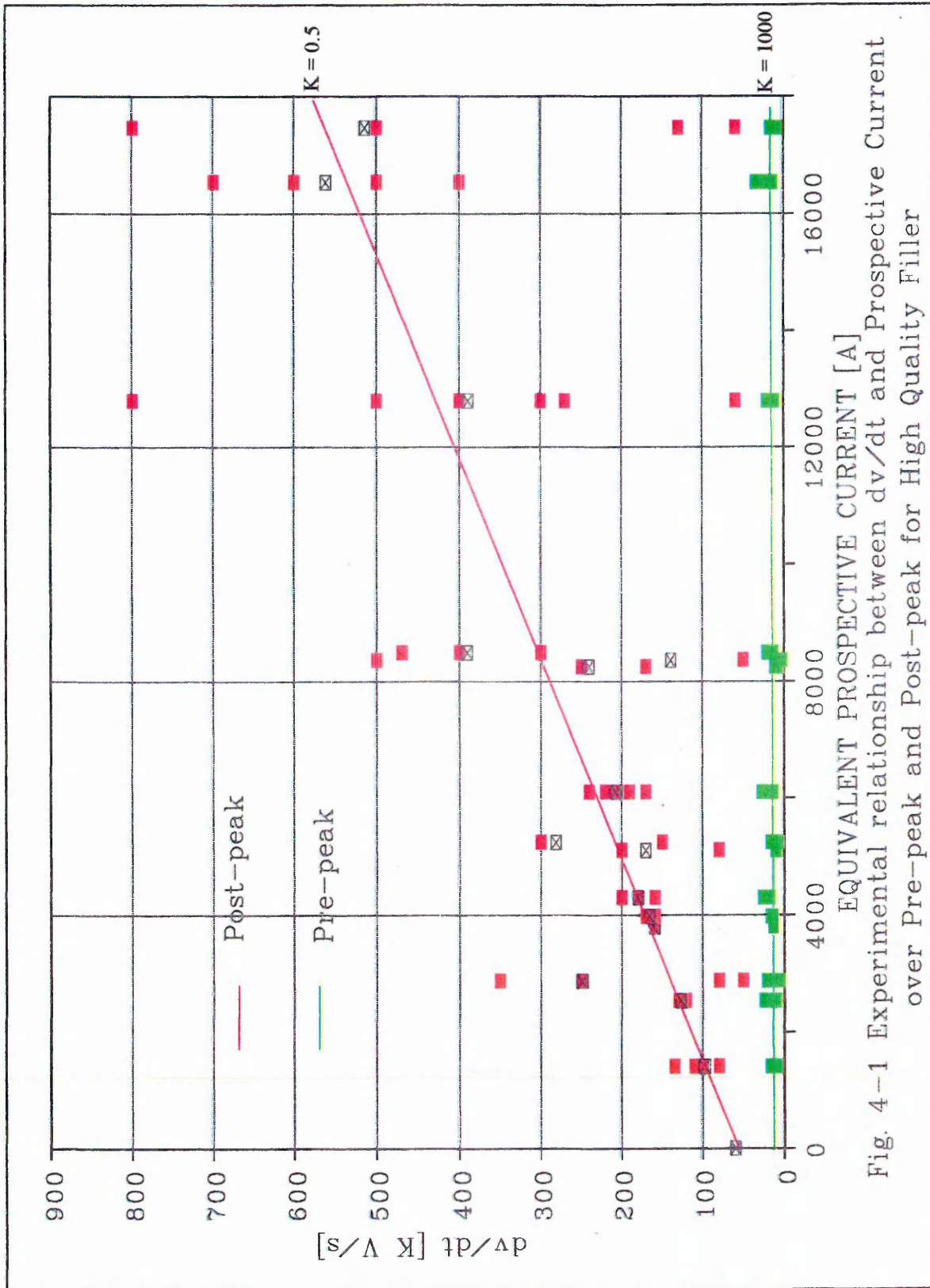


Fig. 4-1 Experimental relationship between  $dv/dt$  and Prospective Current over Pre-peak and Post-peak for High Quality Filler

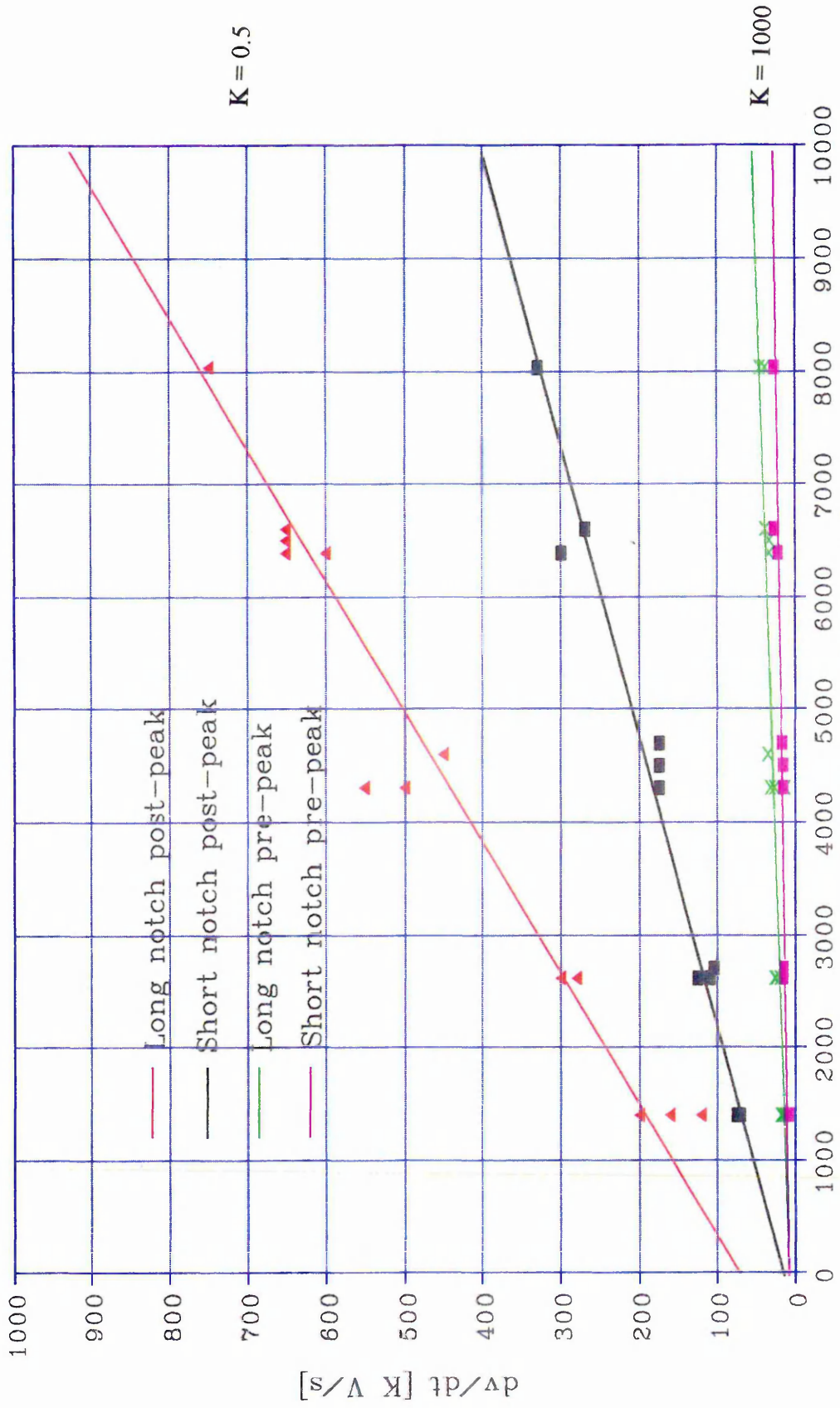


Fig. 4-2 Experimental relationship between  $dv/dt$  and Prospective Current over Pre-peak and Post-peak for Solid Filler

Based on the proposed model, the maximum voltage per arc under these conditions is  $2 \times 49.6$  V, and since the arc number is 20, the maximum arc voltage is 1984 V, which is reached in  $1984/13.5E06$  s (  $147 \mu\text{s}$  ). If a medium current value is considered for example 6.1 kA, the resulting current density is  $23.5 \text{ kA/mm}^2$ .

The examples show that the proposed mechanistic arc behaviour has been simply translated into the conventional parameters adopted in the classical approaches for determining arc voltage.

Examples of the classical approaches are now compared with the work of other researchers together with our findings.

In the classical approach the arc voltage is given by:

$$V_{arc} = n \cdot \{ V_{ak} + E \cdot (dx/dt) \cdot dt \}$$

from Chapter 2, section 2.3.2.:

$$k = E \cdot dx/dt = dv/dt$$

where E is the column voltage gradient and  $dx/dt$  the burn-back rate.

Kroemer obtained a peak arc voltage of 1200 V from testing a 30 mm long strip silver fuse element. In his studies Kroemer assumed only one arc occurred during arcing [5]. According to the proposed model, given an arc-root voltage fall of 32 V, the peak arc voltage of 1200 V would result in  $1200/(2 \times 32) = 18$  arcs and an arc length equal to  $(30/18)$ , 1.67 mm. Based upon the arc voltage rise time from our work of  $150 \mu\text{s}$ , the burn-back rate would then be  $(1.67/150 E04) = 1.11 \text{ m}^3/\text{A.s}$ . This result is in close agreement with Kroemer's value of  $1.15 \text{ m}^3/\text{A.s}$ . The major difference between the respective findings is in the value obtained for the column gradient.

Kroemer showed the plasma gradient to vary with current density where in our model the gradient has been shown to be constant. The values for the gradient were given by

Kroemer to vary between 300 and 40 V/mm for arcing periods in the range 10 to 50 ms. From simple calculations, based on the proposed arc model, the column gradient is given by  $V_{ak}/L_{arc} = (32/1.67) = 19.16$  V/mm.

It is clear from the classical arc equations that Kroemer's assumption of only one arc occurring per notch would result in an error of the order of 18 in the gradient (i.e.  $n=18$ ). If we consider the range of the gradient claimed by him then at 50 ms two arcs could be assumed and at 10 ms, 18 arcs would exist. This would result, in both cases, in a constant column gradient between 16 ~20 V/mm.

Wilkins and Gnanalingham based their studies on Kroemer's assumption of a single arc burning in a notch of a multi-notch element [6]. They determined the burn-back speed of silver strip fuse elements in quartz filled cartridge fuses, based on a modified empirical formula, which show that the velocity depends upon the current according to the following power law:

$$dx/dt = (a + b \cdot i^{0.6}) \cdot i / s$$

where a and b are experimental constants, x is the column length, i instantaneous current and s the cross section.

It is claimed that this equation is valid for instantaneous current densities up to 11 kA/mm<sup>2</sup>. These results and equation were later applied in a mathematical model for the arcing period [6].

Using the constants in the authors' paper [7] in the above equation gives an arc length of 2.3 mm compared with 1.67 mm based on our findings. Again the discrepancy can be put-down to the assumption of only a single arc occurring in notches. The values assumed for the column gradient were similarly exaggerated.

Daalder and Schreurs in 1983 determined that the burn-back rate is a function of the current density, provided that the Joule heating is negligible, because a fuse element heated by load currents will present a burn-back rate 2 or 3 times higher than a cold fuse.

They obtained the erosion constant of  $1.03 \text{ E-}09 \text{ m}^3/\text{A s}$ , which is in close agreement with Kroemer's and our results [8].

Slot, Kalasek and Sikkenga in 1987 proposed a one-dimensional model for the burn-back of silver strips, concluding that the heat loss by conduction in the silver has a delaying influence on the burn-back velocity. The model predicts an exponential increase of the burn-back rate when a current density threshold of  $3 \text{ kA}/\text{mm}^2$  is exceeded. Actual experiments determined that the prediction is somewhat overestimated [9].

Mocsary in 1964 researched the influence of the dependency of recovery voltage frequency on the arc behaviour of high voltage H.B.C. fuses, using non uniform cross-section wire fuse elements. He proposed that the arc voltage is a function of the fuse element length and it is not dependent on the short circuit current, provided that its value exceeds the critical current. He also concluded that the vaporization rate is a function of the current density and thus the arc voltage slope (pre-peak  $dv/dt$ ) is proportional to the current density. The same author concluded that the pre-peak  $dv/dt$  is a function of current density to a power less than unity and to the fuse rated voltage (fuse element length). Both parameters were consequently related to the dimensions of the particular fuse design. A time constant determined by the circuit inductance and fuse element resistance is defined, from which he proposed that the product of  $dv/dt$  and the time constant is a fuse characteristic parameter [10].

The agreement and differences between the findings of the cited authors and our results can be clarified by the following:

- The experimental results show that the pre-peak  $dv/dt$  is constant or weakly dependent on prospective current density.
- The current peak value is approximately a function of the square root of the prospective current increasing eventually to the cube root.
- The change in the instantaneous current value from the start of the arcing period to the moment in which the voltage peak is reached is between 6 to 10 %.

- The burn-back rate has been proposed by many researchers to be a function of current density. The function being between a linear one and a weak exponential one.
- The true voltage variation during the pre-peak arcing time is not a straight line but a curve in (S) form, from which agreement or not with the straight line depends on the instantaneous current density or current change in this short period of time.
- The pre-peak  $dv/dt$  is proportional to the burn-back rate, which is constant for a given fuse geometry.

As explained, the actual pre-peak  $dv/dt$  is only approximately constant. The assumption is valid in the simple model and besides its influence is significant only during the earliest stages of the arcing period.

#### 4.1.3. Determination of the post-peak $dv/dt$ parametric value.

The situation is radically different during the post-peak period where the  $dv/dt$  values are heavily dependent on the prospective current. The figures 4.1 and 4.2 show a higher than linear dependence. The consulted references indicate that the burn-back rate is underestimated when based on a linear relationship with instantaneous current density. The following analysis can explain the reason of the disparity:

The values obtained from the tests, Fig 4.1 and 4.2 are the  $dv/dt$  values for the whole post-peak period for each arc. They show also that the  $dv/dt$  value is proportional to the burn-back rates as explained in the previous section at the precise moment the peak voltage occurs.

From this moment, as the current density decreases so does the burn-back rate. But in the proposed model the  $dv/dt$  is kept constant due to the compensation effect of the number of arcs variation (merging phenomena). This behaviour would show jumps in the voltage trace but, as previously explained, the transient change in number of arcs is counter-balanced by the column diameter decreasing at a faster rate than the length increase. This effect masks the voltage modification and is responsible for eventual arc

de-ionization. The  $dv/dt$  values can be obtained from figures 4.1 or 4.2 or the corresponding equations if free or solid filler is used respectively.

Baxter 1950, determined that the arc voltage is a linear function of the current density.

As an example Baxter obtained a peak voltage of 2050 V for a 50 mm x 0.559 mm diameter fuse element for 240 V d.c.,  $5.0E09$  A/m<sup>2</sup>. This result compares very closely with the value of 1984 V obtained for the 35 mm x 0.6 mm diameter results in this work. The linear dependence proposed by Baxter however conflicts with our findings [11].

Johann 1982 proposed that the arc voltage is approximately proportional to the square root of the current. Using Johann's relationship for the 35 mm x 0.6 mm diameter wire, gives an arc voltage of 1600 V compared with the predicted and measured value of 1984 V. The difference between these values is likely to be because the average current density used in this work is approximately three times the maximum value used by Johann [12].

Mocsary proposed that the arc voltage is function of the fuse element length and it is not dependent on the short circuit current provided that its value exceeds the critical current [10].

Hibner's well known equation [Chapter 2, section 2.1] for the maximum arc voltage is shown to depend on both the fuse length (or notch length) and the square root of the maximum current density. This dependence was found not to be highly relevant to the arcing period in our findings. Hibner's equation is applicable to wire, strip and notched strip fuse elements. It involves the experimental determination of the constant for each element type.

Our results are mostly in agreement with Mocsary's relation. This could be because our tests were confined to a small range of prospective test currents.

## 4.2. Prediction of Arc Performance Characteristics.

### 4.2.1. Fuse characteristic determination

Any of the conventional fuse characteristics can be obtained with relative ease using the proposed arc model and given the model parametric values. For example based upon an arc length of 1.74 mm the number of arcs can be readily determined by dividing the fuse length by 1.74.

It is necessary to take into account of whether the fuse element is uniform or notched. In the latter case the double arc voltage mechanism should be considered using the following methodology:

- The prospective current densities can be calculated knowing the current and cross-sections of the fuse element notch and shoulder.
- Using the model equation or graphs the pre-peak  $dv/dt$  can be obtained and then by considering the notch and shoulder lengths the burn-back rates for the two fuse element sections can be calculated.
- Assuming the notch and shoulder arc burn-back erosion occurs simultaneously the arc voltage waveform can be calculated using a computer program, such as one described below.

The additional data required are the circuit variables: prospective current, supply voltage, power factor and test making angle.

The following fuse characteristics, which are of great interest for the fuse designer and for the fuse user, can be computed, **Figures 4.3 & 4.4:**

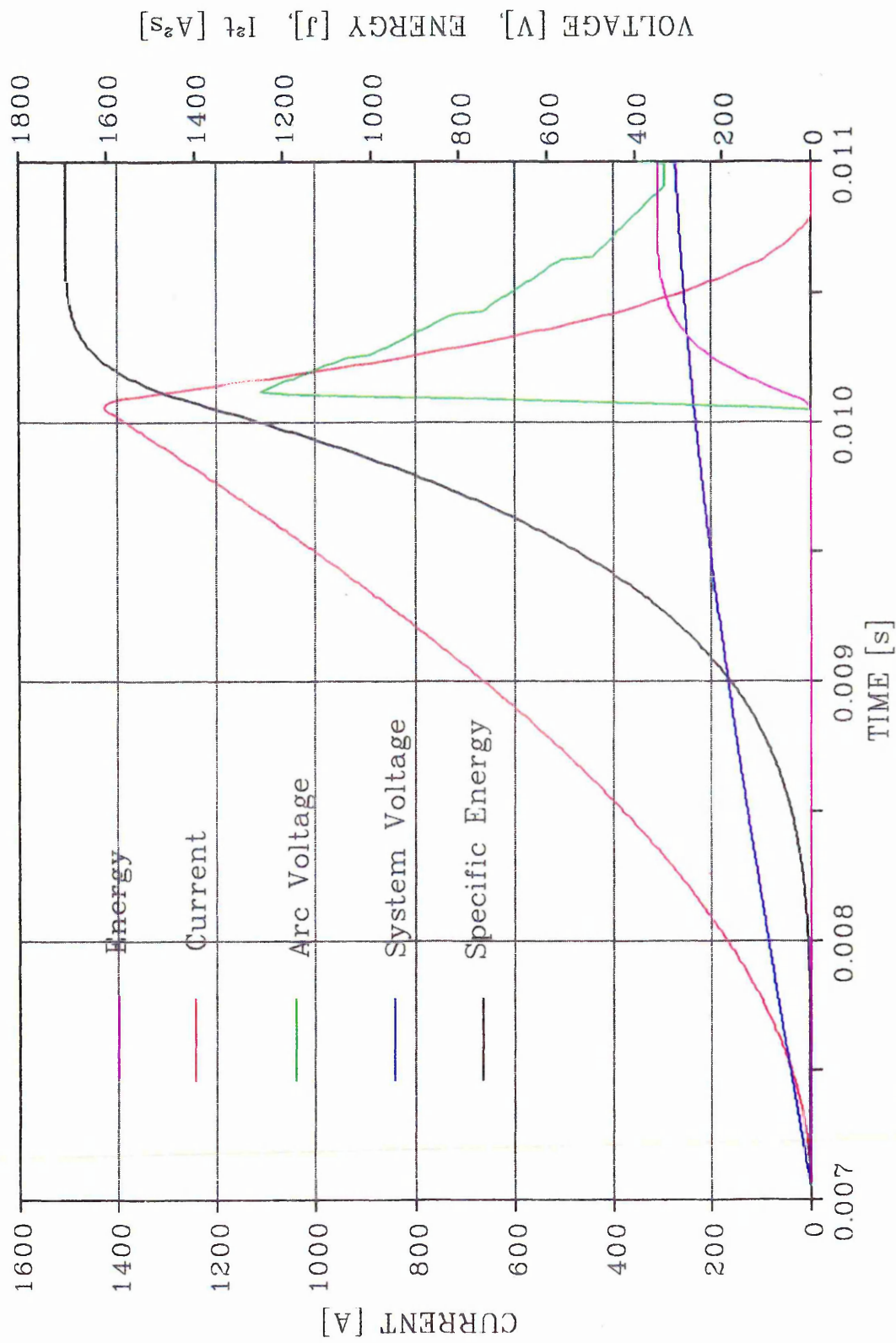


Fig. 4-3 Simulation using a filler with an Hypothetical anode-cathode voltage drop of 125 V,

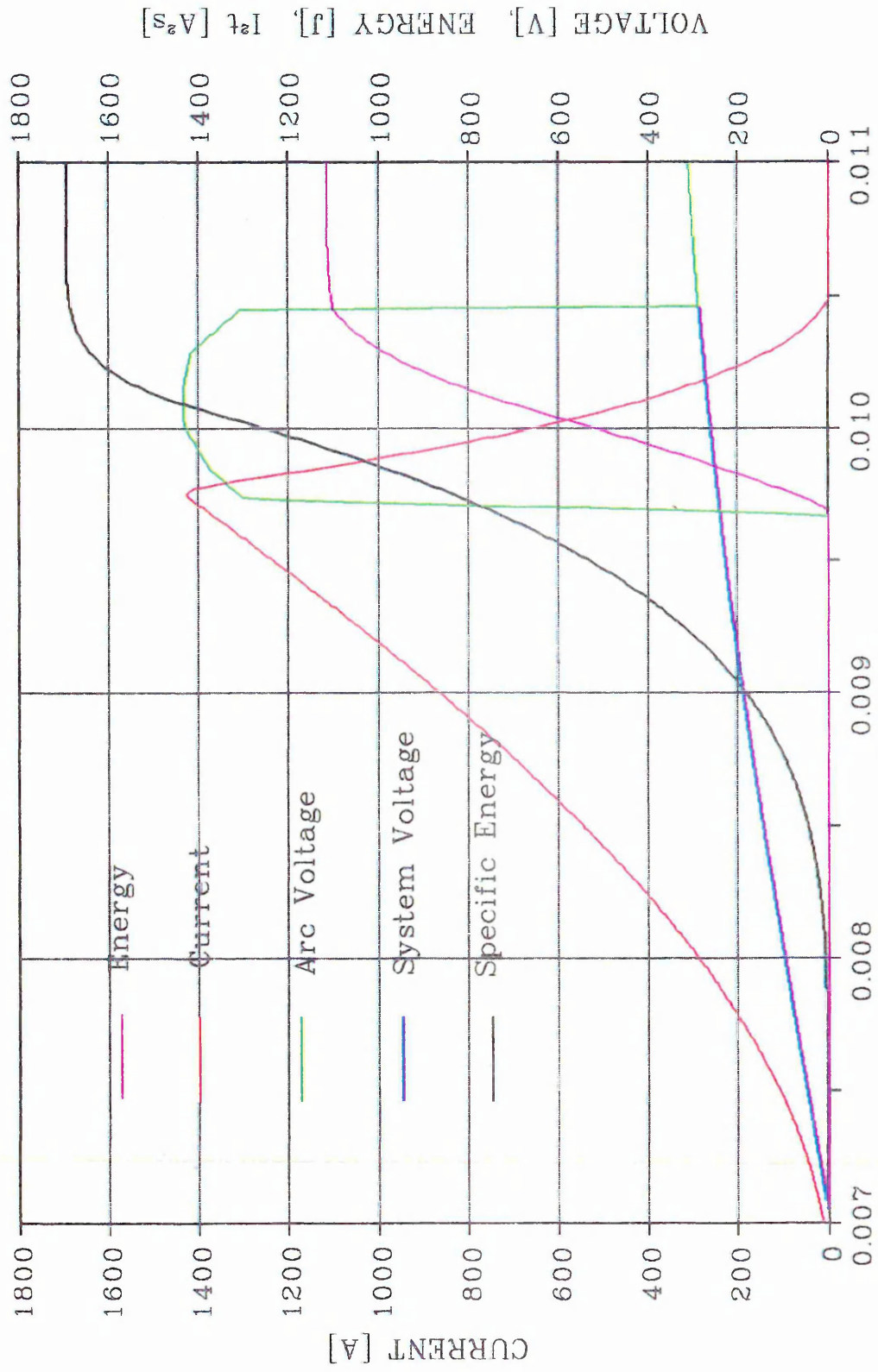


Fig. 4-4 Simulation of HBC Fuse behaviour with a tapered notch fuse element

- Prearc  $\int i^2 dt$
  - Arc  $\int i^2 dt$
  - V arc maximum
  - $dv/dt$  pre-peak
  - $i = f(t)$
  - $V_{arc} = f(t)$
  - Arc energy =  $f(t)$
  - $\int i^2 dt = f(t)$
  - $I_p = f(\text{operation time})$
  - $i_{\text{peak}} = f(I_p)$
- $\int i^2 dt$  maximum and minimum =  $f(I_p, \text{making angle})$

#### 4.2.2. Experimental simulation and Model Accuracy

The model is not only suitable for the simulation of a purpose-designed fuse, but allows also the evaluation of the behaviour of fuse designs when some of the parameters are modified. The modifications for example can include variations in dimensions as well as in the arc-root voltage and/or pre and post-peak  $dv/dt$  values. As a particular example the behaviour of a short notched fuse element immersed in solid filler of hypothetical very high arc-root voltage drop (125 V) can be analysed, keeping the other parameters constant. In **Fig 4.3** the results of such a simulation are shown.

Another interesting application is the study of the effect of a stepped or tapered notch (semicircular and circular) on the pre-peak  $dv/dt$ . The oscillogram of the voltage and current for such an example is shown **Fig 4.4**. Alternatively, the model is able to give the necessary parameters for some desired fuse behaviour, determined by say the required current or arc voltage variation with time.

#### 4.2.3. Practical limitations of proposed arc model

The main discrepancies based on the study of current and voltage traces of hundreds of simulations, including over 800 different fuse element types tested, are summarized as follows:

- The actual voltage peak values are slightly smaller and slightly more rounded than the analytical ones. (obviously the model is just a good approximation leaving aside the burn-back rate variation with instantaneous current density)
- The model shows a better agreement during the first half of the post-peak period, where the arcs perform as wall stabilised ones more precisely.
- The conditions are modified during the second period, where the wall stabilised arc theory gradually fails, because of arc expansion.
- The model agreement is less good at the end of the arcing period where the cooling by the fulgurite inside wall and other types of cooling such as convection are neglected.

#### 4.3. Fuse Design Considerations

##### 4.3.1. Ideal fuse arc characteristics

Based on our results and on well established concepts, the postulation of the ideal H.B.C. fuse is possible as one which meets the following requirements:

- Is able to force the current to zero and therefore operates independently of naturally occurring current zeros [13].
- In order to produce current limitation it is necessary for the arc voltage to exceed the supply voltage. This overvoltage, generated by the fuse, should be controlled according to its application. This overvoltage will produce a reversal of the voltage across the source inductance and hence a linear decline of the current if the arc voltage is maintained constant. Fig 4.5.

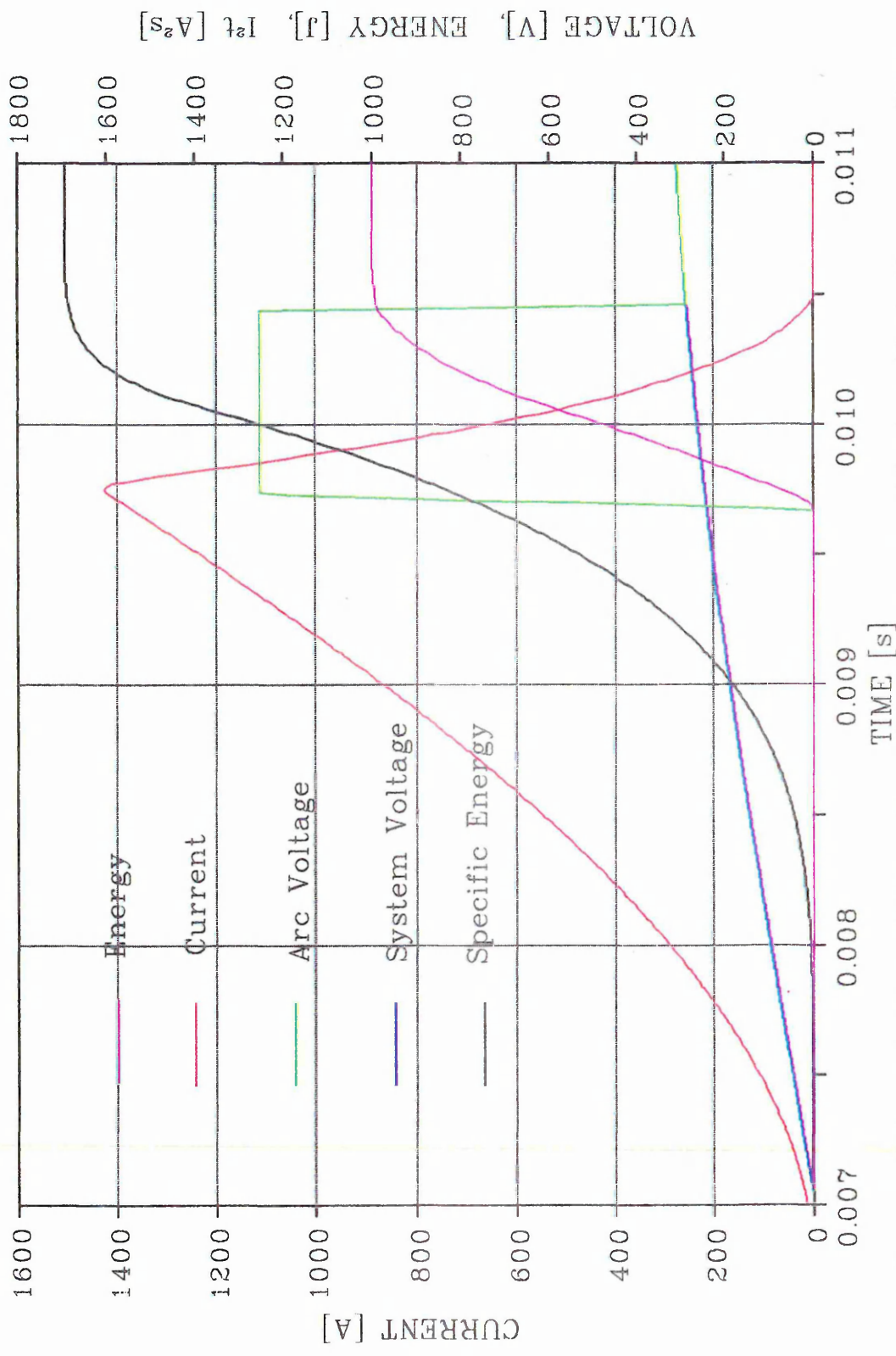


Fig. 4-5 Simulation of HBC Fuse behaviour considering that the overvoltage is constant during the whole arc period

- The overvoltage can be determined by the desired rate of decline in the current or desired arcing  $\int i^2 \cdot dt$  using a computer program. The overvoltage however must be limited according to the voltage withstand capability of the other circuit devices in parallel with the fuse during its operation. The overvoltage withstand of the normal circuit elements depends on the peak value and on the rate of rise. As the latter one is the most dangerous, the control of this overvoltage rise is of utmost importance [14].
- In order to determine the optimum overvoltage shape the study of a simplified circuit should be done, where the circuit resistance is neglected [15, 16].

For these conditions the circuit equation is:

$$v_s = L \cdot di / dt + v_a$$

where  $V_s$  and  $V_a$  are supply and arc voltage respectively,  $L$  is the circuit inductance and  $i$  the circuit current.

From the previous equation it follows that:

$$i = 1 / L \cdot \int (V_s - V_a) \cdot dt$$

In accordance with fuse practice it is assumed that  $V_a = 0$  during the prearcing period,  $t_0 - t_1$ , where  $t_0$  is the instant at which the short-circuit current commences and  $t_2$  is the time when the current is interrupted. **Fig 4.5.**

It follows for  $i \rightarrow 0$  that

$$\int_{t_0}^{t_2} v_s \cdot dt = \int_{t_1}^{t_2} v_a \cdot dt$$

This means, in mathematical terms, that the areas enclosed by the supply voltage during the period  $t_0 - t_2$  and the arc voltage during  $t_1 - t_2$  must be equal. The conclusion which can be deduced from this simple analysis is that the arc voltage shape should

theoretically be square (constant), because this is the shape for which the area is maximum for the shortest arcing time and hence produces the lowest  $\int i^2 \cdot dt$ . In practice, however the optimum shape is trapezoidal, in order to avoid excessive voltage rise rates.

The optimum voltage waveform requires the following problem to be solved. The answer however depends on the fuse application, i.e. at one end of the spectrum is semiconductor protection and at the other are general purpose industrial applications. The maximum value for peak arc voltage pertaining to semiconductor device protection is to limit its value to twice the R.M.S. rated voltage. This limit can be extended to 3.5 to 4 times for general purpose industrial fuses.

The next question is the fuse element design and choice of filler to be able to meet the specific requirements.

Uniform fuse elements, wire or strip, create very sharp arc voltage wave forms, producing a short arcing period. They also produce high peak arc voltage values together with extremely fast rising arc voltage. Such fuse characteristics practically prohibit the use of these element, even in industrial applications. The best solution resides in the notched fuse element, which from our investigations the peak voltage reduces from 1800 V for uniform cross-section to between 1070 V (obtained with a long notch), and 640 V in the case of short notched fuse elements. (all the values are average values)

An increase in the notch length to 0.3 mm did not produce a further reduction in the arc voltage, because the voltage per notch limit was exceeded.

In reference to the ideal wave form, the long notched fuse element produced a peak voltage which was not as sharp as produced by the uniform fuse element. But a big improvement in the smoothing of the voltage was created with the short notched fuse, where the double arc mechanism was significant.

The  $dv/dt$  as a function of current density can be determined from tests on very short notched fuse elements. The notch element is extremely simple, thus the idea can be readily exploited by extending the notch length and gradually increasing the cross-section to modify the arc voltage waveform shape.

The above summary explanation indicates that the fuse arc voltage wave form can be designed through the creation of steps in the notch, where each step will have its own

dv/dt and dx/dt based on its current density and length. The polyhedral notch could be extended to a more uniform shape, as for example in the circular hole, oval-shaped hole or non-axial elliptical indentation, etc.

It is worth noting that the fuse voltage per-arc has two components, the positive column voltage and arc-root voltage drop. The analysis presented above relates only to the positive column. The Vak value can be also altered by changing the filler characteristics as previously explained. The remaining factor which can help in obtaining the desired wave form is the number of arcs, closely followed by the number and shape of the notches.

An interesting idea, not researched here, is the application of differential or gradual notches, used in order to change the simultaneous and/or progressive burn-back. Both behaviours can be analysed using the proposed mechanistic model and computer program. The arc merging phenomena and the possibility of avoiding occurrence of shoulder arcs can also be studied by the application of the proposed model.

#### 4.4 References

1. Mikulecky, H.W.; Current-Limiting Fuse Arc-Voltage Characteristics; IEEE Trans. on PAS, Vol. PAS-87, n° 2, pp. 438-448, February 1968.
2. Reineri, C. et al; Experimentación sobre el comportamiento de distintos tipos de elementos extintores en fusibles h.b.c. en baja tensión (Experimental study of the behaviour of different type of filler in H.B.C. Fuses); IX Congreso Chileno de Ingeniería Eléctrica, Octubre 1991, pp. 3.6.1., Arica, Chile.
3. Lipski, T. Ossowicki, J.; Some aspects of application of stone-sand arc-quenching medium in H.B.C. fuses; Seventh Int. Conf. on Swit. Arc Phen., pp. 231-235, Lodz, 1993.
4. Wright, A. Beaumont, K.J.; Analysis of high-breaking-capacity fuselink arcing phenomena; Proc. IEE, vol. 123, n° 3, pp. 252-258, March 1976.
5. Kroemer, H.; Der Lichtbogen an Schmelzleitern in sand, (The arc in Elements Fusing in Sand); Archiv fur Elektrotechnik; Heft 8, Band 36, pp.455-470, 1942.
6. Wilkins, R. Gnanalingam, S.; Burn-Back rates of silver fuse elements; 5th. IEE Conf. Gas Discharges, n° 165, pp. 195-197, Liverpool, September 1978.
7. Gnanalingam, S. Wilkins, R.; Digital simulation of fuse breaking tests; IEE Proc., vol. 127, Pt. C, n° 6, PP. 434-440, November 1980.
8. Daalder, J.E. Schreurs, E.F.; Arcing Phenomena in High Voltage Fuses; EUT Report 83-E-137, Eindhoven University of Technology the Netherlands, March 1983.
9. Sloot, J. et al; A one dimensional mathematical model for the dynamical burnback velocity of silver strips; Third Int. Conf. on Elec. Fuses and their App.; pp. 72-77, Eindhoven, 1987.

10. Mocsary J.; Untersuchungen von strombegrenzenden Hochspannungs-Hochleistungs-Sicherungen in Stromkreisen mit unterschiedlichen Netzeinschwingfrequenzen; (Investigation of High Voltage High Breaking Capacity Current Limiting Fuses in circuits with variable recovery frequency); Elektrotechnik und Maschinenbau, Jahrgang 81, Heft 23, pp. 655-661, 1964.
11. Baxter H.W.; Electric Fuses; Edward Arnold, London, 1950.
12. Johann H.; Elektrische Schmelzsicherungen für Niederspannung; (Low Voltage Electric Fuses); Springer-Verlag, Berlin, 1982.
13. Lerstrup K.; The current-limiting fuse with special reference to discrimination and breaking capacity; Ingenieron - International Edition, Vol. 2, n° 1, pp. 1-10, 1958.
14. Lerstrup K.; The dimensioning of fuses for diodes or thyristors; Days of Danish Science and Technology, Moscow, September 1975.
15. Bohene E.W.; The geometry of arc interruption; AIEE Transactions, Vol. 60, pp.524-532, 1941.
16. Vermij, L.; Electrical Behaviour of Fuse Elements; Thesis, Eindhoven University, The Netherlands, May 1969.

## Chapter 5 : Review of Research and Concluding Observations

### 5.1 Review of H.B.C. Fuse Arc Mechanism Model

#### 5.1.1 Pre-peak arc voltage mechanism

Figure 5.1 shows the voltage per arc profile for uniform fuse elements in filler, subjected to short-circuit critical current, over the arcing period up to the instant when the arc voltage reaches its maximum value. This period is referred to as the pre-peak arc voltage time. The arc voltage profile has the familiar sawtooth characteristic shape, which results from the arc mechanisms and underlying principles of wall-stabilised arcs discussed in Chapter 2. It is instructive to review the arc model from a circuit point of view to bring out its important features and some aspects of its behaviour which require further clarification and understanding.

From a mathematical stand-point, it can be readily shown that the curve characterising the minimum voltage per arc is given by the relation for  $V_{arc}$  below, which, interestingly, is a very simple function of  $V_{ak}$  and the arc number  $n$ . A characteristic of the proposed model is its simplicity throughout which leads to other simplifications for what has, in the past, been considered to be a very complex mechanism. Continuing with this simple approach, it follows from the analysis of the relation that the maximum value of this voltage will occur when  $n = \hat{n}$  and that in the limit (i.e.  $n \Rightarrow \infty$ ) the relation results in  $\hat{V}_{arc} = 2V_{ak}$ .

$$V_{arc} = 2 \times V_{ak} \frac{(n-1)}{n}$$

Also it can easily be shown, mathematically from the same figure, that the pre peak arc voltage gradient is given by

$$k_1 = \left[ \frac{dv}{dt} \right]_{PP1} = \frac{2 \times V_{ak}}{T} \quad \text{from which} \quad k_1 = \frac{\hat{n} \times 2V_{ak}}{t_{1arc}} = \frac{\hat{V}_{arc}}{t_{1arc}}$$

where  $T$  is the time interval between successive arcs and  $t_{1arc}$  is the time for the arc voltage to reach its maximum value from the beginning of the arcing period.

The maximum value of the arc voltage may be obtained from Hibner's well known equation or directly from test . The maximum number of arcs for uniform elements (wires) is given by

$$\hat{n} = \frac{L}{h} \quad \text{where } h = 0.555 + 2.08 \times d \quad (\text{from Chapter 2})$$

The only unknown parameter is  $t_{1\text{arc}}$  which would need to be determined from tests on fuse samples

### 5.1.2 Post-peak arc voltage mechanism

Figure 5.2 shows the voltage per arc over the remaining part of the arcing period, referred to as the post-peak arc voltage period . The equations for the arc voltages above apply equally to the post-peak period . For this period it is clear that the gradient of the arc voltage change per arc is constant but the time between arc extinctions is not . If the gradient is obtained, however, it is relatively simple to determine the arc voltage profile over the whole arcing period .

The gradient during extinction of the first arc is the same as the gradient during the formation of the last arc, i.e. the value is equal to  $k_1$  . It follows, therefore, that it is now possible, from only two tests at different current densities, to predict the whole of the arcing performance of any HBC type fuse, comprising uniform section elements and long notched elements and, in the case of bound fillers, of HBC fuses comprising medium and short restrictions, although care must be exercised in using the models for elements with short restrictions . The approach is valid also for parallel elements, as discussed in Chapter 3

The model is applicable for predicting the arcing wave forms of HBC fuses comprising any element shape by determining the arc voltage gradients for the various cross-sections of the elements . This is not as major a task as it seems since the ratio of the gradients are in direct relation to the ratio of the shoulder to notch cross-sections .

The accuracy of the model and how well it simulates fuse arc formation and extinction mechanisms, based on over 800 short-circuit tests on twenty fuse types, can be assessed from inspection of figures 5.2 & 5.3 .

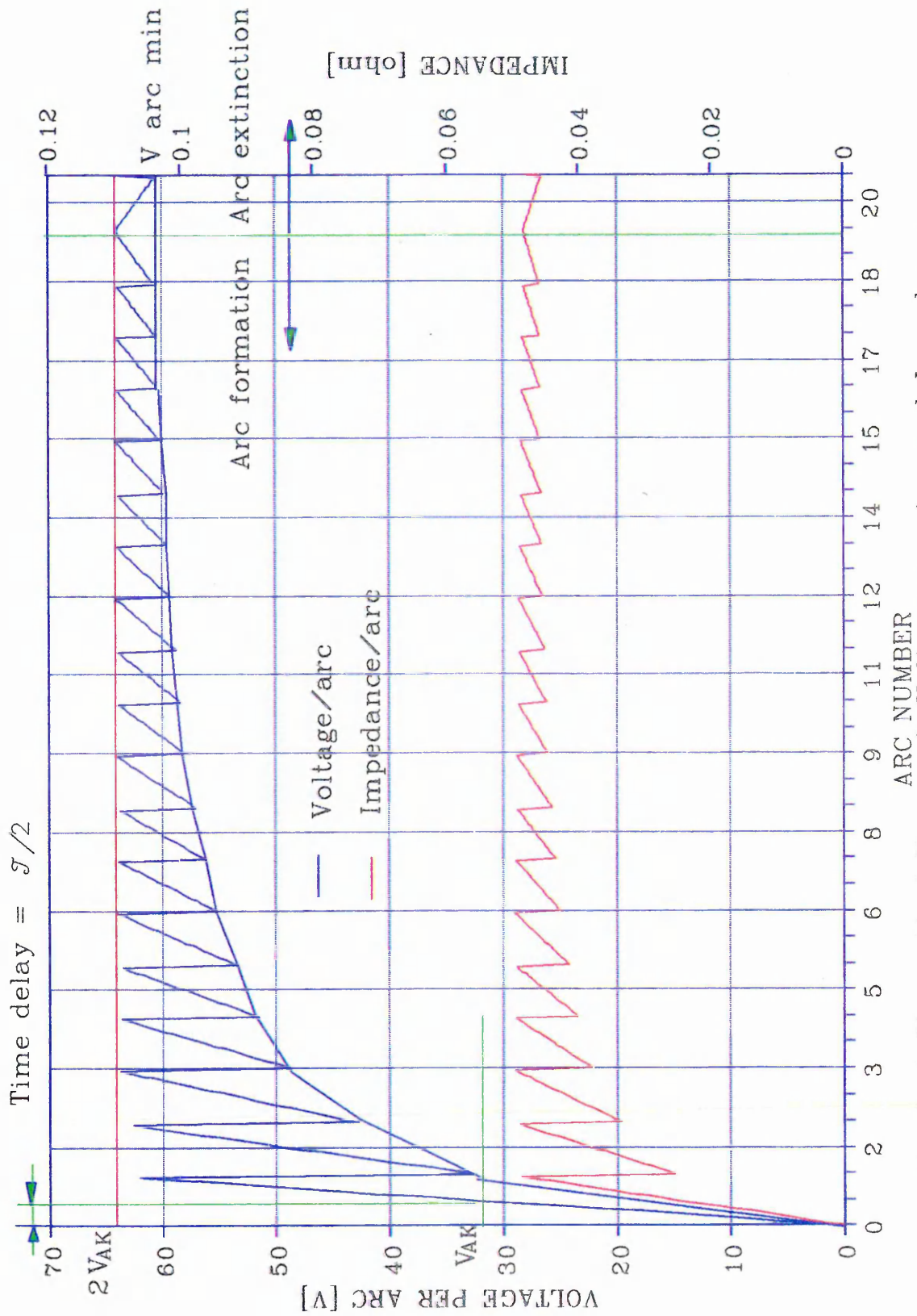


fig. 5-1 Theoretical Pre-peak Voltage per Arc and Impedance

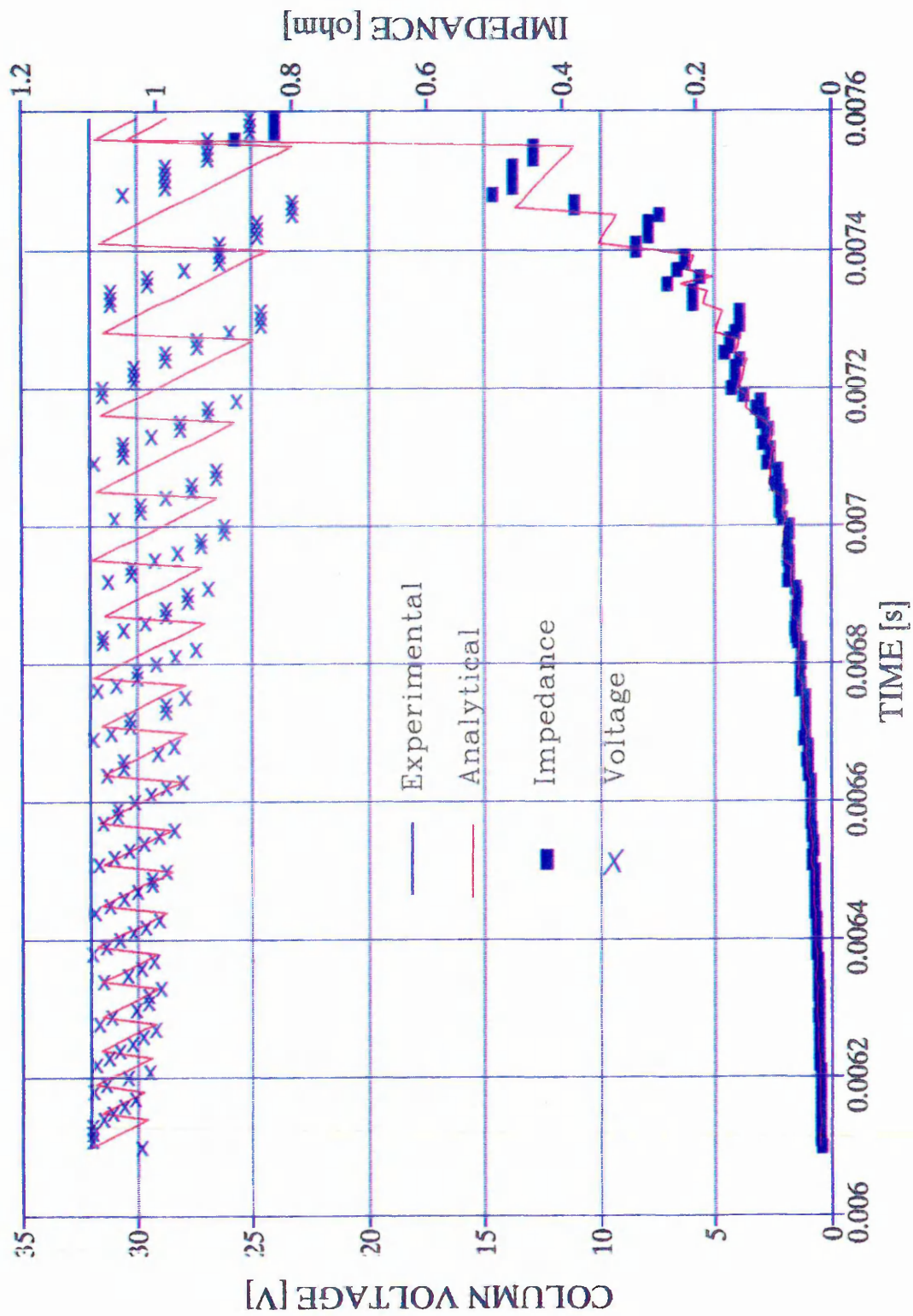


Fig. 5-2 Post-peak voltage/arc and impedance

## 5.2 Review of arc physical formation and extinction processes

The melting disintegration process precipitating arcing, known to occur in wires, has been found to occur in exactly the same way in uniform strip and notched fuse elements. This work has demonstrated that the number of arcs in these elements for interruption of short-circuit currents, including the 'critical current', is the same for elements of the same length, cross-section and material type, irrespective of the surrounding filler medium. The work has also demonstrated that the respective arc formation and extinction processes, occurring in wires, are also the same for these elements and can, hence, be represented by a single arc model. It has been demonstrated in this work too, that the grain composition, compaction and structure of fillers effect the rates of arc formation and arc extinction and the value of the arc-root voltage and, hence, how the filler influences the peak arc voltage, its rate of rise and its effect in limiting current and the arcing  $I^2t$ , Fig. 5.4. It is clear, therefore, from the results of this work that the arcing mechanism for all fuses is, fundamentally, the same.

### 5.2.1 Arc physical formation processes

The physical processes in the formation of arcs in fuses are considered to be as follows. At commencement of arcing during short-circuit interruption, the whole wire, or reduced sections, are assumed to be in a molten state, as described previously and by many other researchers. Deformation of the element shape takes place, as described in Chapter 2 and by Arai, which produces points of increased current density along the element where the element will vaporise first. The filler properties, particularly the grain shape, size and packing density, influence the onset of deformation (**Photograph 1**, Chapter 2).

The findings in this work demonstrate that the arcing process starts with the commencement of one arc. It is proffered, based on the model for the proposed arc mechanism, Fig. 5.1, that the first arc takes a short, but finite, time to establish the arc

roots and, hence, the corresponding arc-root voltage fall, before significant electrode erosion (burn-back by thermionic emission) occurs. This time, equal to  $\frac{T}{2}$ , is shown in figure 5.1 as the delay between the commencement of arcing and the instant the column voltage first appears. The delay has been found, in this work, to be of the order  $3 \approx 5 \mu\text{s}$ , which is in good agreement with the findings of Mikulecky [1]. The burn-back, which becomes highly significant at this point, produces extension of the roots and is responsible for establishing the first 'so-called' positive column. The voltage fall, associated with the consequent plasma column, and its dimensions, increases as the burn-back and the column length increase. It is assumed in this work that the filler plays a role probably by confining the arc co-axially and, hence, effects the speed of the burn-back significantly at this juncture. This influence is evidenced by the higher rise rates of the initial arc voltage for high compaction and bound fillers, Fig. 5.4.

The next critical stage is when the column voltage attains the same value as the established arc-root voltage fall  $V_{ak}$ . It has been demonstrated by experiment and logic in this work that the column voltage can not exceed this value and, hence, if the column voltage is rising, at the instant it reaches the value  $V_{ak}$ , another arc ignites. This is the fundamental reason why arcs behave in a mechanistic manner and, hence, it is believed to be a new principle and, therefore, a fundamental discovery.

The arc extension process progresses by burn-back, as before, until the second arc column voltage attains the (critical) value  $V_{ak}$ , after which another arc forms. This process is replicated thereafter until the maximum number of arcs is reached in accordance with the fuse element properties and dimensions.

The fuse arc voltage is a maximum at the instant the last column to be established attains the arc-root voltage critical value.

At the instant, during arc formation, that the arc voltage exceeds the instantaneous value of the circuit supply voltage, the voltage across the circuit inductance reverses and, hence, the circuit current begins to fall and current density in the fuse elements reduces.

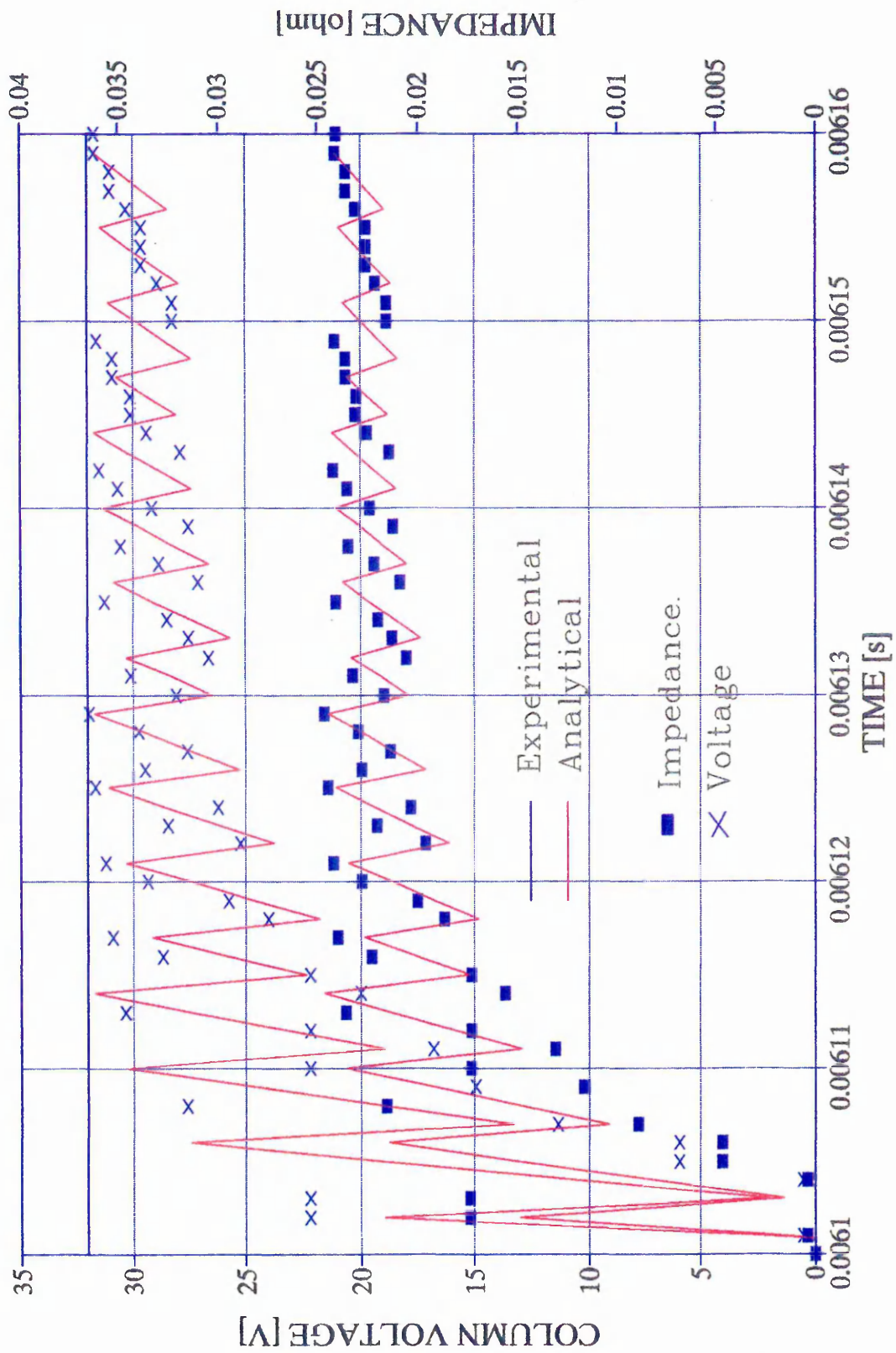


Fig. 5-3 Pre-peak voltage/arc and impedance

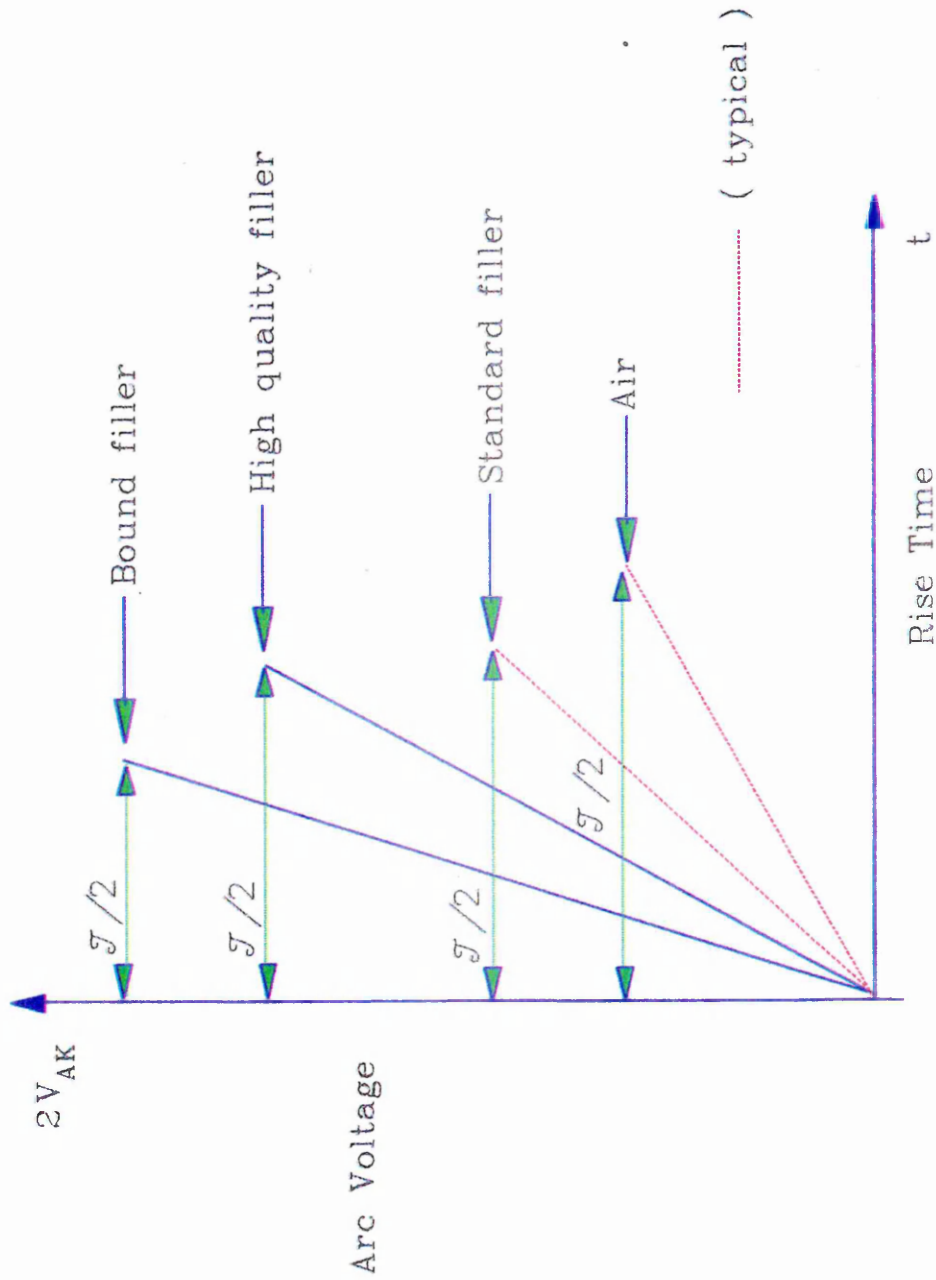


Fig. 5-4 Initial Arc Voltage Rise Times for Different Arc quenching media

Arc formation will still continue and, hence the arc voltage will continue to rise even when the current is falling .

The formation of consecutive arcs, as described, has implications for some unexplained fulgurite lumen formations, observed early on in the work, and for the existence of un-melted element particles, deposited some way from arc lumens, found from tests on wires in filler, **Photograph 5**, Chapter 2 . The arc mechanism provides possible answers to some of the puzzling observations regarding the size and length of arcs and the apparent mixed combination of long fat arcs and short uniform ones, **Photographs 10 & 11**, Chapter 2 . The existence of long and short arcs is self-evident if arcs commence consecutively and, consequently, burn for longer periods . This behaviour would also account for short arcs of different lengths, evidenced by the common occurrence of different widths of light and dark bands in fulgurites of wire filled fuses .

The deposits of un-melted element material close too, but away, from the extremities of arc lumens, can also be explained with a reasonable degree of confidence, based on the arc mechanism findings . The explanation, in this case, is that maximum expulsion of un-melted arc products would occur in the region of the first arc at the instant the second arc ignites . This is because when the second arc-root voltage is established the voltage across the first column, practically, collapses, although the arc is continuing to burn back . For this to occur , the arc resistance must fall suddenly which would necessitate, since the length, if anything, is increasing, that the arc cross-section must expand rapidly. The net effect would be a massive increase of pressure around the arc in regions where the filler is still un-melted and porous . This could result in the expulsion of arc products well beyond the region of the arc, and, therefore could well account for the un-melted element deposits observed in **Photographs 5&13** .

The apparent phenomena of long arcs subsequently reforming into short arcs, which switched the direction of the work towards investigating arc mechanisms, can not be explained by the proposed arc mechanism process . It, therefore remains a puzzle, although it is suspected that the process does not, in fact, occur, as what is, likely, being observed is the fulgurite remains of two or three adjoining arcs coalescing after the

current in the fuse has been by-passed . This would also account for the occasional variation in the number of arcs observed for the same test setting which was, initially, put down, solely, to variations in fuse sample manufacture .

### 5.2.2 Arc physical extinction processes

Some interesting physical insights have been gained in applying the arc mechanism model to the arc extinction process since the arc extinction physical process is far more complex than the arc extinction mechanism .

Study of the post peak arc voltage per arc wave form, **Fig. 5.2**, indicates that the commencement of arc extinction occurs when arcs begin to merge due to extended burn-back . As described in Chapter 2, the merging of two arcs results in a reduction in the magnitude of the arc voltage of  $2V_{ak}$ , although the actual voltage fall at the instant of merging will be between  $V_{ak}$  and  $2V_{ak}$  . What happens next is not very clear in the physical sense, based on the data available . A theory, predicated on reasoning, nonetheless, is advanced as the most logical explanation of wall-stabilised arc extinction . The situation which exists upon the merger of two arcs is, clearly, that the arc length is increased at the same time the voltage across the merged arc exceeds the maximum permissible value, i.e.  $2V_{ak}$  . The current is, of course, falling but, arguably, the change is not significant over the time interval of an arc merger . What is clear is that the resistance of the arc must increase for the arc voltage to increase which implies that the arc cross-section and/or the plasma electrical conductivity must reduce .

The conductivity would fall due to increased cooling and reduction of available energy from the circuit, caused in part, by the fall in current and increase in area of the outer surface of the arc . However the more likely explanation is that the arc cross-section decreases marginally at first, as evidenced by the increase in the impedance per arc, **Fig. 5.2** . After arc merger the arc continues to increase in length due to burn-back and the column voltage falls further. This process continues for consecutive arcs until, for a good fuse, the remaining 4 to 5 arcs extinguish, virtually together . This behaviour is very noticeable in the graph portrayed in figure 5.5.

It is concluded that wall-stabilised arcing breaks down when the wave form departs from the classical sawtooth shape but this does not automatically imply it is a bad fuse . A bad fuse is likely to be one where wall-stabilised arcing breaks down early in the extinction process, in which case it is suggested that final extinction will occur later, if at all . Under the most onerous conditions, one arc would be left burning which may well burn through the end caps or at the least cause high volatilisation of the filler and considerable pressure within the fuse; a condition frequently met in clearing low over-current faults .

### 5.3 Fuse arcing and circuit interaction

Figure 5.6 shows the fuse transient electrical impedance determined experimentally and from the model, together with the corresponding current and voltage wave forms . Apart from drawing attention to the accuracy of predictions, using the model, it is instructive, at this juncture, to consider how the model may be applied to practical situations . One interesting application is to use the fuse impedance characteristic as input data to a CAD circuit simulator, such as SPICE, to enable the circuit interaction to be analysed . This, in fact, has been achieved and combined with electro-thermal models for power semiconductors to assess whether semiconductor fuse will protect the power semiconductor devices for non-sinusoidal application [2] .

There are, obviously, other applications which can be analysed in this manner . In this context, therefore, the model adds to the so-called 'tool kit' for extending the use of simulation by computer and heralds the day when fuse testing in short-circuit power stations will be a thing of the past and all design will be done by computer . The presented work has, probably, inched this realisation a little further along this inevitable path .

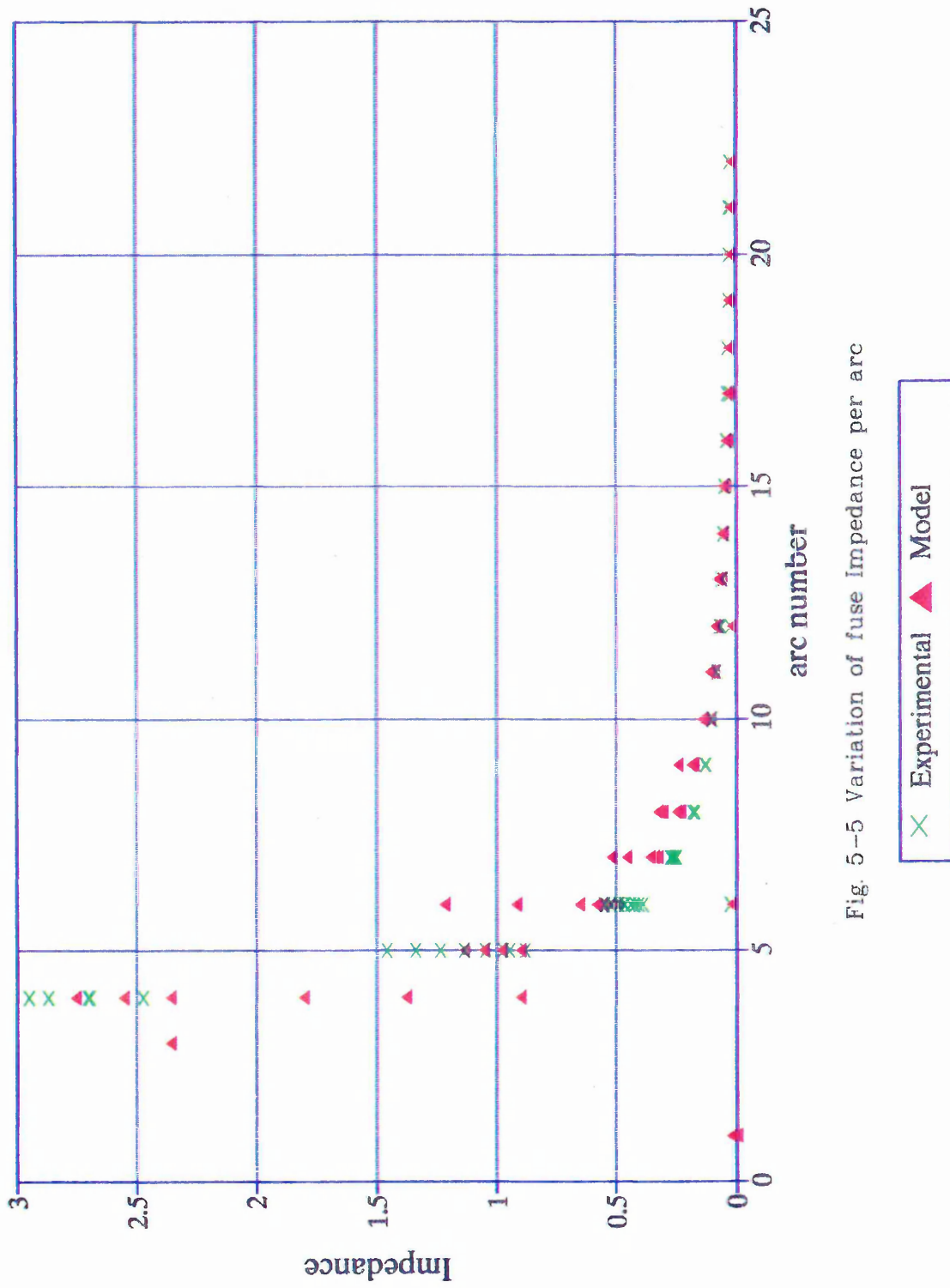


Fig. 5-5 Variation of fuse Impedance per arc

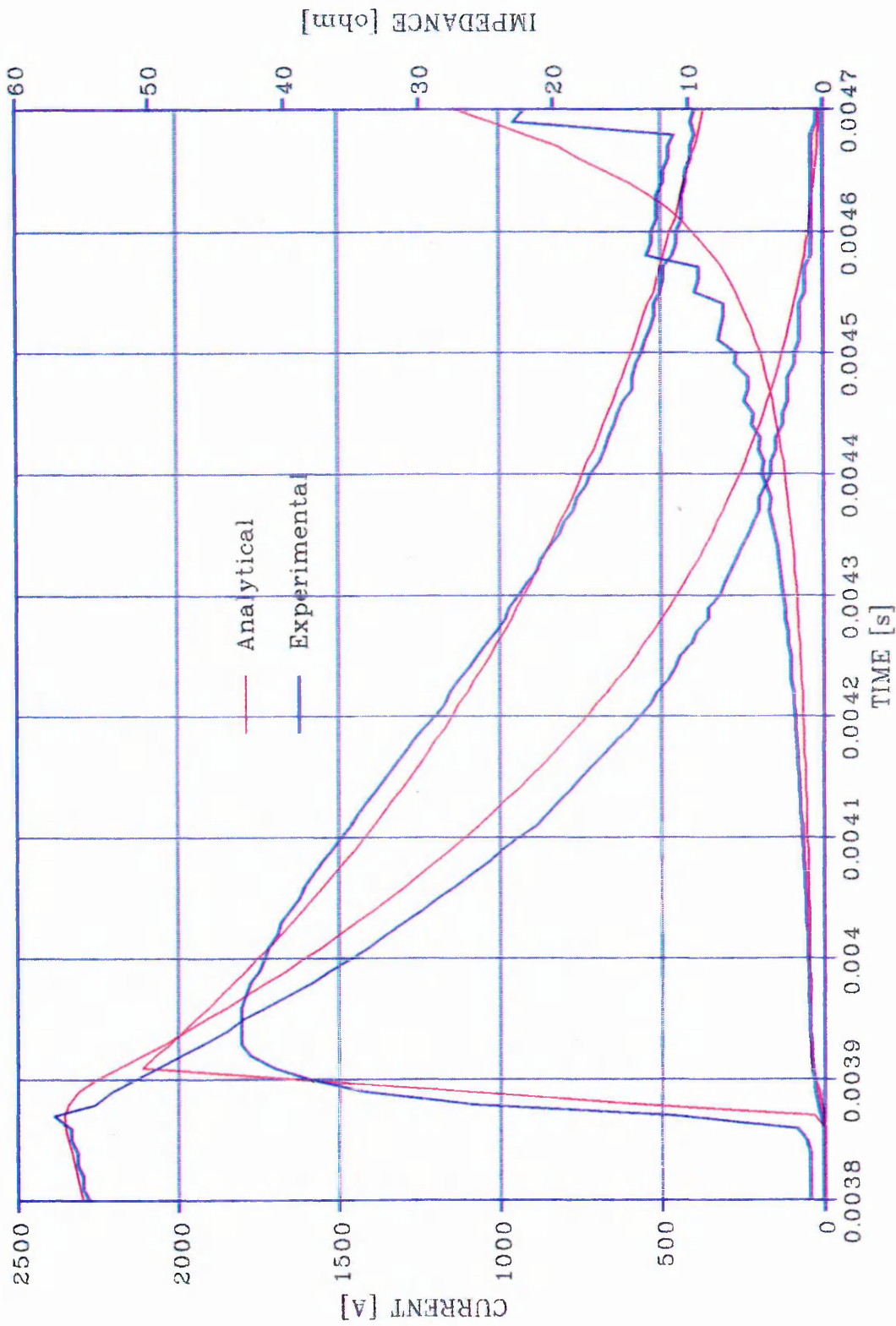


Fig. 5-6 Fuse arc current and voltage wave forms and transient impedance

#### 5.4 Unresolved problems and future work

Clearly an improved understanding of the arc mechanism is necessary to develop full confidence in its use . On matters of detail, the quest to determine the time interval between consecutive arc formations is important as is also to obtain a closer prediction of fuse performance under a variety of other conditions . Not least would be simulation of low overcurrent interruption . Then again there are other fuse technologies to research and understand . The list is non-ending .

#### 5.5 References

1. Mikulecky, H.W.; Current Limiting Fuse Arc-Voltage Characteristics; IEEE Trans PAS, Vol 87, No 2, 1968 .
2. Magnago F., McEwan P.M., Gomez J.C., Zamanillo G.; Computer Modelling of HBC Fuses and their Co-ordination with Power Electronic Devices for Sinusoidal and Non-sinusoidal Short-circuit Fault Conditions; submitted to IEEE APEC'95 Conf., Aug. 1994.

## 6 : The Author

Juan Carlos Gomez Targarona, born in Mendoza, Argentina, in 1952, obtained his bachelor degree in Mechanical and Electrical Engineering from The University of San Juan in 1975. He began his academic career, at the same university, as Assistant Professor in 1976.

He has been active in fuse research and development since 1973 and also as a consultant to the Argentinean electrical power industry for over 20 years.

He joined The University of Rio Cuarto, Argentina, in 1978 where he established The Institute of Electrical Power System Protection and a research group in electrical apparatus and systems. In 1988 he spent a secondment in England working with Professor Dr. Peter McEwan on fuse research . In 1991 he commenced his doctorate degree under Professor McEwan, at Sheffield Hallam University, England .

He has recently achieved the level of Senior Professor at the rank of highest level of university teacher, in Argentina.

He has published over 30 papers on electrical apparatus and systems and has developed extensive post-graduate and undergraduate courses in a wide range of electrical engineering topics.

## Acknowledgments

My very special thanks goes to my family who supported me during the period of this research. Above all my gratitude goes to Sofia, my wife, and my two daughters who suffered orphanhood on too many occasions at an age when they needed their father most.

I am also extremely grateful to Professor Dr. Peter McEwan , who, as Director of Studies and friend, continuously encouraged me in this research on fuses and for his advice, valuable discussions and guidance .

I am also grateful to Professor Dr. Juana Chessa de Silber, Universidad Nacional de Rio Cuarto, Argentina, who, as my Second Supervisor, assisted me in carrying out this project .

My sincere gratitude goes to my colleagues and friends at The Universidad Nacional de Rio Cuarto, Institute of Electrical Power System Protection, for their generous assistance and support of my research .

I wish to express also my thanks to The University of Rio Cuarto, and The Sheffield Hallam University , England , for providing facilities and financial support for the research and my sincere thanks to my colleagues and the technical staff of the School of Engineering Information Technology, Sheffield Hallam University, who were always willing to help me during my periods in Sheffield .

My special thanks also goes to :

Semikron and Reproel SACI, Buenos Aires, Argentina, who supplied fuse components and data for the experimental research .

The British Council , Argentina , in particular to Mr. Harold Fish , Director, for financial support and encouragement of the Argentinean/UK University link .

Table 1

## Short-Circuit Test Data for Wire Elements

lprosp. A.	Con. angle $e^\circ$	lpeak Ac.	Vpeak Vc.	Spec. energy $I^2t$	Energy J	Arc num. n	dv/dt pre-p. -	dv/dt post-p. -	Sample n° -
1404	5	1942	1873	5350	891.2	20	15	80	1ag
1404	5	1942	1907	5350	891.2	20	15	80	2ag
1404	70	1809	1803	5350	773.3	20	15	100	3ag
1404	90	1500	1872	5350	531.7	20	10	135	4ag
2540	25	2471	1820	5400	797.4	20	23	120	5ag
2540	5	2383	1803	5400	741.6	21	23	130	6ag
2540	75	2560	1803	5800	855.9	20	23	125	7ag
2540	78	2471	1942	5800	797.4	21	20	130	8ag
3990	12	2780	1700	5750	626	19	15	170	9ag
3990	32	2890	1768	5800	676.5	19	15	170	10ag
4300	76	3053	1942	5850	755	21	17	200	11ag
4300	85	3045	1768	5850	751	19	24	180	12ag
6100	40	3353	1699	5900	611.6	19	20	200	13ag
6100	5	3000	1699	5600	489.6	18	24	220	14ag
6100	76	3530	1664	5600	677.9	19	26	170	15ag
6100	85	3486	1812	5600	661.1	19	26	190	16ag

Table 2

## Short-Circuit Test Data for Strip Elements

lprosp. A.	Con. angle $e^\circ$	lpeak Ac.	Vpeak Vc.	Spec. energy $I^2t$	Energy J	Arc num. n	dv/dt pre-p.	dv/dt post-p.	Sample n°
1404	25	2030	2081	-	973.8	-	-	-	1lg
1404	12	2030	2011	6150	973.8	20	8	80	2lg
1404	80	1721	1769	6100	699.9	19	7	110	3lg
1404	60	1941	2011	6400	890.3	21	11	100	4lg
2540	20	2471	1803	6000	797.4	21	9	125	5lg
2540	5	2471	1872	6100	797.4	21	9	125	6lg
2540	75	2560	1942	6300	855.9	21	9	125	7lg
2540	80	2560	1422	6300	855.9	19	15	130	8lg
3990	25	2912	1942	6400	686.9	21	11	160	9lg
3990	29	3045	1890	6500	751	21	11	160	10lg
3800	80	3111	1751	7000	783.9	20	11	160	11lg
4300	75	3177	1751	6500	817.6	19	20	160	12lg
6100	32	3398	1734	6800	628.1	20	12	220	13lg
6100	0	3177	1768	6900	549.1	19	15	240	14lg
6100	72	3618	1834	6500	712.1	20	22	190	15lg
6100	95	3574	1942	6600	694.9	20	20	210	16lg

Table 3

## Short-Circuit Test Data for Long Notch Elements

Iprosp. A.	Con. angle e°	Spec. energy A <sup>2</sup> s	dv/dt pre-p.n	dv/dt pre-p.s	dv/dt post-p.n	dv/dt post-p.s	Arc n.n n°	Arc n.s n°	Arc n.c n°	Sample n°
1435	0	1360	20	1.5	250	45	11	10	9	el1g
1435	0	1360	20	0.9	250	35	11	8	9	el2f
1435	0	1360	12	0.9	50	35	12	8	8	el10f
1435	27	1360	12	0.9	50	45	11	8	8	el3f
1435	27	1360	12	0.6	80	25	9	7	7	el2g
1435	72	1360	12	0.9	50	45	10	8	8	el4f
1435	72	1360	12	0.9	50	60	12	8	8	el3g
1435	90	1360	12	3.5	80	55	11	11	11	el6f
1435	90	-	-	-	-	-	-	-	-	el6g
2620	0	1350	5	2.5	300	70	11	10	10	el7g
2620	0	1400	12	2.5	300	40	10	8	8	el7f
2620	23	1350	15	2.5	300	90	11	10	10	el8g
2620	23	1350	15	2.5	300	70	11	10	10	el8f
2620	72	1380	15	2.5	150	60	11	10	10	el9g
2620	72	1380	15	2.5	300	50	11	9	10	el9f
2620	90	1380	15	2.5	300	70	11	10	10	el10g
2620	95	1380	15	2.5	300	80	12	10	10	el11f
4119	0	1340	10	4.5	250	85	10	8	8	el11g
4119	0	1340	6	4.5	170	170	12	10	10	el12f
4250	25	1400	12	3.5	300	35	10	7	8	el13f
4250	25	1400	12	3.5	300	100	11	10	10	el12g
4250	72	1300	17	4.5	470	70	12	9	9	el14f
4250	72	1300	17	1.5	470	80	11	8	10	el13g
4250	90	1300	20	4.5	400	90	12	10	11	el15f
4250	90	1300	20	4.5	400	90	12	10	11	el14g
6397	1	1580	15	4.5	270	140	11	8	9	el16f
6397	0	1430	15	4.5	270	200	11	9	10	el15g
6397	25	1400	12	3.5	300	100	11	8	9	el17f
6397	25	1450	12	3.5	300	150	12	10	10	el16g
6397	72	1430	15	4.5	500	50	11	7	7	el18f
6397	72	1480	17	4.5	500	80	11	8	8	el17g
6397	90	1300	20	4.5	400	120	11	10	10	el20f
6397	90	1260	20	4.5	400	60	11	8	8	el18g
8270	0	1290	16	4.5	500	180	11	8	8	el21f
8270	0	1290	16	4.5	500	200	11	8	9	el19g
8270	25	1320	12	3.5	600	150	11	8	8	el22f
8270	25	1320	14	5.5	600	240	12	9	10	el20g
8270	85	1290	20	4.5	500	100	12	8	9	el25f
8270	85	1290	22	4.5	700	100	11	8	8	el21g
8270	90	1290	32	4.5	700	80	11	8	7	el24f
8270	90	1290	26	4.5	400	90	9	9	9	el23g

Table 4  
Short-Circuit Data for Medium Notch Elements

A.	e°	A²s	-	-	-	-	-	-	n°	n°	n°	n°	n°
1435	0	1300	-	-	0.7	-	-	350	-	-	5	8	5 ec1g
1435	0	1300	-	-	0.4	-	350	-	-	6	8	5 ec2g	
1435	0	1300	-	-	0.4	-	350	-	-	6	7	5 ec1f	
1435	20	1250	-	-	0.16	-	350	-	-	5	6	3 ec3g	
1435	20	1250	-	-	0.7	-	350	-	-	5	8	5 ec4g	
1435	20	1250	-	-	0.4	-	350	-	-	5	7	5 ec2f	
1435	85	1350	-	-	0.12	-	350	-	-	5	6	3 ec5g	
1435	85	1350	-	-	0.4	-	350	-	-	5	7	5 ec3f	
1435	90	1250	-	-	0.195	-	350	-	-	5	6	3 ec5f	
1435	90	1250	-	-	0.18	-	350	-	-	5	6	3 ec4f	
1435	90	1250	-	-	0.35	-	350	-	-	6	6	5 ec6g	
2560	0	1350	-	-	0.6	-	200	-	-	6	6	6 ec7g	
2560	0	1350	-	-	0.6	-	200	-	-	6	6	6 ec6f	
2560	95	1350	-	-	0.8	-	80	-	-	6	7	6 ec10g	
2560	95	1350	-	-	0.6	-	200	-	-	6	6	5 ec10f	
4180	4	1300	-	-	-	-	50	-	-	7	-	5 ec11f	
4180	6	1550	-	-	1.5	-	50	-	-	6	6	6 ec11g	
4180	6	1550	-	-	1.5	-	50	-	-	6	6	5 ec12f	
4180	25	1200	-	-	2	-	50	-	-	7	7	6 ec12g	
4180	25	1400	-	-	0.7	-	500	-	-	6	6	5 ec14f	
6397	6	1650	-	-	1.5	-	60	-	-	7	-	5 ec15g	
6397	6	1650	-	-	1.5	-	60	-	-	6	-	5 ec17f	
6397	27	1550	-	-	0.85	-	800	-	-	6	5	4 ec16g	
6397	27	1550	-	-	1.5	-	800	-	-	7	6	5 ec18f	
6397	120	1550	-	-	0.9	-	400	-	-	6	6	5 ec20f	
8737	0	1120	-	-	-	-	130	-	-	7	-	ec22g	
8737	18	1180	-	-	-	-	60	-	-	6	-	5 ec21f	
8737	19	1220	-	-	1.5	-	500	-	-	6	5	4 ec19g	
8737	65	1120	-	-	1.2	-	800	-	-	6	6	5 ec21g	
8737	90	1080	-	-	1.5	-	800	-	-	6	6	4 ec20g	
8737	90	1080	-	-	0.35	-	800	-	-	6	5	3 ec22f	

Table 5

## Short-Circuit test data for wire and strip elements in bound filler

lprosp. A.	Con. angle e°	Spec. energy I <sup>2</sup> t	dv/dt pre-p. -	dv/dt post-p. -	Sample n° -
1435	10	6350	10	90	51adg
1435	80	5050	30	200	53adg
1435	80	5950	25	150	53ldg
2540	13	5650	35	380	54adg
2540	13	5650	35	380	64adf
2540	18	5750	25	250	54ldg
2540	18	5750	25	250	64ldf
2540	82	5500	30	400	55adg
2540	82	5500	30	380	65adf
2540	82	6400	25	260	55ldg
2540	82	6400	25	250	65ldf
5930	12	5350	36	700	58adg
5930	11	6100	36	500	58ldg
6200	80	5000	36	500	59adg
6100	80	6000	36	300	59ldg
6200	80	5000	36	500	69adf
6100	80	6000	36	300	59ldf

Table 6

## Short-Circuit Test data for long notch elements in Bound Filler

lprosp. A.	Con. angle e°	Spec. energy I <sup>2</sup> t	dv/dt pre-p. -	dv/dt post-p. -	Sample n° -
1404	5	1450	10	120	el1fd
1404	5	1400	18	200	el24fd
1404	17	1450	12	160	el2fd
1404	65	1500	12	160	el3fd
1404	80	1500	16	200	el4fd
2621	5	1500	20	280	el5fd
2621	13	1480	20	300	el6fd
2621	72	1550	24	300	el7fd
2621	85	1300	26	300	el8fd
4306	7	1600	26	550	el9fd
4306	10	1500	13	550	el10fd
4306	70	1350	32	500	el11fd
4600	90	1450	35	450	el12fd
6397	5	1580	34	600	el13fd
6397	12	1500	34	600	el14fd
6397	12	1500	34	650	el15fd

Table 7

## Short-Circuit Test data for Medium notch elements in Bound Filler

lprosp. A.	Con. angle e°	Spec. energy I <sup>2</sup> t	dv/dt pre-p. -	dv/dt post-p. -	Sample n° -
1404	5	1450	10	70	ec2fd
1404	7	1500	8	75	ec5fd
1404	72	1500	8	75	ec4fd
1404	80	1500	8	75	ec6fd
2621	5	1400	14	125	ec7fd
2621	13	1500	14	125	ec8fd
2621	72	1450	14	110	ec9fd
2700	90	1400	14	105	ec10fd
4306	1	1580	14	175	ec12fd
4500	10	1510	14	175	ec13fd
4500	72	1510	14	125	ec14fd
4700	90	1400	16	175	ec15fd
6397	0	1480	22	300	ec16fd
6397	10	1340	22	300	ec17fd
6600	72	1500	26	270	ec18fd
6600	90	1280	26	270	ec19fd

Table 8

## Short-Circuit Test data for two parallel wire elements in fine grain filler

lprosp. A.	Con. angle e°	Spec. energy I <sup>2</sup> t	dv/dt pre-p. -	dv/dt post-p. -	Sample n° -
2840	8	20000	9	90	1fg
2840	15	24000	5	90	1dg
2840	84	19700	9	120	2fg
2840	80	22000	9	120	2dg
5070	11	20500	20	115	3fg
5070	18	23600	10	140	3dg
5070	22	20500	20	115	12ff
5070	8	22400	10	140	18df
5070	85	19500	10	180	4fg
5070	86	22000	11	150	9dg
5070	85	19500	14	160	13ff
5070	86	20000	12	130	13df
11584	10	19000	17	275	7fg
11584	7	22500	17	225	7dg
11584	100	19000	17	225	8fg
11584	100	22000	17	225	8dg